

International Atomic Energy Agency

INDC(CCP)-408

Distr.: L

---

**INDC**

**INTERNATIONAL NUCLEAR DATA COMMITTEE**

---

**SELECTED ARTICLES TRANSLATED FROM  
JADERNYE KONSTANTY (NUCLEAR CONSTANTS)  
VOLUMES 1 - 2, 1995**

Translated by Dr. Alex Lorenz

August 1997

---

**IAEA NUCLEAR DATA SECTION, WAGRAMERSTRASSE 5, A-1400 VIENNA**

Reproduced by the IAEA in Austria  
August 1997

INDC(CCP)-408  
Distr.: L

**SELECTED ARTICLES TRANSLATED FROM  
JADERNYE KONSTANTY (NUCLEAR CONSTANTS)  
VOLUMES 1 - 2, 1995**

Translated by Dr. Alex Lorenz

August 1997



## Contents

### *Neutron Data and Parameters*

The MENDL-2 cross section data library for the ..... 7  
investigation of the activation and transmutation of  
materials subjected to the irradiation of intermediate  
energy nucleons (Part 1. Neutron Data)  
By Yu.N. Shubin, V.P. Lunev, A.Yu. Konobeev and A.I. Ditok

The universal library of fission products and delayed ..... 37  
neutron group yields  
By A.B. Koldobskiy and V.M. Zhivun

The evaluation of the  $^{237}\text{Np}$  fission cross section in the ..... 55  
20 keV - 20 MeV energy range  
By V.N. Dushin, V.A. Kalinin and V.I. Shpakov

### *Nuclear Structure and Nuclear Reaction Data Parameters*

Evaluation of the photoneutron reaction cross sections of ..... 73  
radioactive fission product nuclei  
By Yu.N. Shubin, A.G. Gusseyinov, N.S. Rabotnov and V.P. Lunev

### *Nuclear Reactor Data*

The analysis of reaction rate measurements for the determination ..... 93  
of neutron energy spectra  
By A.V. Zvonarev, G.N. Manturov, Yu.S. Khomyakov,  
A.M. Tsibulya, V.P. Netsvet, N.V. Skorikov and I.M. Proshin



# THE MENDL-2 CROSS SECTION DATA LIBRARY FOR THE INVESTIGATION OF ACTIVATION AND TRANSMUTATION OF MATERIALS SUBJECTED TO IRRADIATION BY INTERMEDIATE ENERGY NUCLEONS.

(Part 1. Neutron data).

*Yu.N. Shubin, V.P. Lunev, A.Yu. Konobeev, A.I. Ditok.*

*State Research Centre of the Russian Federation  
Institute Of Physics and Power Engineering, Obninsk*

## Abstract

A new version of the MENDL data library is presented. This library consists of neutron and proton cross sections for more than 32000 reactions for 505 stable and unstable nuclei having a half-life  $T_{1/2} \geq 1$  day. Most of the data were obtained with the aid of the geometry dependent hybrid exciton model taking the pre-equilibrium deuteron and alpha-particle emission into account.

## Introduction

Currently, there is an increasing demand for cross section data for reactions induced by intermediate and high energy particles. The knowledge of these cross sections is necessary for the investigation of the activation and transmutation processes of materials irradiated by hard neutron spectra in thermonuclear installations, neutron generators, accelerators, as well as in the study of processes induced by the irradiation of long-lived fuel decay products in intensive high energy particles beams.

For reactions induced by neutrons having incident energies up to 20 MeV, in stable and long lived target nuclei, there exist data libraries, such as the REAC [1] and EAF [2] libraries, which consist of more than tens of thousands excitation functions. The use of rigorous theoretical models to describe neutron reaction cross sections makes it possible to significantly improve the content of activation data libraries. The last version of the ADL-3 [3] data library is an example of such an approach.

The demand for analogous/similar nuclear data for nucleons in the intermediate energy range ( $E < 100$  MeV) has so far not been satisfied. The MENDL (Medium Energy Nuclear Data Library) data library has been created to satisfy the neutron data requirements in that energy range. This library consists of information on nuclear reaction cross sections for stable and unstable nuclides in the energy range up to 100 MeV. The description of the first version of this library was published earlier in reference [4]. The creation of the second version of this library, MENDL-2, incorporated the modified version of the ALICE-92 program. This

program takes into account the competing gamma ray process in the decay of the compound system, the emission of complex particles (e.g. deuterons and alpha particles) in the pre-equilibrium mechanism, the utilization of the relationships of the generalized superfluid model of the nucleus in the calculation of level densities and the increase in the volume of the represented nuclides.

A brief description of the formulation of cross section library, the calculational method used in the evaluation process, and a description of the content of the library are presented below.

## 1. Content of the MENDL Cross Section Data Library

The MENDL library comprises cross sections compiled by the authors, for more than 32000 threshold reactions for the interaction of neutrons with nuclei of elements ranging from Al to Po in the 0-100 MeV energy range. The data for 505 stable and unstable nuclides having half-lives of  $T_{1/2} \geq 1$  day are given in the MENDL library.

The description of the library and part of the library content are given in Chapter 3.

## 2. Method Used in the Cross Section Compilation

The neutron data included in the MENDL library were derived from theoretical calculations on the basis the geometry dependent hybrid exciton model and on Weisskopf's evaporation model. The nuclear level densities were calculated in the framework of the superfluid model. The calculated cross section values for a number of channels were adjusted so as to agree with existing experimental data.

### 2.1 Calculation of cross sections

#### 2.1.1 Pre-equilibrium emission of nucleons

The calculation of pre-equilibrium spectra of nucleons is performed by using the geometry dependent hybrid exciton model (GDH) [5,6]. The calculations were performed with the aid of the following expression:

$$\frac{d\sigma^{pre}}{d\varepsilon_x} = \pi\lambda^2 \sum_{l=0}^{\infty} (2l+1)T_l \sum_{n=n_0}^{\bar{n}} R_x(n) \cdot \frac{\omega(p-l, h, E - Q_x - \varepsilon_x)}{\omega(p, h, E)} \cdot \frac{\lambda_c^x}{\lambda_c^x + \lambda_+^x} \cdot g \cdot D_n, \quad (1)$$

where  $\lambda$  is the wave length of the incident particle,  $T_l$  is the partial transmission coefficient calculated using the optical model (see par. 2.1.7),  $\varepsilon_x$  is the energy of the nucleon emitted from the nucleus,  $Q_x$  is the binding energy of the nucleon in the compound nucleus,  $\omega(p, h, E)$  is the density of the exciton states having  $p$  particles and  $h$  holes ( $p+h=n$ ) for an excitation energy  $E$ ,  $\lambda_c^x$  is the velocity of the emitted nucleon,  $\lambda_+^x$  is the velocity of the inner nuclear transition corresponding to the absorption of the nucleon in the nucleus,  $g = A/14.0$  is the density of the single particle state,  $R_x(n)$  is the number of particles of type  $x$  in the  $n$ -exciton

state,  $D_n$  is the “depletion” factor for the  $n$ th exciton state taking into account the change in the population states at the expense of emission at the previous stages, and where  $n_0$  is the initial number of excitons ( $n_0=3$ ).

The density of the exciton states was calculated using the Strutinsky-Erickson formula:

$$\omega(p, h, E) = \frac{g(gE - A)^{n-1}}{p!h!(n-1)!}, \quad (2)$$

where  $A$  is the correction, which takes the Pauli principle into consideration, which is equal to

$$A = (p^2 + h^2 + p - 3h) / 4.$$

The following expression was used to calculate the nucleon emission velocity:

$$\lambda_c^x = \frac{(2s_x + 1)\mu_x \epsilon_x \sigma_{inv}^x(\epsilon_x)}{\pi^2 \hbar^3 g_x}, \quad (3)$$

where  $s_x$  and  $\mu_x$  are the spin and the reduced mass of the particle of type  $x$ ,  $\sigma_{inv}^x$  is the inverse reaction for the particle under consideration,  $g_x$  is the density of the single particle states that is equal to  $g_n = N/14$  for neutrons and  $g_p = Z/14$  for protons.

The nucleon absorption velocity was calculated with the aid of the formula:

$$\lambda_+^x = V \sigma_0(\epsilon_x) \rho_1 \quad (4)$$

where  $V$  is the nucleon velocity inside of the nucleus,  $\sigma_0$  is the nucleon-nucleon interaction cross section, effectively taking Pauli's principle into consideration [7],  $\rho_1$  is the nuclear matter density. At the initial stage ( $2p1h$ ), the average value of the nuclear density  $\rho_1$ , corresponding to the distance from the centre of the nucleus  $1\lambda < r_1 < (l+1)\lambda$ , was taken for each partial wave and each value of the radius  $r_1$ . For the other exciton states the value of the density was determined by averaging over the volume of the nucleus.

For neutron induced reactions, the  $R_x(n)$  factor in equation (1) was determined as follows:

$$R_n(3) = (Z+2A)/(2Z+A) \quad (5a)$$

$$R_p(n) = 2 - R_x(3) \quad (5b)$$

$$R_x(n) = R_x(3) + (n-3)/4 \quad (5c)$$

In the course of these calculations multiple pre-equilibrium nucleon emission was taken into account. In accordance with reference [6], it was assumed that the number of particles emitted from one and the same exciton state was equal to:

$$P_{np} = P_n P_p \text{ (in the case of the emission of a neutron and a proton)} \quad (6a)$$

$$P_{nn} = P_n P_n / 2 \text{ (in the case of the emission of two neutrons)} \quad (6b)$$

whereby  $P_n$  and  $P_p$  represent the total number of neutrons and protons being emitted by the  $n$ -exciton configuration under consideration. The pre-equilibrium component of the  $(n, n')$ ,  $(n, 2n)$  and  $(n, np)$  were calculated with the aid of the following equations:

$$\sigma^{Z,A}(E_n - \varepsilon) = \frac{C_n}{\sigma_n} \cdot \frac{d\sigma_n(\varepsilon)}{d\varepsilon}, \quad (7a)$$

$$\sigma^{Z,A-1}(E_n + Q_{(n,2n)} - \varepsilon - \bar{\varepsilon}_n) = \frac{C_{nn}/2}{\sigma_{2n}} \cdot \frac{d\sigma_n(\varepsilon)}{d\varepsilon}, \quad (7b)$$

$$\sigma^{Z-1,A-1}(E_n + Q_{(n,np)} - \varepsilon - \bar{\varepsilon}_p) = \frac{C_{np}}{2\sigma_{np}} \left( (1 - V_p/\varepsilon) \cdot \frac{d\sigma_n(\varepsilon)}{d\varepsilon} + \frac{d\sigma_p(\varepsilon)}{d\varepsilon} \right) \quad (7c)$$

where  $Z, A$  are the characteristics of the target nucleus,  $E_n$  is the energy of the initial neutrons,  $Q_{(n,2n)}$  and  $Q_{(n,np)}$  are the energies of the  $(n, 2n)$  and  $(n, np)$  reactions,  $V_p$  is the proton Coulomb potential, where  $C_n$ ,  $C_{nn}$  and  $C_{np}$  are respectively, the cross sections for the emission of a single pre-equilibrium neutrons, the simultaneous emission of two pre-equilibrium neutrons from the same exciton states, and the emission of a neutron and a proton from such states, where  $\sigma_n$  and  $\sigma_{2n}$  are the values of the integrals of the entire pre-equilibrium neutron spectra ( $d\sigma_n/d\varepsilon$ ) in the energy range corresponding to the  $(n, n')$  and  $(n, 2n)$  reactions, and where  $\sigma_{np}$  is the integrated pre-equilibrium spectrum of neutrons ( $d\sigma_n/d\varepsilon$ ) in the energy range from 0 to  $E - B_n - B_p$  respectively, and where  $\bar{\varepsilon}_n$  and  $\bar{\varepsilon}_p$  are the average kinetic energies of the second neutron and proton corresponding to the kinetic energy of the first emitted particle.

### 2.1.2 Pre-equilibrium emission of $\alpha$ -particles

The pre-equilibrium emission of  $\alpha$ -particles was described with the aid of the coalescence model taking the particle pick-up reaction into consideration [8,9], in association with the hybrid exciton model. Calculations of the pre-equilibrium  $\alpha$ -spectra were performed using the following expression:

$$\frac{d\sigma^{\text{pre}}}{d\varepsilon_x} = \sigma_{\text{non}} \sum_{l+m=4} \sum_n F_{l,m}(\varepsilon_\alpha) \cdot \frac{\omega(p-1, h, E - Q_\alpha - \varepsilon_\alpha)}{\omega(p, h, E)} \cdot \frac{\lambda_c^\alpha}{\lambda_c^\alpha + \lambda_+^\alpha} \cdot g_\alpha \cdot D_n, \quad (8)$$

where  $\sigma_{\text{non}}$  is the inelastic cross section for the interaction of incident particles with the nucleus,  $F_{l,m}(\varepsilon_\alpha)$  is the probability for the formation of an  $\alpha$ -particle with energy  $\varepsilon_\alpha$  from  $l$  excited and  $m$  non-excited quasi particles in the nucleus [8], and where  $g_\alpha$  is the density of single particle states for  $\alpha$ -particle.

The  $\alpha$ -particle emission velocity was calculated using the equation:

$$\lambda_c^\alpha = \frac{\mu_\alpha \varepsilon_\alpha \sigma_{mv}^\alpha(\varepsilon_\alpha)}{\pi^2 \hbar^3 g_\alpha}, \quad (9)$$

The  $\alpha$ -particle absorption velocity was calculated using the equation:

$$\lambda_+^\alpha = 2W_{\text{opt}}^\alpha / \hbar \quad (10)$$

In these calculations, the value of  $\sum_{l+m=1} F_{l,m}$  for all nuclei was taken to be equal to 0.41.

Serving as illustration, Fig. 1 shows the cross sections of nuclear reactions which were calculated with the aid of the given approach to describe the non-equilibrium  $\alpha$ -particle spectra, as well as selected experimentally determined excitation functions for the reactions  $^{197}\text{Au}(n,\alpha)^{194}\text{Ir}$  and  $^{98}\text{Mo}(n,\alpha)^{96}\text{Zr}$  which are reasonably well reproduced by calculations taking pre-equilibrium  $\alpha$ -particle emission into consideration. The excitation function of the  $^{202}\text{Hg}(p,2n2p)^{199}\text{Au}$  reaction was taken as an example for high energy incident particle reactions. In this case, it can be seen that the equilibrium component of the  $\alpha$ -particle emission reaction does not reproduce experimentally determined data. The same figure shows the calculated  $\alpha$ -particle spectrum for the  $^{120}\text{Sn}(p,\alpha)$  reaction, in which the hard part of the spectrum is represented by the pre-equilibrium  $\alpha$ -particle emission mechanism.

The comparison of data given in Fig. 1 shows that the use of the given approach to calculate pre-equilibrium  $\alpha$ -particle spectra significantly improves the agreement between calculated and experimental data.

### 2.1.3 Pre-equilibrium emission of deuterons

Deuteron spectra resulting from reactions induced by nucleon having energies between 14.8 and 90 MeV have been analyzed in the framework of the exciton model, coupled with the coalescence model including the pick up reaction mechanism [8,9]. Figure 2 shows the calculated spectrum of deuteron resulting from the irradiation of  $^{54}\text{Fe}$  by 62 MeV protons. It can be seen from this figure that the calculated cross section values differ significantly from the experimental data in the hard part of the spectrum. The variation of the calculation parameters, in particular the imaginary part of the optical potential for deuterons, did not result in a noticeable improvement in the agreement of the calculated differential cross sections with the measured spectra as follows from the comparison of the data given in Figure 2. Analogous results were obtained by using the "closed" form of the exciton model described in reference [9].

The reason for the discrepancy between calculated and experimental data is related to the fact that the calculational procedure does not include the direct channel in the creation of the deuterons which yields, according to reference [10], a noticeable contribution to the differential emission cross section of the particle under consideration.

The contribution of the direct channel to the deuteron creation cross section can be included using a phenomenological approach based on the pre-equilibrium hybrid exciton model. In order to do that, it is necessary to analyze the nucleon pick-up process and the emission of the deuteron from the initial (1p,0h) configuration [11,12]. The formal representation of the differential pre-equilibrium deuteron emission cross section can be written in the form of :

$$\frac{d\sigma^{\text{pre}}}{d\varepsilon_d} = \sigma_{\text{non}} \left\{ \frac{\omega^*(E - Q_d - \varepsilon_d)}{\omega(1p,0h, E)} \cdot \frac{\lambda_c^d}{\lambda_c^d + \lambda_+^d} \cdot g_d + \sum_{n=3} \sum_{l+m=2} F_{l,m}(\varepsilon_d) \cdot \frac{\omega(p-1, h, E - Q_d - \varepsilon_d)}{\omega(p, h, E)} \cdot \frac{\lambda_c^d}{\lambda_c^d + \lambda_+^d} \cdot g_d D_n \right\}, \quad (11)$$

where  $\omega^*(U)$  is the density of the excited nuclear states formed after the emission of the deuteron, and  $g_d$  is the density of the single particle state of the deuteron.

It must be noted that the second term enclosed in the braces of equation (11) describes part of the non-equilibrium deuteron spectrum which is shown in Fig. 2, and computed in ref. [9].

Following the emission of the deuteron, created as a result of the pick-up of the nucleon, the nucleus ends up in the  $(p-1, h+1)$  state. As a result, the density of the terminal states  $\omega$  can be represented by the following equation:

$$\omega^*(U) = \omega(0p, 1h, U) \gamma / g_d , \quad (12)$$

where  $\gamma$  is the quantity which characterizes the process of the deuteron formation.

In as much as the exciton model cannot be expected to give a rigorous description of direct processes, the  $\gamma$  quantity must be arrived at by the superposition of the spectra calculated using equation (11) and experimental data. It must be noted that, the values of empirical quantities in various forms of the exciton model [9,10] describing the emission of composite particles are chosen in an analogous manner.

The superposition of deuteron emission spectra, calculated with the use of equation (11) and experimental data made it possible to ascertain that the  $\gamma$  quantity has a weak dependence on the mass number of the target nucleus, and can be assumed to be constant to a good degree of accuracy.

The resulting deuteron emission spectra, calculated on the basis of the  $\gamma$  quantity which is derived from experimental data, are shown in Figures 3 and 4 for nuclei ranging from C to Au for a variety of incident particle energies. The plots show the contribution of the "semi-direct" component, the pre-equilibrium component corresponding to the deuteron preparation coefficients  $F_{1,1}$  and  $F_{2,0}$  in equation (11), and the equilibrium emission spectrum. The sum of the direct component and the equilibrium spectrum, whose superposition with the total spectrum illustrates the contribution to the deuteron emission spectrum of the  $n>3$  exciton states is shown as well (see equation (11)). The calculations for all nuclei were made for the following parameter values:  $\gamma = 2 \cdot 10^{-3}$ ,  $\sum_{l-\max} F_{ln} = 0.3$ , the value of the imaginary part of the deuteron optical potential parameter as given in reference [6] was taken to be  $W=16$  MeV. As can be seen from Figure 2, the value of the imaginary part of the deuteron optical potential does not affect the contribution of the pre-equilibrium component of the deuteron spectrum to any large extent.

The calculated deuteron spectra from reactions induced by neutrons having an incident energy of 14.8 MeV are shown on Figure 3 together with experimental data for iron, nickel and copper. Because of the absence of higher incident neutron energy data, experimental deuteron spectrum data resulting from proton reactions were used instead. Figure 4 shows calculated deuteron spectra resulting from reactions induced by protons having an initial energy of 62 MeV for a number of target nuclei. Calculated deuteron spectra resulting from 90 MeV proton scattered by  $^{58}\text{Ni}$  are also shown on the same figure. As shown on Figures 3 and 4, the calculated deuteron spectra are in good agreement with experimental data. At the same time, the agreement between the calculated and measured spectra for light nuclei could be improved by taking the dependence of the  $\gamma$  quantity on the mass of the target nucleus into account.

### 2.1.4 The equilibrium emission of particles

The calculation of equilibrium emission spectra was calculated by using the Weisskopf model. At the same time, emission of neutrons, protons, deuterons and  $\alpha$ -particles from excited nuclei was investigated as well.

### 2.1.5 Nuclear level densities

Nuclear level densities were calculated on the basis of the phenomenological description of atomic level densities [13] for all nuclei formed in the evaporation cascade.

In the process of describing level densities of atomic nuclei in the generalized nuclear model, it is possible to separate the excited states into quasi-particulate and coherent collective states. It is then possible to express level densities by the equation:

$$\rho(U) = \rho_{qp}(U') \cdot K_{vib}(U') \cdot K_{rot}(U') \quad (13)$$

where  $\rho_{qp}(U')$  is the density of the quasi-particulate (non-collectivized) state of the nuclear excitation,  $K_{vib}(U')$  and  $K_{rot}(U')$  are the enhanced level density coefficients related to the vibrational and rotational states corresponding to the effective excitation energy  $U'$ .

The energy dependence of the quasi-particulate level density was calculated on the basis of the superfluid model of the nucleus [13], in this connection, the correlation function for the basic state of the nucleus was taken to be equal to  $\Delta_0 = 12.0/A^{1/2}$  MeV. On the average, this choice agrees with the nuclear mass systematics [15] as well as with the results of the analysis of the experimental values of the neutron resonance density of heavy nuclei [14]. The critical temperature of the phase transition from the superfluid to the normal state, the critical energy of the phase transition, the condensation energy, and the effective excitation energy related to the correlation function  $\Delta_0$ :

$$\begin{aligned} t_{cr} &= 0.567 \Delta_0 \\ U_{cr} &= 0.472 a_{cr} \Delta_0^2 - n \Delta_0 \\ E_{con} &= 0.152 a_{cr} \Delta_0^2 - n \Delta_0 \\ U' &= U + n \Delta_0 + \delta_{shift}, \end{aligned} \quad (14)$$

where  $n=0$ ,  $n=1$  and  $n=2$  for the even-even, odd and odd-odd nuclei respectively, the empirical shift  $a$  of the excitation energy  $\delta_{shift}$  was chosen by the simultaneous description of the density of the low-lying collective levels and the neutron resonance data.

Shell effects are included in the analysis on the basis of the phenomenologically selected energy dependence of the level density parameter  $a(U, A)$ :

$$\begin{aligned} a(U, Z, A) &= \tilde{a}(A) \cdot \left( 1 + \delta W(Z, A) \cdot \frac{\varphi(U' - E_{cond})}{U' - E_{cond}} \right), \quad \text{for } U' > U_{cr} \\ a(U, Z, A) &= a(U_{cr}, Z, A), \quad \text{for } U' < U_{cr} \end{aligned} \quad (15)$$

where the asymptotic value of the level density parameter at high energy was chosen according to

$$\tilde{a}(A) = 0.073A + 0.115A^{2/3} \quad (16)$$

$\delta W(Z,A)$  is the shell correction to the nuclear binding energy derived from experimental values of masses or by using the Meyers-Swiatetsky formula [16] if the former was not available, where  $\phi(U) = \{1 - \exp(-\gamma U)\}$  is a dimensionless function which determines energy changes of the level density parameter for low excitation energies and where the quantity  $\gamma = 0.4/A^{1/2}$  is selected according to the description of neutron resonance densities [13].

The vibrational enhancement of the level density can be expressed by:

$$K_{\text{vib}} = \exp\{\delta S - (\delta U/t)\}, \quad (17)$$

where changes in the entropy and excitation energy, related to the collective modes of excitation, can be obtained from the correlation for the Bose particle gas:

$$\begin{aligned} \delta S &= \sum_{i=1}^{\infty} (2\lambda_i + 1) \{ (1 + n_i) \ln(1 + n_i) - n_i \ln(n_i) \} \\ \delta U &= \sum_{i=1}^{\infty} (2\lambda_i + 1) \omega_i n_i, \end{aligned} \quad (18)$$

where  $\omega_i$  and  $\lambda_i$  are the energy and multiplicity of the collective excited state, and  $n_i$  is its population for a given temperature. The reduction of the vibrational enhancement of the level density at high temperatures is taken into account in the expression for level population:

$$n_i = \frac{\exp\{-\gamma_i / (2\omega_i)\}}{\exp\{\omega_i / t\} - 1} \quad (19)$$

with the help of empirically selected simultaneous description of low-lying levels and from neutron resonance parameter data given by  $\gamma_i$ :

$$\gamma_i = 0.0075A^{1/3}(\omega_i^2 + 4\pi^2 t^2) \quad (20)$$

In the calculations, only quadrupole and octopole states were considered; only the lowest level states for all nuclei, with the exception of  $^{208}\text{Pb}$ , were determined by phenomenological expressions which gave reasonable agreement with experimental data:

$$\omega_2 = 30A^{-1/3}; \quad \omega_3 = 50A^{-1/3} \quad (21)$$

The position of the lowest  $2^+$  state of  $^{208}\text{Pb}$  was chosen to be equal to the experimental value of 4.1 MeV.

For all spherical nuclei, only the vibrational level density enhancement coefficient  $K_{\text{vib}}(U')$  was taken into consideration in equation (11). For deformed nuclei, the level density enhancement  $K_{\text{rot}}(U')$ , representing the rotational mode of collective nuclear excitation, is taken into

consideration, which is expressed by [13]:

$$K_{rot}(U) = \sigma_{\perp}^2 g(U) = \sigma^2 (1 + \beta/3) g(U), \quad (22)$$

where  $\sigma$  is the spin cut-off factor, and  $g(U)$  is an empirical function which takes into consideration the quenching of the rotational mode at high temperatures, proposed in reference [17] in the form of:

$$g(U) = \{1 + \exp [(U - U_r)/d_r]\}^{-1}, \quad (23)$$

where the quenching function parameters are related to the nuclear quadrupole deformation parameter  $\beta$ :

$$U_r = 120A^{1/3}\beta^2; \quad d_r = 1400A^{-2/3}\beta^2 \quad (24)$$

The nuclear quadrupole deformation parameter  $\beta$  is determined by the mass formulas given in reference [16].

The advantage of this approach to the calculation of nuclear level densities over others is realized primarily in the calculations of cross sections for magic and near magic nuclei. Figure 5 shows cross sections for the following reactions (p,2n2p), (p,3n2p), (p,4n,2p) and (p,6n4p) for  $^{90}\text{Zr}$ , calculated on the basis that the level densities were determined using the superfluid and the Fermi gas models with a density parameter  $a = A/9.0$ . It can be seen from Figure 5 that the best agreement of the calculated data with the experimental data is obtained by using the superfluid model.

### 2.1.6 Equilibrium emission of gamma quanta

The probability to have a  $\gamma$ -quantum emitted was determined by the following formula:

$$\Gamma_{\gamma}(E) = \frac{1}{\pi \hbar^2 c^2 \rho(E)} \int \epsilon_{\gamma}^2 \alpha_{\gamma}(E - \epsilon_{\gamma}) \rho(E - \epsilon_{\gamma}) d\epsilon_{\gamma}, \quad (25)$$

where  $\sigma_{\gamma}$  is the  $\gamma$ -quantum absorption cross section and  $\rho$  is the nuclear level density.

The photo-absorption cross section was calculated by using the Lorenz formula:

$$\alpha_{\gamma}(\epsilon_{\gamma}) = \sum_{k=1}^2 \frac{\sigma_k \epsilon_{\gamma}^2 \Gamma_{k\gamma}^2}{(\epsilon_{\gamma}^2 - E_{k\gamma}^2)^2 + \epsilon_{\gamma}^2 \Gamma_{k\gamma}^2}, \quad (26)$$

taking into account the spallation/splitting (?) of the giant dipole resonance in deformed nuclei. The location of the giant dipole resonance  $E_{k\gamma}$  maximum, taking the quadrupole deformation of the nucleus  $\beta$ , is determined by:

$$E_{1\gamma} = E_0 (1 - \beta/3)^2; \quad E_{2\gamma} = E_0 (1 - 0.16\beta); \quad E_0 = 43.4A^{-0.215} \quad (27)$$

its width being equal to:  $\Gamma_1 = 0.232E_1$  and  $\Gamma_2 = 0.275E_2$ , and the value of the photo absorption cross section  $\sigma_{k\gamma}$  at its maximum expressed in mb is determined by: (28)

$$\sigma_{1\gamma} = 145A/E_1; \quad \sigma_{2\gamma} = 235A/E_2 \quad (29)$$

were selected from the systematics used in reference [18].

The density of nuclear levels for the gamma channel agrees with the partial channels in context of the superfluid model.

The importance of taking into account the competing gamma ray emission in the calculation of the excitation function of various reactions induced by intermediate energy nucleons on neutron deficient nuclei, in particular  $^{124}\text{Xe}$ , was repeatedly noted in earlier works described in reference [19]. Only by taking into account the competition of gamma rays together with particles is it possible to avoid the appearance of sharp “non-physical” peaks in the near-threshold region of calculated excitation functions of proton induced reactions, namely:  $^{124}\text{Xe}(p,pn)^{123}\text{Xe}$ ,  $^{126}\text{Xe}(p,pn)^{125}\text{Xe}$ , and  $^{126}\text{Xe}(p,2np)^{124}\text{Xe}$  (see upper part of Figure 6). The solid curves represent results of calculations with the inclusion of competing gamma rays, the dotted curves represent the results of analogous calculations without the competing gamma rays. The experimental data for the proton induced reactions were taken from references [27,28,29] for  $^{124}\text{Xe}$ , and from reference [30] for  $^{126}\text{Xe}$ . In many cases the inclusion of competing gamma rays leads only to a change of the effective reaction threshold, and does not alter substantially the energy dependence of the excitation function. Results of analogous calculations of the excitation functions for neutron induced reactions in  $^{93}\text{Mo}$  are shown in the lower part of Figure 6. Experimental data for the  $^{95}\text{Mo}$  nuclide were taken from the EXFOR data library. From the data presented here, it can be seen that the calculations performed with the modified ALICE-92 computational program using a consistent choice of level densities in particle and  $\gamma$ -channels, are in reasonable agreement with the experimental data.

### 2.1.7 Calculation of inelastic interaction and reverse reaction cross sections

The calculations of the reaction cross sections were performed with the aid of the optical model. The parameters used in these calculations for the optical potential for neutrons, protons, deuterons and  $\alpha$ -particles are listed in Table I.

### 2.1.8 The performance of numerical calculations

The numerical calculations were performed using the modified ALICE-92 computational program. The algorithm of this program was altered for the calculation of nuclear level densities based on the superfluid model [13], and for the calculation of the pre-equilibrium spectra from complex particles on the basis of the coalescence model including the particle pick-up reaction [8,9].

In addition, the following alterations were incorporated in the program:

1. The calculation of the level densities in the framework of the generalized superfluid model [17]. Using this approach, comparison of calculated excitation functions for various reactions

in the energy range up to 100 MeV reactions, with experimental data shows a better agreement than with using assorted modifications of the Fermi-gas model.

2. This version of the program makes it possible to take into account the pre-equilibrium mechanism in the emission of deuterons and  $\alpha$ -particles. The calculation of the pre-equilibrium emission of  $\alpha$ -particles was executed in the framework of the coalescence pick-up model [8] and the hybrid exciton model. The calculations of the non-equilibrium component of the deuteron spectra included the direct processes in the framework of the phenomenological model described in Section 2.1.3. The calculation of excitation function with the emission of complex particles were compared with the available experimental data for incident nucleon energies up to 100 MeV.

3. The elimination of the uncertainty in the calculation of the second pre-equilibrium particle emission. In the calculations of the simultaneously emission of two particles in the pre-equilibrium process in the (n,np) and (p,np) reactions in conformity with equation 7c, the correction related to the Coulomb barrier in the proton pick-up coefficients  $(1-V_0/\omega)$  is taken into account.

4. At energies larger than 100 Me, the data of Barashenkov [20] derived from the analysis of experimental data and theoretical considerations were used in the determination of total neutron and proton induced reaction cross sections.

5. The corrected neutron optical potential parameters were used to achieve the agreement between calculational results and evaluated (BROND-2, ENDF/B-VI, JENDL-3) and experimental reaction cross section data for heavy nuclei ( $A>230$ ).

6. The error which arises in the calculation of the reaction cross section, taking the gamma quantum emission from the residual nucleus into account, was corrected. (This error arises as a result of the incorrect accounting of the contribution of gamma quanta emitted by the residual nuclei  ${}_Z X^{A-1}$  or  ${}_{Z-1} X^{A-1}$  in the course of calculating the reaction cross section with the formation of the residual nucleus  ${}_Z X^A$ ).

### 2.1.9 Examples of cross section calculations

Nuclear reaction cross sections were calculated using one set of calculation model parameters. In those cases where the calculated cross sections were not in agreement with the experimental neutron cross section data for energies up to 20 MeV, the calculational results were adjusted so as to achieve agreement with the calculational results.

Typical examples of discrepancies between experimental data and cross section values calculated with the aid of a single set of calculational parameters are illustrated in Figs. 7-13. These figures show the results of calculations for neutron and proton induced cross sections for a number of nuclides. Cross sections for the (n,p), (n, $\alpha$ ) and (n,2n) reactions are given on Figs. 7-12, and proton induced reaction cross sections for nuclides having secondary particles having numbers  $X>3$  are shown in Fig.13. Experimental neutron induced reaction cross section data were taken from the EXFOR data library, and proton induced reactions were taken from experiments described in the first version of MENDL [4].

**Table 1. Optical potential parameters used in cross section calculations**

Parameter	Neutrons	Protons	Deuterons	$\alpha$ -particles
Real part V (MeV)	48.0	60.0	$79.0+2Z/A^{1/2}$	50.2
Imaginary part W (MeV)	9.0	5.0	16.0	12.3
Type W	surface	volume	surface	volume
Spin-orbital potential $V_{ls}$ (MeV)	7.0	7.5	5.6	0.001
Radius $r_v$ (fm)	$1.151+1.77(A-2Z)/A^{4/3}$	1.2	1.15	$1.2+1.5/A^{1/2}$
$r_w$	$r_v$	1.55	$1.01+1.26/A$	$r_v$
$r_{so}$	$r_v$	1.25	0.98	1.00
Coulomb radius (fm)		1.25	1.3	1.3
Difusivity $a_v$ (fm)	0.66	0.60	0.81	0.564
$a_w$	0.64	0.50	0.68	0.564
$a_{so}$	0.64	0.51	1.00	1.000

## 2.2 Semiempirical evaluation of cross sections

In the case of stable nuclides, the adjustment of the calculated cross sections was made on the basis of available experimental data and systematics. In most cases the calculated quantities were normalized to the known cross section value at 14.5 MeV.

The cross section normalization procedure was performed simultaneously for the (n,p), (n, $\alpha$ ), (n,2n) and (n,np) reaction cross sections. The data used for the normalization of the (n,p), (n, $\alpha$ ) and (n,2n) reactions cross sections was taken from the EXFOR data library and the compilation published in reference [21]. The 14.5 MeV cross section values used in this process were taken from references [22 and 23]; these cross sections were evaluated on the basis of experimental data and the systematical dependence of the cross section on the number of neutrons and protons in the nuclei. The following empirical equation was used to determine the (n,p) reaction cross section at 14.5 MeV:

$$\sigma_{np} = \pi r_0^2 (A^{1/3} + 1)^2 \left\{ A^{1.07} [1.1935S^2 - 0.8(S + 0.12906)]^3 + 0.41066 \exp(-233.0S^2 + 0.027613S) \right\} \quad (30)$$

where  $r_0 = 1.3$  fm,  $S=(N-Z+1)/A$ .

Equation (30) was derived from 156 experimental data sets which are given in reference [22]. It includes the contributions of pre-equilibrium (the first term within the braces) and the equilibrium (second term) mechanisms of the (n,p) reaction at 14.5 MeV. As can be gleaned from Table 2, equation (30) appears to give the best approximation of the experimental data, yielding a best  $\chi^2$  value.

In the case of the (n,np) reaction at 14.5 MeV, the systematic derived in reference [24] as well as the cross sections evaluated in that work on the basis of experimental data, were used in the normalization.

Figure 14 shows an example of the adjustment made to the calculated cross sections for the  $^{56}\text{Fe}$  and  $^{58}\text{Ni}$  nuclides. The calculated cross section values for all reactions given in Figure 14, were normalized to the cross section value at 14.5 MeV obtained as a result of processing data from various measurements.

**Table 2. Results derived from 156 experimental (n,p) reaction data sets [22] using various approximation**

Formula	$\Sigma(\sigma_i^{\text{exp}} - \sigma_i^{\text{calc}})^2 / (\Delta\sigma_i^{\text{exp}})^2$	$\chi^2$	Reference
(30)	441.71	2.96	Present
Forrest	474.28	3.12	[22,24]
Bychkov et al.	588.68	3.87	[22,25]
Ait-Tahar	756.50	4.91	[26]

### 3. Format of the Data Stored in the MENDL Data Library

Data in the MENDL data library are stored in the ENDF-6 format. The information is stored in the MF=1 and MF=3 files. The MF=1 file contains general information and the detailed description of the reactions stored in the M=3 file, and the M=3 file contains the numerical reaction cross sections. Standard numerical designators, which are described in more detail in the M=1 file, are used for the storage of the data for each of the nuclides.

#### 3.1 Catalog of the MENDL data library

The catalog of the MENDL library contains the following information. Records which start with the symbol \* contain the target nucleus parameters: the atomic number, the chemical symbol, the mass number, the half life and the designating number of the reaction whose data are included in the file. The record which contains the description of the reaction contains:

- the atomic number Z,
- the chemical symbol of the element and the mass number A of the target nucleus,
- the type of reaction, which are represented in the form of "(n,X)" assumed to be the sum of all reactions leading to the given residual nucleus without taking decay chain

- of the latter into account;
- Z, the chemical symbol and the mass number A of the daughter nuclide;
- half life (lifetime) using the symbols "S, M, H, D, Y" representing seconds, minutes, hours, days and years respectively;
- the number of energy data points for which data of a given reaction is given in the library;
- minimum reaction energy Q (threshold reaction in the laboratory system) for the given resulting nucleus;
- designation of the primary source of cross section data included in the library.

### EXAMPLE

13-Al-26 (NIX) 11-Na-22 2.60E+00Y 68 -9.450E+00 Original
--

**Notation:**

13-Al-26	target nucleus aluminium isotope having mass number A=26
(NIX)	sum of reaction cross sections (n,n $\alpha$ ) and (n,3n2p)
11-Na-22	resulting nucleus in the sodium reaction isotope with mass A=22
2.60E+00Y	Half life of 11-Na-22 = 2.6 years
68	number of energy data points for which reaction cross sections are given
-9.450E+00	value of the Q reaction energy for the (n,n $\alpha$ ) reaction
original	the given cross section data were obtained by the authors.

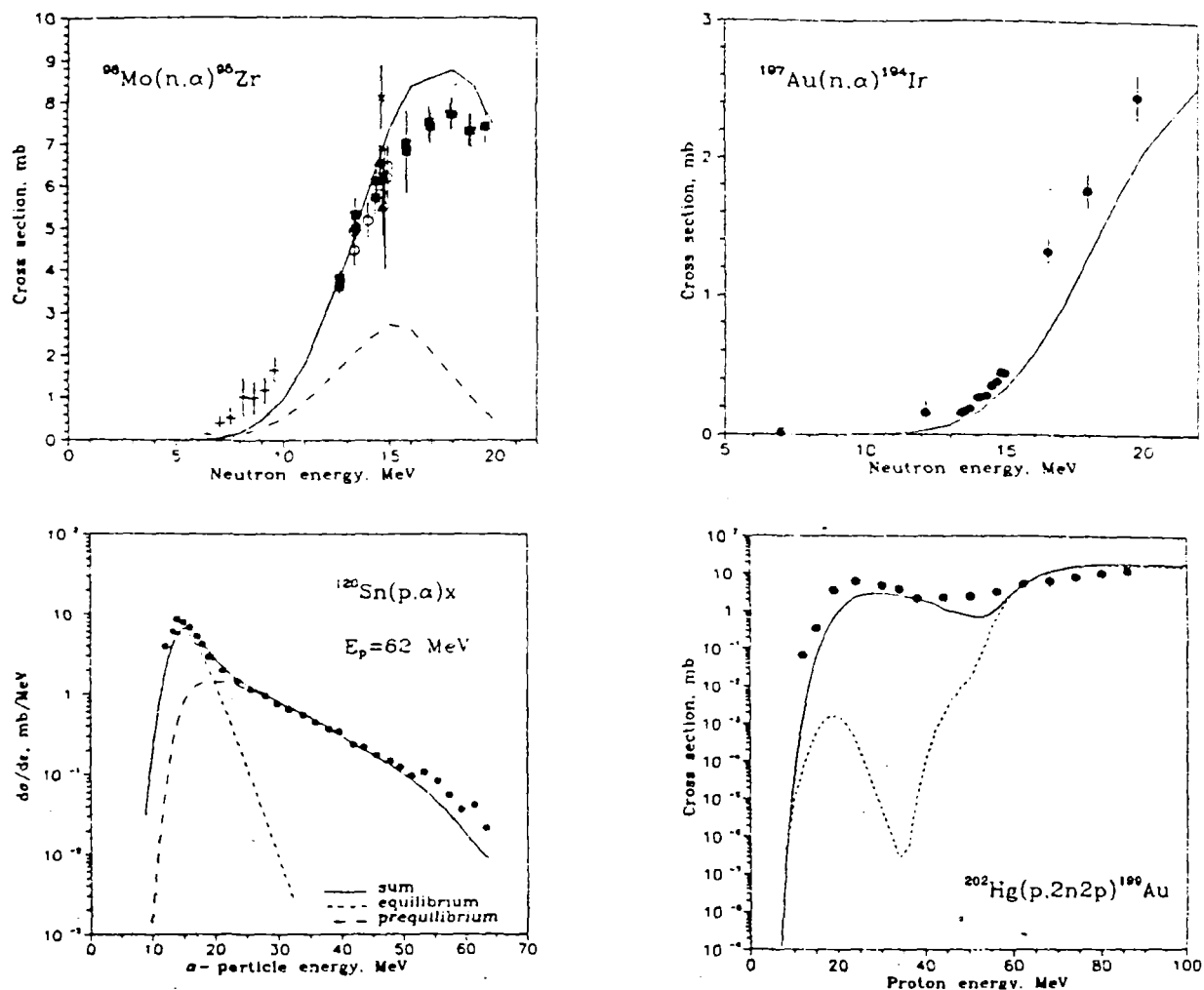


**Figure 1.** Experimental data and calculated curves on the pre-equilibrium emission of  $\alpha$ -particles. For the  $^{197}\text{Au}(n,\alpha)$  reaction, the solid curve represents the sum of equilibrium and pre-equilibrium reaction mechanism contributions. For the proton induced  $^{202}\text{Hg}(p,2n2p)^{197}\text{Au}$  and neutron induced  $^{98}\text{Mo}(n,\alpha)^{95}\text{Zr}$  reactions, the dashed curve represents the equilibrium mechanism contribution. The  $\alpha$ -particle spectrum is given for the  $^{120}\text{Sn}(p,\alpha)$  reaction (the long dashed curve represents the pre-equilibrium contribution, the solid curve represents the sum of the equilibrium and pre-equilibrium processes). The difference between the curves is determined completely by the pre-equilibrium  $\alpha$ -particle emission.

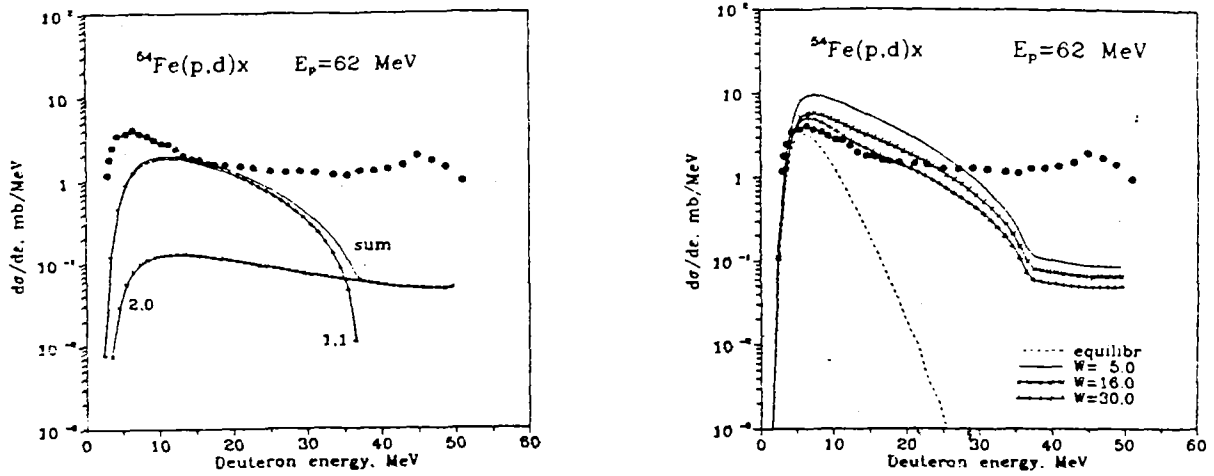


Figure 2. Deuteron emission spectra calculated without the the contribution of the direct reaction mechanism. The calculated contributions of the pre-equilibrium components of the deuteron emission from the  $F_{1,1}$  and  $F_{2,0}$  configuration [9] are given in the figures.

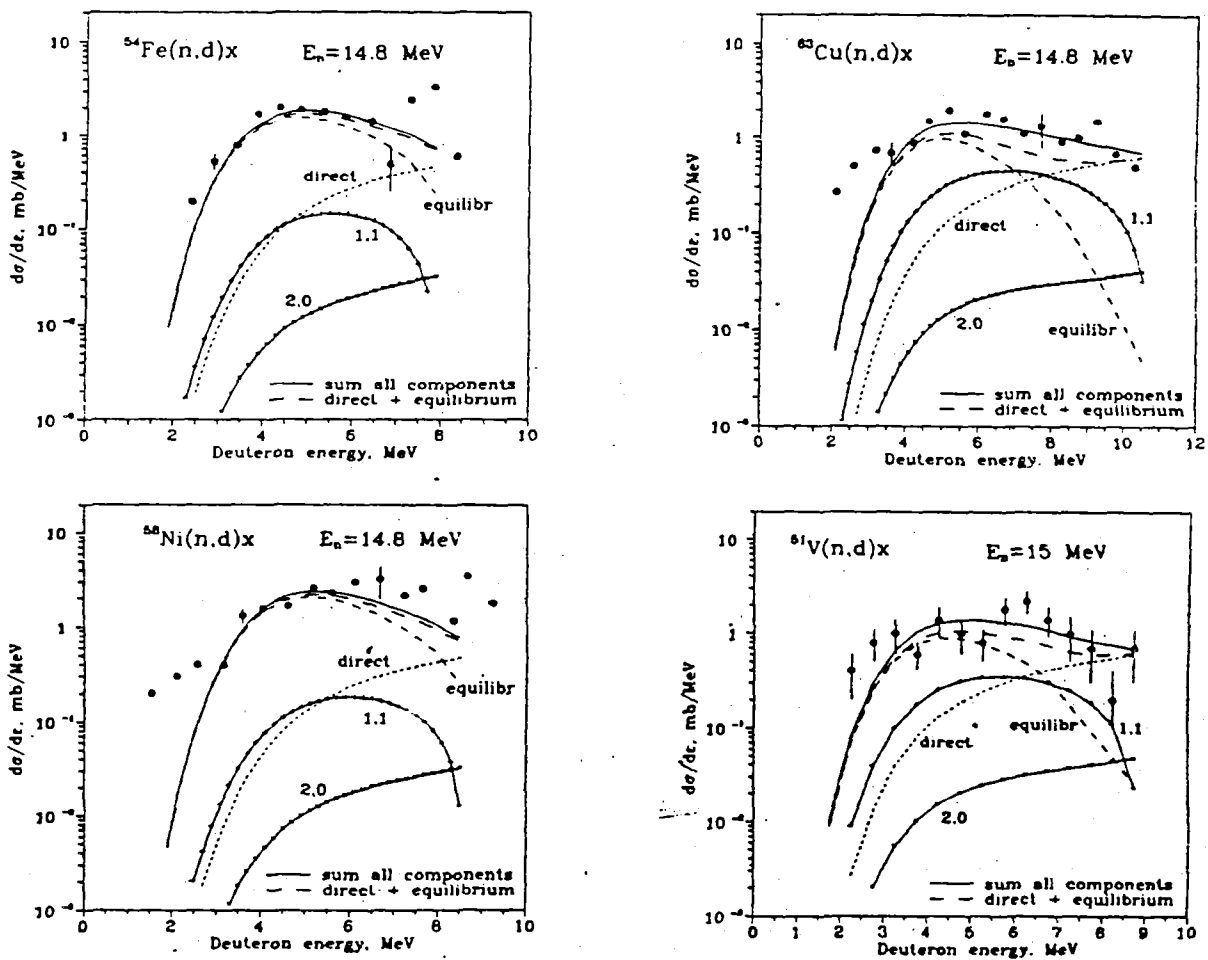


Figure 3. Deuteron spectra from neutron induced reactions with an initial energy of 14.8 MeV. The contributions of the direct,  $F_{1,1}$  and  $F_{2,0}$  pre-equilibrium and equilibrium processes are given in the figures.

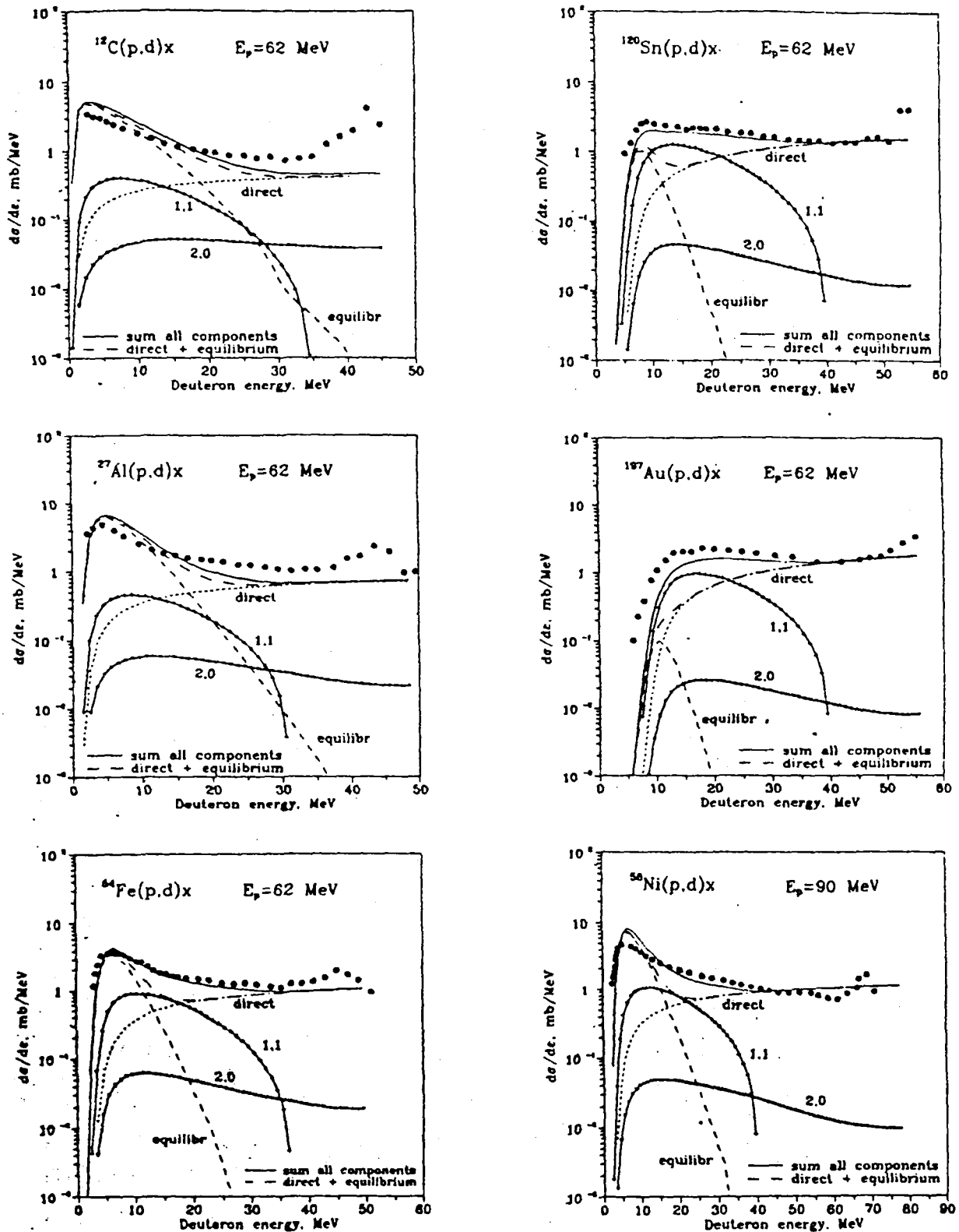
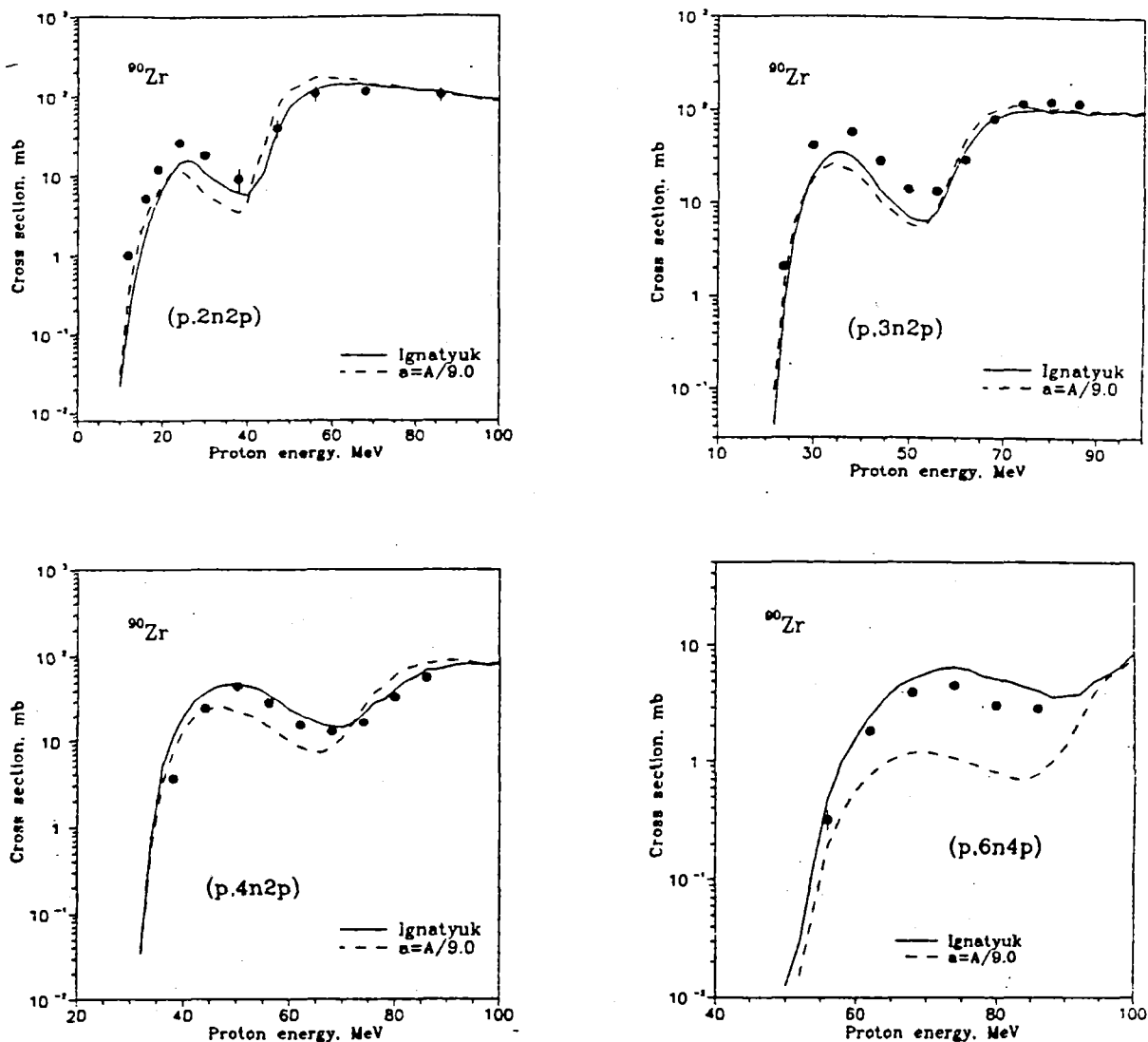
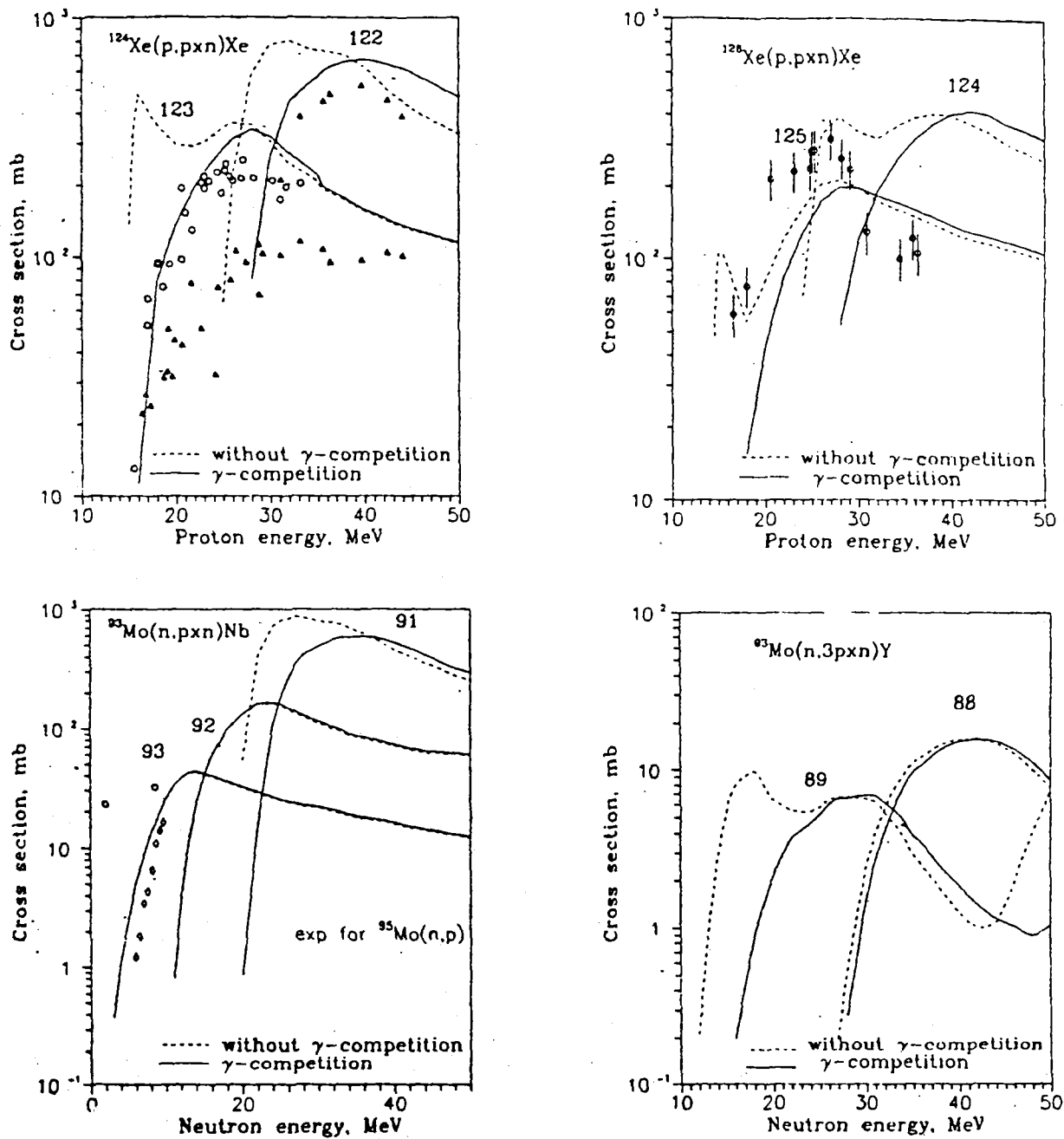


Figure 4. Comparison of calculated and experimental deuteron spectra from proton induced reactions at intermediate energies. The contributions of various reaction mechanisms are shown in the figures.



**Figure 5.** Influence of various models to calculate level densities on the excitation function of proton induced reactions. The dashed curve represents calculations based on the Fermi gas model using the parameter ( $a=A/9$ ), the solid curve represents calculational results based on the generalized superfluid model.



**Figure 6.** Influence of the competing effect of gamma rays on the calculation of excitation functions for the  $^{124}\text{Xe}(p,pxn)\text{Xe}$  and  $^{126}\text{Xe}(p,pxn)\text{Xe}$  proton induced reactions (upper part of the illustration) and the  $^{93}\text{Mo}(n,pxn)\text{Nb}$ , the  $^{93}\text{Mo}(n,3p2n)^{89}\text{Y}$  and the  $^{93}\text{Mo}(n,3p3n)^{88}\text{Y}$  neutron induced reactions (lower part of the illustration).

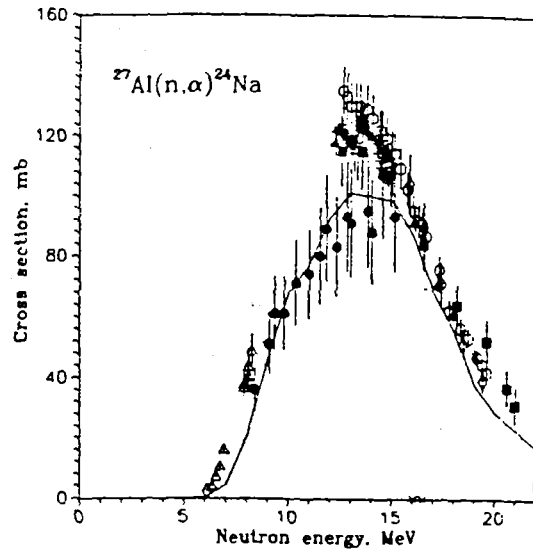
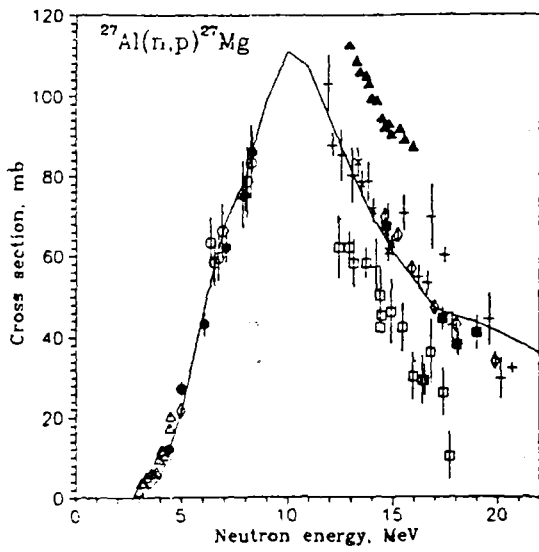


Figure 7. Neutron induced  $^{27}\text{Al}$  reaction cross section calculated with the aid of a global set of parameters for the  $^{27}\text{Al}(n,p)^{27}\text{Mg}$  and the  $^{27}\text{Al}(n,\alpha)^{24}\text{Na}$  reactions.

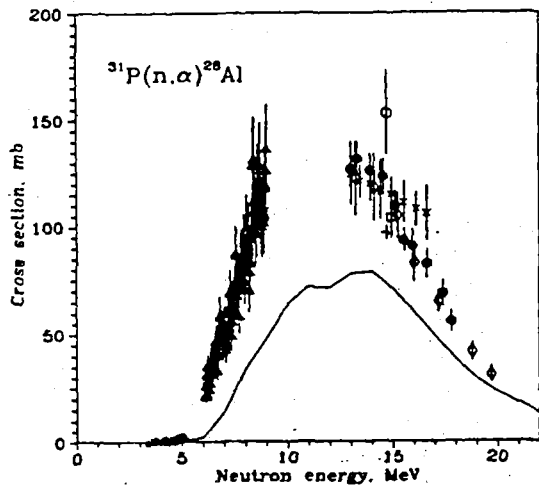
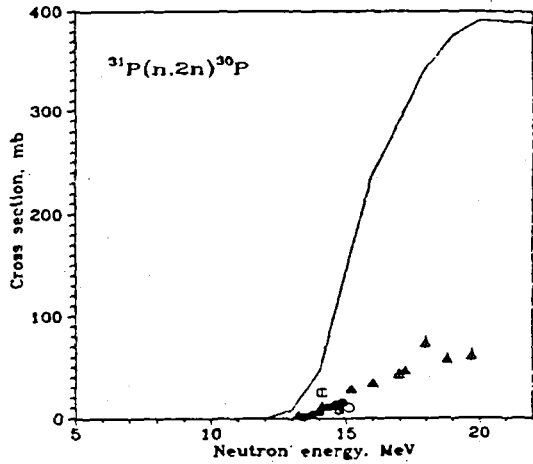
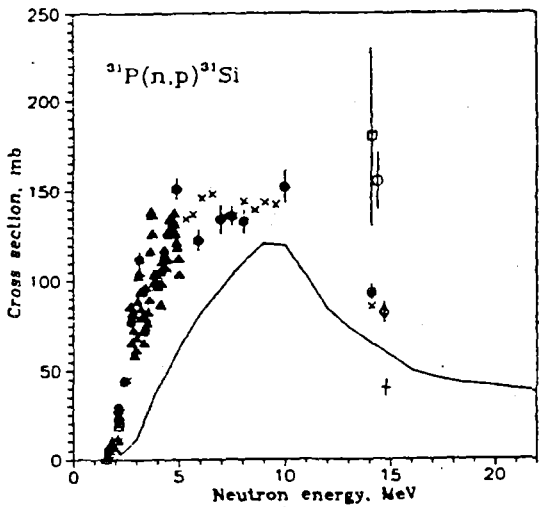


Figure 8. Calculations of various neutron induced reactions for the  $^{31}\text{P}$  nuclide with the use of a global set of parameters.

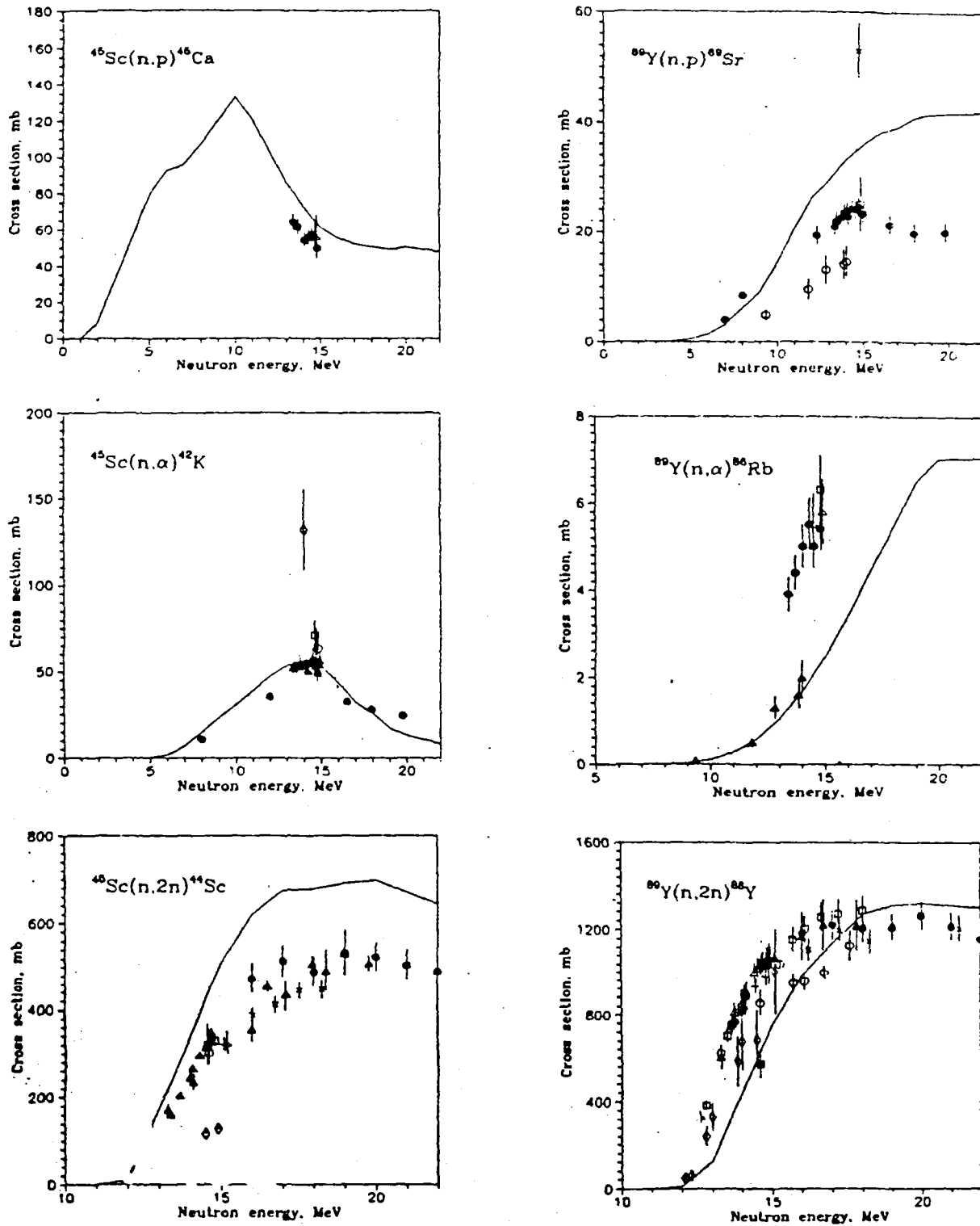


Figure 9. Calculational results of various neutron induced reactions for the  $^{45}\text{Sc}$  and the  $^{89}\text{Y}$  nuclides with the use of a global set of parameters.

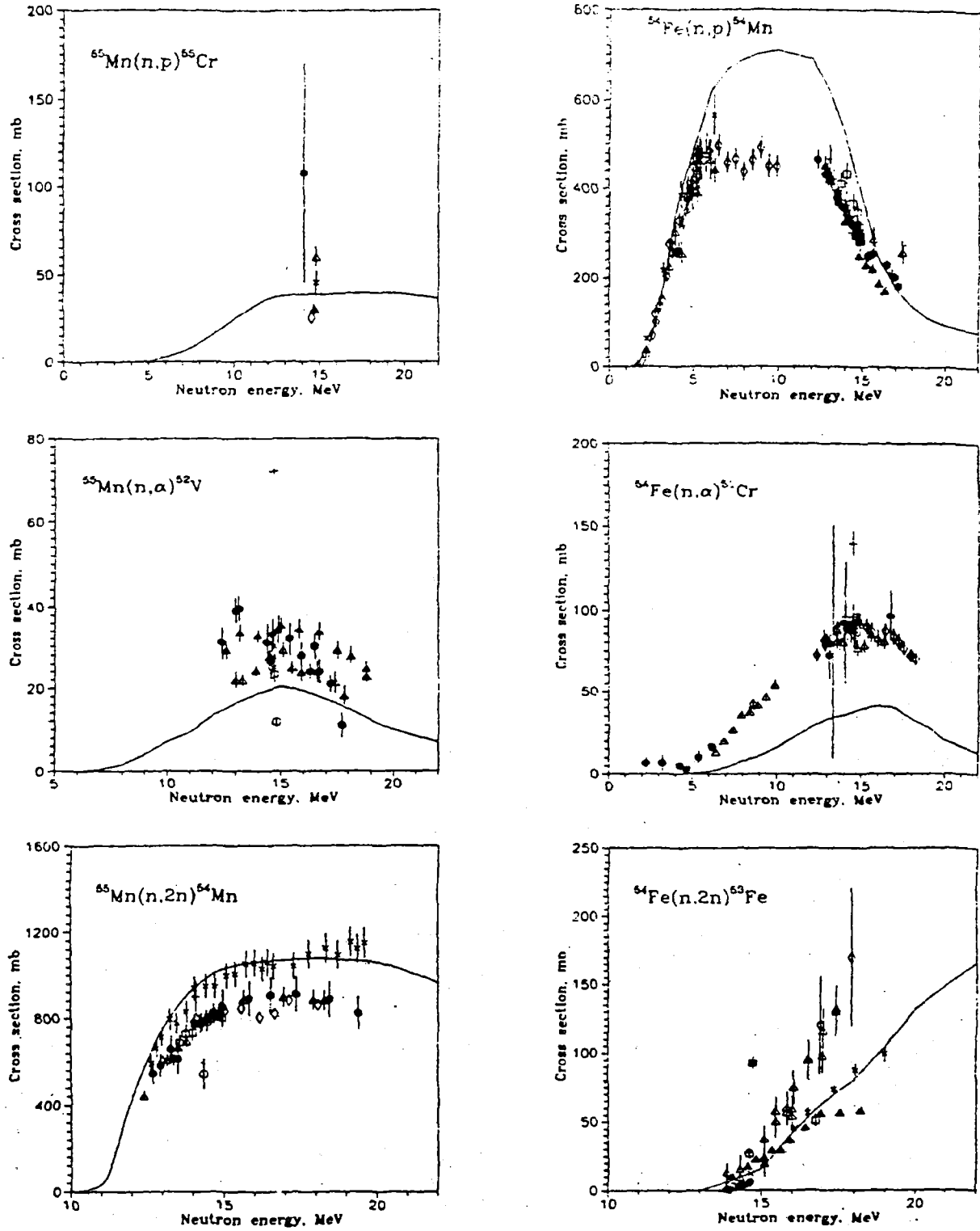


Figure 10. Calculational results of various neutron induced reactions for the  $^{55}\text{Mn}$  and the  $^{54}\text{Fe}$  nuclides with the use of a global set of parameters.

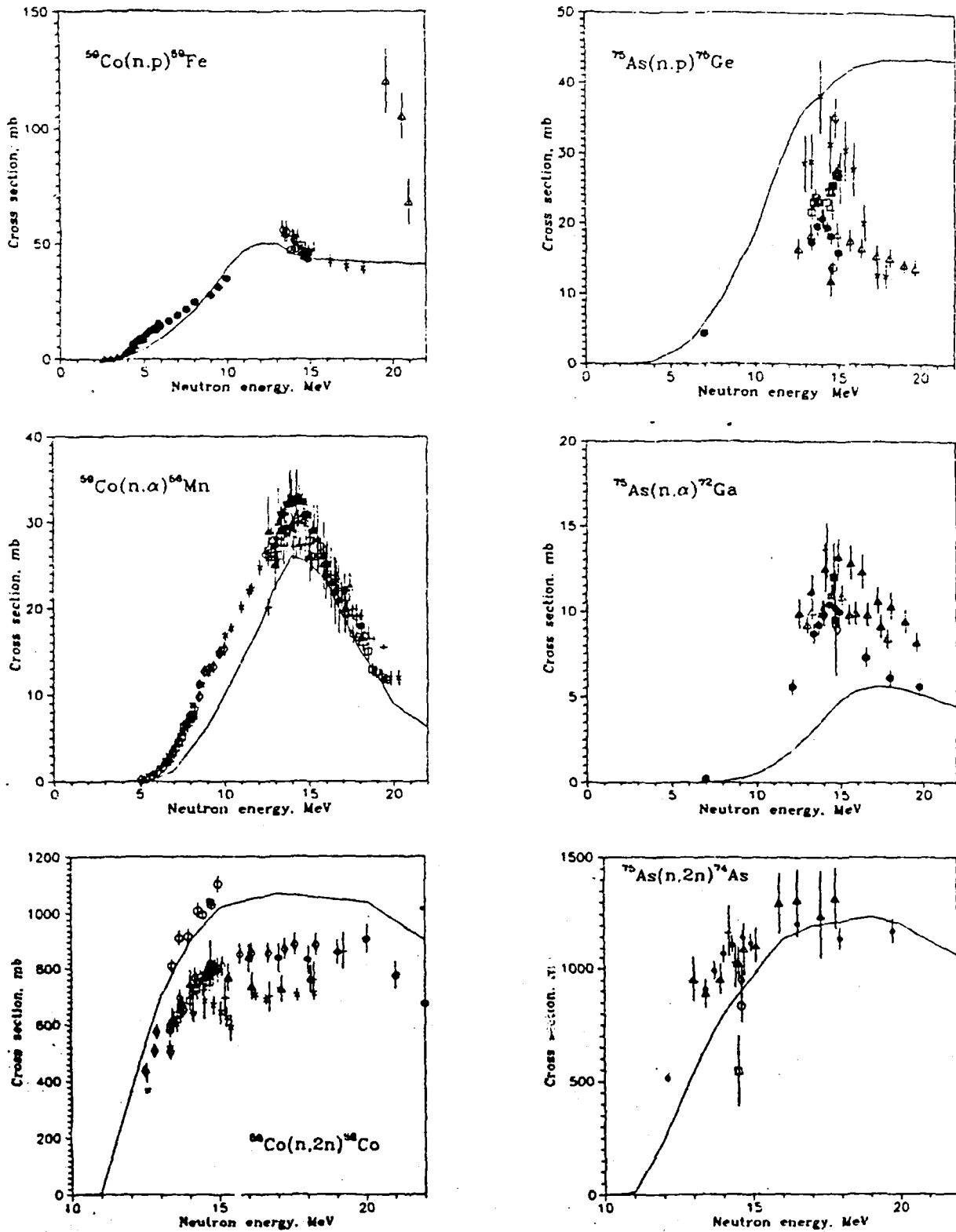


Figure 11. Calculational results of various neutron induced reactions for the  $^{59}\text{Co}$  and the  $^{75}\text{As}$  nuclides with the use of a global set of parameters.

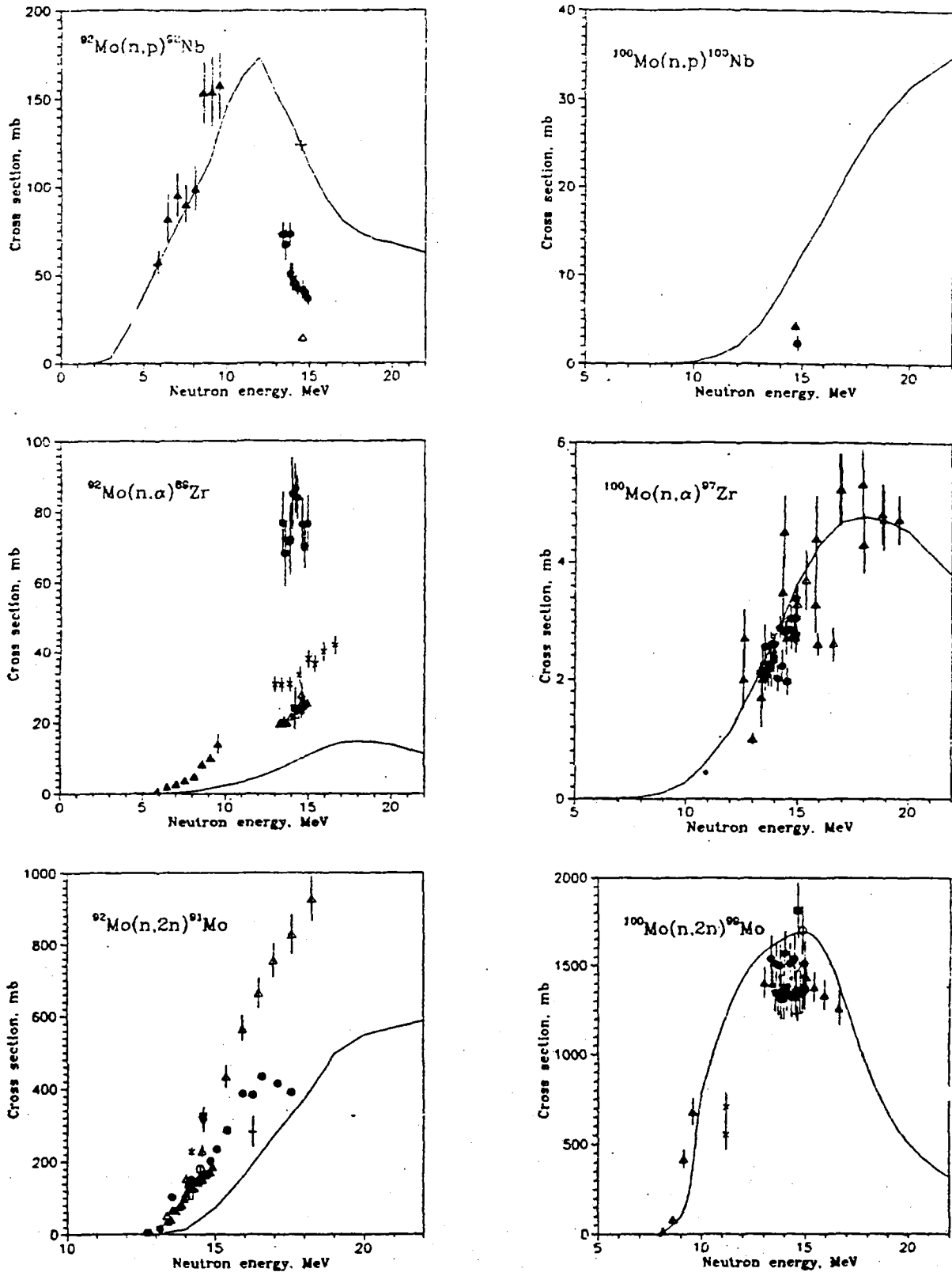


Figure 12. Calculational results of various neutron induced reactions for the  $^{92}\text{Mo}$  and the  $^{100}\text{Mo}$  nuclides with the use of a global set of parameters. In the case of the  $^{92}\text{Mo}(n,p)$  reaction, the illustration shows the experimental data and the value of the reaction cross section derived from the systematics ("+" ) corresponding to equation (30).

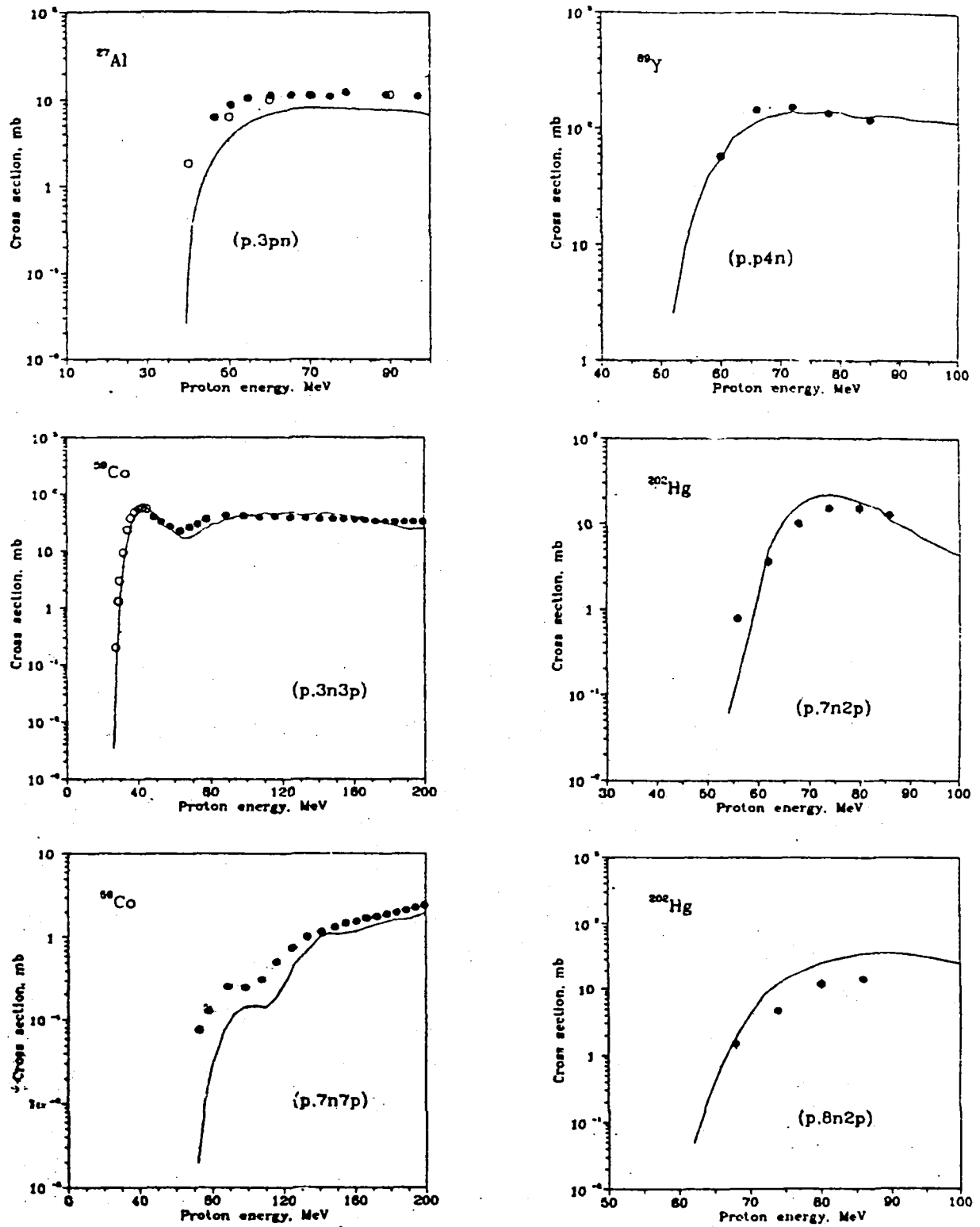


Figure 13. Calculational results of proton induced reactions at intermediate energies obtained with the use of a global set of parameters compared with experimental data.

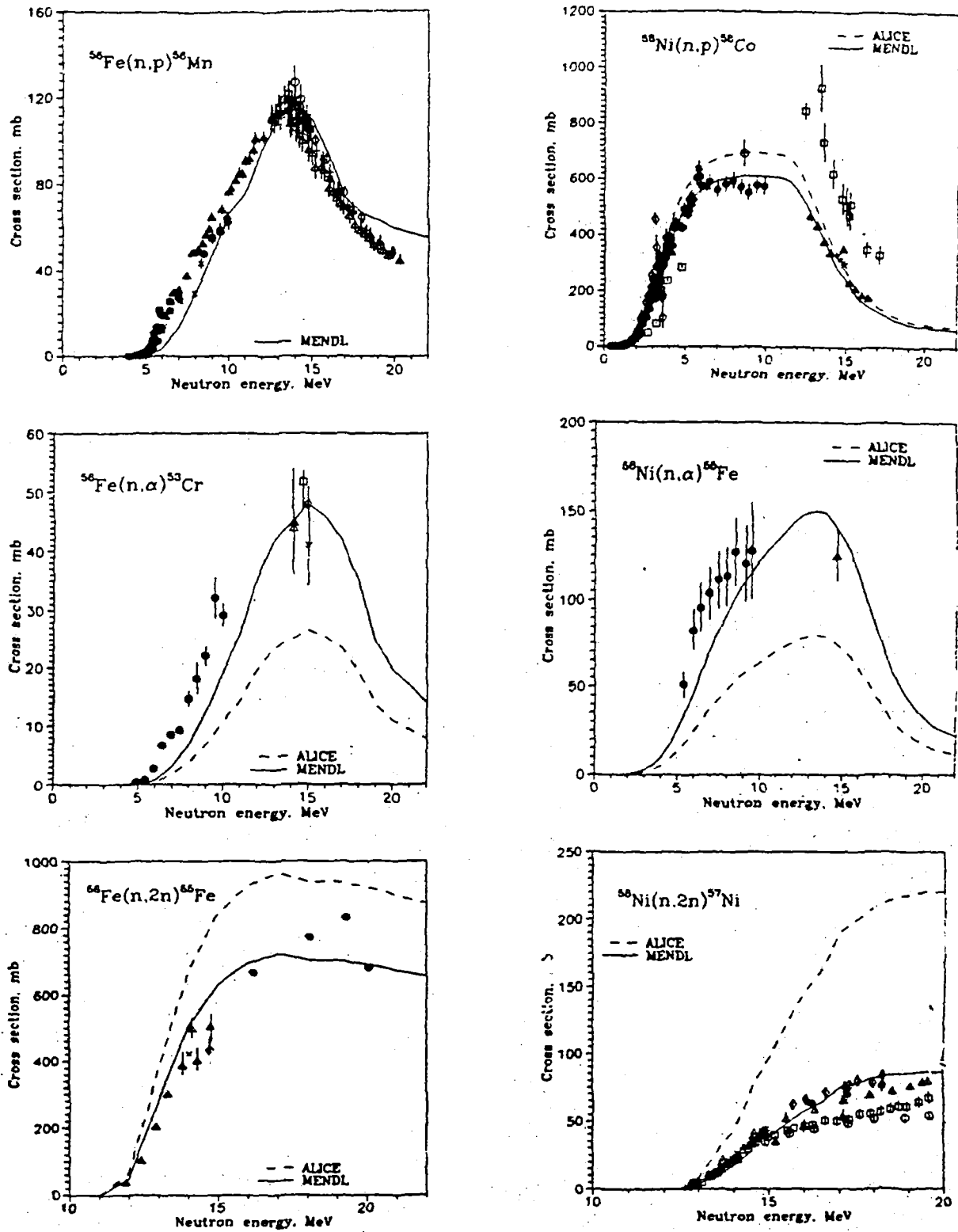


Figure 14. Example of the adjustment of the neutron induced excitation function for the (n,p), (n, $\alpha$ ) and (n,2n) reactions of the  $^{56}\text{Fe}$  and  $^{58}\text{Ni}$  nuclides with the use of experimental data. The solid curves represent data from the MENDL-2 data library.

CONTENT

(The total content of the library is stored in a special file)

Target		Half-life		Number of reactions		
*13-Al-26	unstable		7.205E+05Y	74 reactions		
Target	Reaction	Product	Half-life	Points	Q-value	Comments
13-Al-26	(N,2N)	13-Al-25	7.18E+00S	67	-1.137E+01	Original
13-Al-26	(N,3N)	13-Al-24	2.07E+00S	47	-2.830E+01	Original
13-Al-26	(N,4N)	13-Al-23	4.70E-01S	31	-4.319E+01	Original
13-Al-26	(N,5N)	13-Al-22	7.00E-02S	18	-6.253E+01	Original
13-Al-26	(N,6N)	13-Al-21	short	10	-7.813E+01	Original
13-Al-26	(N,P)	12-Mg-26	stable	90	4.786E+00	Original
13-Al-26	(N,X)	12-Mg-25	stable	81	-4.082E+00	Original
13-Al-26	(N,X)	12-Mg-24	stable	65	-1.141E+01	Original
13-Al-26	(N,X)	12-Mg-23	1.13E+01S	46	-2.794E+01	Original
13-Al-26	(N,X)	12-Mg-22	3.86E+01S	32	-4.109E+01	Original
13-Al-26	(N,X)	12-Mg-21	1.23E-01S	19	-6.047E+01	Original
13-Al-26	(N,X)	12-Mg-20	9.50E-02S	11	-7.419E+01	Original
13-Al-26	(N,2P)	11-Na-25	5.96E+01S	70	-9.358E+00	Original
13-Al-26	(N,X)	11-Na-24	1.50E+01H	58	-1.614E+01	Original
13-Al-26	(N,X)	11-Na-23	stable	90	2.968E+00	Original
13-Al-26	(N,X)	11-Na-22	2.60E+00Y	68	-9.450E+00	Original
13-Al-26	(N,X)	11-Na-21	2.25E+01S	53	-2.052E+01	Original
13-Al-26	(N,X)	11-Na-20	4.46E-01S	35	-3.762E+01	Original
13-Al-26	(N,X)	11-Na-19	3.00E-02S	24	-5.178E+01	Original
13-Al-26	(N,X)	11-Na-18	short	12	-7.353E+01	Original
13-Al-26	(N,X)	11-Na-17	short	3	-9.166E+01	Original
13-Al-26	(N,3P)	10-Ne-24	3.38E+00M	53	-2.006E+01	Original
13-Al-26	(N,X)	10-Ne-23	3.72E+01S	46	-2.670E+01	Original
13-Al-26	(N,X)	10-Ne-22	stable	73	-5.826E+00	Original
13-Al-26	(N,X)	10-Ne-21	stable	59	-1.396E+01	Original
13-Al-26	(N,X)	10-Ne-20	stable	52	-2.072E+01	Original
13-Al-26	(N,X)	10-Ne-19	1.77E+01S	34	-3.759E+01	Original
13-Al-26	(N,X)	10-Ne-18	1.67E+00S	24	-4.923E+01	Original
13-Al-26	(N,X)	10-Ne-17	short	15	-6.846E+01	Original
13-Al-26	(N,X)	10-Ne-16	short	6	-8.611E+01	Original

## References

- [1] MANN, F.M., Transmutation of Alloys in the MFE Facilities as Calculated by REAC (A Computer System for Activation and Transmutation), Report HEDL-TME 81-37 (1982).
- [2] KOPECKE, J., NIEROP, D., Report ECN-1-91-053 (1991).
- [3] GRUDZEVICH, O.T., et al., Catalog of the ADL-3 data library. Problems in Nuclear Science and Technology, Series: Nuclear Constants, No.3-4 (1993). [in Russian].
- [4] KONOBEV, A.Yu., et al., Cross section library for the study of the transmutation and activation of materials irradiated by neutrons and protons up to 100 MeV. Problems in Nuclear Science and Technology, Series: Nuclear Constants No.3-4 (1992) 55 [in Russian].
- SHUBIN, Yu.N., et al., MENDL Activation Data Library for Intermediate Energies. Report IAEA-NDS-136, Rev.0 (1994).
- [5] BLANN M., Importance of the Nuclear Density Distribution on Pre-equilibrium Decay, Phys. Rev. Lett. 28 (1972) 757.
- [6] BLANN, M., VONACH H.K., Global Test of Modified Precompound Decay Models, Phys. Rev. C28 (1983) 1475.
- [7] KIKUCHI, K., KAWAI, M., Nuclear Matter and Nuclear Interactions. North Holland, Amsterdam (1968).
- [8] IWAMOTO, A., HARADA, K., Mechanism of Cluster Emission in Nucleon-induced Pre-equilibrium Reactions. Phys. Rev. C26 (1982) 1821.
- [9] SATO, N., IWAMOTO, A., HARADA, K., Pre-equilibrium Emission of Light Composite Particles in the Framework of the Exciton Model. Phys. Rev. C28 (1983) 1527.
- [10] GADIOLI, E., Emission of Complex Particles in Pre-compound Reactions, Rep. INFN/BE-88-2, Istituto Nazionale di Fisica Nucleare, Milano (1988).
- [11] DOBES, J., BETAK, E., Proc. Int. Conf. React. Models 77, Balatonfured (1977) 195.
- [12] KALBACH, C., The Griffin Model, Complex Particles and Direct Nuclear Reactions, Z. Physik A283 (1977) 401.
- [13] IGNATYUK, A.V., Contribution to the Collective Motion in the Density of Excited Nuclear States, Jadernaya Fizika 21 (1975) 401. [in Russian].
- BLOKHIN, A.I., IGNATYUK, A.V., et al., The Analysis of the Excitation Function of Threshold Reactions in the Generalized Superfluid Model, Izv. Akad. Nauk USSR, Series: Physics 49 (1985) 962. [in Russian].

- BLOKHIN, A.I., IGNATYUK, A.V., SHUBIN, YU.N., Vibrational Enhancement of the Level Density of the Iron Nuclei, *Jadernaya Fizika* **48** (1988) 371 [in Russian].
- IGNATYUK, A.V., et al., Density of Discrete Levels in  $^{116}\text{Sn}$ . *Phys. Rev.* **C47** (1993) 1504.
- [14] IGNATYUK, A.V., ISTEKOV, K.K., SMIRENKIN, G.N., The Role of Collective Effects in the Systematics of Nuclear Level Densities, *Jadernaya Fizika* **29** (1979) 875 [in Russian].
- [15] MEYERS, W.D., *Droplet Model of Atomic Nuclei*, IFI/Plenum Press, New York (1977).
- [16] MEYERS, W.D., SWIATECKI, W.J., Anomalies in Nuclear Masses., *Ark. Fys.* **36** (1967) 343.
- [17] HANSEN, G., JENSEN, A.S., Energy dependence of the Rotational Enhancement Factor in the Level Density, *Nucl. Phys.* **A406** (1983) 236.
- [18] BLANN, M., REFFO, G., FABRY, F., Calculation of  $\gamma$ -ray Cascades in the ALICE Code, Proc. Meeting on the Methods for the Calculation of Neutron Nuclear Data, Bologna (1986) 107.
- [19] SHUBIN, Yu.N., in IAEA report, Proc. IAEA Advisory Group Meeting on Intermediate Energy Nuclear Data for Applications, Vienna (1990).
- LUNEV, V.P., et al., An Analysis of Reaction Cross Section Computational Methods for the Production of Medical Radioisotopes. Proc. Int. Conf., on Nuclear Data for Science and Technology, Juelich (1991) 609.
- BLANN, M., et al., Effect of Gamma Emission Competition on the Excitation Function Description for Reactions Induced by Intermediate Energy Nucleons. Proc. Int. Conf. on Nuclear Data for Science and Technology, Gatlinburg (1994).
- [20] BARASHENKOV, V.S., Nucleon-Nuclear Cross Sections, Preprint P2-89-770, OIYaI, Dubna (1989) [in Russian].
- [21] BYCHKOV, V.M., MANOCHIN, V.N., PASHCHENKO, A.B., PLYASKIN, V.I., Cross Sections for Neutron Induced Threshold Reactions, Energoatomizdat, Moscow (1982) [in Russian].
- [22] BADIKOV, S.A., PASHCHENKO, A.B., Comparative Analysis of (n,p) Reaction Cross Section Systematics at Energies of 14 to 15 MeV. FEI Preprint N-2055, Institute of Physics and Power Engineering, Obninsk (1989) [in Russian].
- [23] PASHCHENKO, A.B., Cross Sections for Reactions Induced by 14.5 MeV Neutrons of Cf-252 and U-235 Fission Spectra. Preprint No236, TSNI Atominform, Moscow (1990) [in Russian].

- [24] FORREST, R.A., Systematics of Neutron-Induced Threshold Reactions with Charged Particles at about 14.5 MeV. Rep. AERE-R12149, Harwell Laboratory (1986).
- [25] BYCHKOV, V.M., PASHCHENKO, A.B., PLYASKIN, V.I., Interpretation of the (N-Z) Dependence of (n,p) Reaction Cross Sections at 14 - 15 MeV, FEI Preprint N809, Institute of Physics and Power Engineering, Obninsk (1978) [in Russian].
- [26] AIT-TAHAR, S., Systematics of (n,p) Cross Sections for 14 MeV Neutrons, J.Phys. G: Nucl. Phys. 13 (1987) 121.
- [27] KUREŃKOV, et al., Excitation Functions of Proton-Induced Nuclear Reactions on  $^{124}\text{Xe}$ : Production of  $^{123}\text{I}$ . J. Radioanal.Nucl.Chem.Lett. 135 (1989) 39.
- [28] TARKANYI, F., et al., Excitation Functions of the (p,2n) and (p,pn) Reactions and the Differential and Integral Yields of  $^{123}\text{I}$  in Proton -Induced Nuclear Reactions in Highly Enriched  $^{124}\text{Xe}$ . Appl. Rad. Isot. 42(1991) 221.
- [29] TARKANYI, F., et al., Nuclear Reaction Cross Sections Relevant to the Production of the  $^{122}\text{Xe} - ^{122}\text{I}$  Generator System Using Highly Enriched  $^{124}\text{Xe}$  and a Medium-sized Cyclotron. Appl. Rad. Isot. 42 (1991) 229.
- [30] VENIKOV, N.I., et al., Excitation Functions of Proton Induced Reactions in  $^{126}\text{Xe}$ :  $^{125}\text{I}$  Impurity in  $^{123}\text{I}$ . Appl. Rad. Isot. 44 (1993) 51.

# THE UNIVERSAL LIBRARY OF FISSION PRODUCTS AND DELAYED NEUTRON GROUP YIELDS.

*A.B. Koldobskiy, V.M. Zhivun*

*Moscow Institute of Engineering Physics, Moscow*

## Abstract

A new fission product yield library based on the Semiempirical method for the estimation of their mass and charge distribution is described. Contrary to other compilations, this library can be used with all possible excitation energies of fissionable actinides. The library of delayed neutron group yields, based on the fission product yield compilation, is described as well.

## Introduction

Fission product yields constitute the most important data for the determination of the radiation characteristics of fission fragments and their mixtures. The need to perform such calculations arises in the solution of a broad class of practical problems in connection with the use of the byproducts of nuclear technology, radiation safety consideration at power plants and nuclear industry sites, monitoring of international material safeguards agreements, etc... For these reasons, it was deemed to be of utmost importance to create a body of reference data on fission product yields having a high degree of reliability, and at the same time be adaptable to be used as input to calculational programs in universal formats for their international exchange.

Although there are theoretical models to describe the final stages of nuclear fission, from the saddle point to the rupture point, which can give a qualitative description of the mass and charge distribution of fission products, they are not suitable for the calculation of fission product yields to accuracies required for the solution of problems mentioned above. Nevertheless, there are a number of theoretical approaches, which, together with the existing body of experimental information, could be used in the development of calculational methods which could predict fission product yields. These methods are described in this report.

Contemporary experimental nuclear analysis methods guarantee a considerably high degree of accuracy of yield values in comparison to any of the existing calculational methods (although even in this case the accuracy is not always satisfactory). At the same time, to depend on purely experimental fission product yield compilations in practical applications is completely unrealistic. The reasons for this are technical, for instance the problems arising in the high speed separation of short-lived fission products, in the difficulties to obtain neutron beams of high enough intensity in practically significant energy intervals, in the problems to obtain the required measurement statistics (particularly in the analysis of threshold actinides and low

yield fission products), etc., as well as economical, arising as a result of the complexity and high cost of construction and use of the instrumentation necessary for the performance of the experiments, the acquisition of high purity materials, and others. It must also be taken into consideration that the energy dependence of the yields does not have a structure like the resonance structure of cross sections. Therefore, the use of neutron spectra having fine energy structures (having a large number of energy groups) results in very large amounts of superfluous information, which do not lead to any significant improvement in data accuracy, and is absolutely unjustified in view of the large expenditure of funds and time in the performance of the measurements. One can make a similar comment regarding the sharp differentiation of the practical significance with respect to fission products as well as to the fission reaction where they originated.

Taking these comments into consideration, at the present time, the only realistic basis for the creation of a definitive compilation of fission product yields are the semi-empirical calculational methods which give the possibility to evaluate any given yield value and its uncertainty on the basis of the compiled experimental information and the established physical principles of the fission process, with the use of approximation formulas having relatively simple parametric dependencies on the composition of the actinide nucleus and the energy of the fissioning neutron.

There are a number of fission product yield libraries which are based on these principles. However, even among the more complete libraries, the data are given in a "three-group" representation; that is, they consist of compilations of evaluated thermal data, of "fission spectrum" averaged data (which includes fission reactor neutrons spectra of usually unspecified hardness), and for neutrons in the vicinity of 14.7 MeV (fusion neutrons). This is conditioned by the fact that the overwhelming majority of measured yields relate to these three energies at which it has been relatively easy to perform the corresponding experiments. The information regarding these energies are practically non-existent, are not systematized and are often contradictory.

This "three-group" representation of fission product yields has two significant shortcomings. First, it is difficult to represent yield values at intermediate energies (particularly in the neutron energy range between "fission spectrum" energies and 14.7 MeV), a range in which the energy dependence is significant. As a result of this there is a high probability for the introduction of serious errors. Second, there are difficulties in the systematic combination of the "three-group" yield compilations with the data used in reactor analysis computations which have a significantly more detailed neutron spectrum structure.

These circumstances lie at the basis of the requirement for the creation of the fission product yield library described in this article. Without compromising the accuracy of the data, this compilation must be universal, not only with respect to the fission product and actinide characteristics, but also with respect to the energy of the fissioning neutrons (which has been omitted until now).

### **Calculation of the independent yields**

The adopted method is based on the generally accepted Gaussian description of the isobar distribution of the fission product yields corrected for even-odd effects:

$$y_f(A,Z) \Big|_{A=\text{const}} = \frac{(1 \pm \delta_Z \pm \delta_N)}{c\pi} \exp \left[ - \frac{(Z - Z_p(A))^2}{c} \right], \quad (1)$$

where  $y_f(A,Z)$  is the relative independent fission product yield of mass A and charge Z, where  $Z_p(A)$  is the most probable charge for a given A (whose magnitude is not necessarily whole number and is most often not), and where c is the dispersion of the distribution:

$$c = 2(\sigma^2 + \frac{1}{12}), \quad (2)$$

where  $\sigma^2$  is the dispersion of the "classical" Gauss distribution, where 1/12 is Sheppard's correction which takes into account the essential integer distribution as given by equation (1), and where  $\delta_Z$  and  $\delta_N$  are the corrections for the even-odd effects of the fission product nuclear composition. The  $\sigma$  parameter is a constant equal to  $0.56 \pm 0.04$ .

The "adjustment method" was used to calculate the  $Z_p$  parameters [1,2]. In the case of the well studied thermal neutron induced fission cross section of uranium-235, this parameter was determined using the method of "direct search" of the experimental values of independent yields; this method was implemented with the aid of interpolation and extrapolation procedures for those fission product masses for which these data were partly or entirely unavailable. For all of the other fission reactions, the values of  $Z_p$  were determined by adjusting the corresponding values for the uranium-235 fission induced by thermal neutrons:

$$[Z_p(A)]_x = [Z_p(A)]_{^{235}\text{U}_n} + \{[\Delta Z_p](A)\}_x, \quad (3)$$

where the "x" index corresponds to the investigated reaction. The value of  $\{[\Delta Z_p](A)\}_x$  was determined using the following expression [2]:

$$\{[\Delta Z_p(A)]\}_x = a(Z_x - 92) + b(A_x - 236) + c(E_x^* - 6,5). \quad (4)$$

Here,  $Z_x$ ,  $A_x$  and  $E_x^*$  are, respectively, the charge, the mass and the excitation energy (in MeV), for the investigated compound nucleus in reaction "x"; where

$$E_x^* = (E_0)_x + (E_n)_x, \quad (5)$$

and  $E_0$  and  $E_n$  are, the neutron separation energy and the fissioning neutron energy in reaction "x", respectively. The coefficients a, b and c in equation (4) are numerical parameters chosen from the available experimental fission product independent yield information. In total, there are 49 such coefficients [2].

The  $\delta_Z$  and  $\delta_N$  parameters are calculated using the following equation:

$$\delta = \begin{cases} \delta_0 - \frac{\delta_0}{2}(E_0 + E_n + E_\delta), & E_0 + E_n - E_\delta < 2 \text{ МэВ} \\ 0, & E_0 + E_n - E_\delta \geq 2 \text{ МэВ}. \end{cases} \quad (6)$$

Here  $E_\delta$  is the fission barrier height of the compound nucleus being investigated and  $\delta_0$  is the magnitude of the corresponding correction near the barrier (for even-even compound nuclei, for thermal fission).

The following notation will be used in the evaluation of the errors of the evaluated independent yield values:

- $N$  number of nuclides in the chosen fission product decay chain ( $I=1, \dots, N$ ),
- $y_n$  value of the corresponding independent yield for the  $i$ th nuclide,
- $\sigma_y$  their uncertainties, for the calculated values of the yields which are dependent on the errors of the  $Z$  and  $\sigma$  parameters,
- $y_{fi}$  evaluated values of the corresponding independent yields, whose sum for all fission products for the given isobaric chain are normalized to unity.

In order to determine the value of  $y_{fi}$  it is necessary to minimize the function  $R$ :

$$R = \sum_{i=1}^N \sigma_{y_n}^{-2} (\hat{y}_{fi} - y_{fi})^2 + \lambda \left( \sum_{i=1}^N \hat{y}_{fi} - 1 \right), \quad (7)$$

where  $\lambda$  is the undetermined Lagrange multiplier [3], and the term  $\sum_{i=1}^N \hat{y}_{fi} - 1$  is introduced in order to comply with the normalization.

The minimum of the function (7) is found by solving the  $(N+1)$  system of equations:

$$\begin{cases} \frac{\partial R}{\partial y_{fi}} = 0, & i=1, \dots, N \\ \frac{\partial R}{\partial \lambda} = 0. \end{cases} \quad (8)$$

Transposing equation (8), we obtain the following set of equations:

$$\begin{cases} 2\hat{y}_{fi} \sigma_{y_n}^{-2} + \lambda = 2y_{fi} \sigma_{y_n}^{-2}, & i=1, \dots, N \\ \sum_{i=1}^N \hat{y}_{fi} = 1 \end{cases}$$

Or, using matrix notation:

$$A \cdot \hat{\vec{y}}_f = \vec{B} \quad (9)$$

where  $A$  and  $B$  have the form:

$$A = \begin{pmatrix} 2\sigma_{y_n}^{-2} & 0 & \dots & 0 & 1 \\ 0 & 2\sigma_{y_n}^{-2} & \dots & 0 & 1 \\ \vdots & \vdots & \ddots & \vdots & \vdots \\ 0 & 0 & \dots & 2\sigma_{y_n}^{-2} & 1 \\ 1 & 1 & \dots & 1 & 0 \end{pmatrix}; \quad \vec{B} = \begin{pmatrix} 2y_{f1} \sigma_{y_n}^{-2} \\ \vdots \\ 2y_{fN} \sigma_{y_n}^{-2} \\ 1 \end{pmatrix}$$

The solution of that system leads to

$$\hat{\vec{y}}_f = A^{-1} \cdot \vec{B} \quad (10)$$

and the evaluated values of the corresponding independent yields may be arrived at using

$$\hat{y}_{jk} = \sum_{j=1}^{N+1} a_{kj}^{-1} \cdot b_j, \quad k = 1, \dots, N, \quad (11)$$

where the terms  $a_{kj}^{-1}, b_j$  are the matrix elements  $A^{-1}$  and  $B$  respectively. The errors of the evaluated independent yields were calculated using equation:

$$\sigma_{\hat{y}_{jk}} = \sqrt{a_{kk}^{-1}}, \quad k = 1, \dots, N.$$

### Calculation of mass yields

In contrast to the charge distribution of fission products, which generate independent yields, at the present time there are no generally accepted analytical approximation methods to produce fission product mass distributions, and in choosing such an approximation method, it is inevitable to infer a certain degree of subjectivity. At the same time, we believe that any function that would approximate a fission products mass distribution would have to satisfy two criteria:

- it would have to incorporate a minimum number of fitting parameters, and
- the dependence of these parameters on the nuclear composition of the fissioning nucleus and the energy of the fissioning neutrons must be expressed in the form of simple functions.

The approximation function chosen in this analysis was originally suggested in reference [4] by the authors in the framework of the so-called "method of three energies reference points":

$$Y(A, \vec{q}) = \left[ Y_1(A, \vec{q}) + Y_2(A, \vec{q}) + Y_3(A, \vec{q}) \right] \cdot \left[ 1 + q_8 \cos(\pi Z_p(A)) \right]. \quad (12)$$

The first and second terms enclosed by the square brackets define the peaks of the lightweight and heavy fission products respectively; the last term of the equation describes the region of symmetric fragmentation.

In expression (12):

$$Y_i = \begin{cases} (q_4 + q_3 T_i^2) \exp \left[ -\frac{1}{2} T_i^2 \exp(q_6 T_i (-1)^{i+1}) \right], & i=1,2 \\ q_7 \exp \left( -\frac{2(A-\bar{A})^2}{A_c} \right), & i=3, \end{cases} \quad (13)$$

where  $\bar{A} = \frac{1}{2}(A_c - \bar{\nu})$ ,  $T_i = (A - q_i)(q_3)^{-1}$  and where:

- $q_1$  and  $q_2$  are the position of the maxima of the lightweight and heavy fission products,
- $q_3$  is the parameter which characterizes the peaks' widths,
- $q_4$  is the parameter which characterizes the peak's heights,
- $q_5$  is the parameter which characterizes the degree of flattening of the peaks' tops,
- $q_6$  is the parameter which characterizes the asymmetry of the peaks,
- $q_7$  is the parameter which characterizes the region of fission fragmentation symmetry,

- $q_8$  is the parameter which characterizes the fine structure of the mass distribution,
- $A_c$  is the mass of the compound nucleus,
- $\bar{\nu}$  is the average number of prompt fission neutrons ,
- $A$  is the mass of the number of fission products,
- $Z_p(A)$  is the most probable charge of the fission product of mass  $A$ .

The parameters of this method allow for the possibility to describe their dependence on the mass of the compound nucleus by a second order polynomial:

$$q_i = \alpha_i + \beta_i(A_c - 200) + \gamma_i(A_c - 200)^2, \quad i = 1, \dots, 8, \quad (14)$$

where  $\alpha_i$ ,  $\beta_i$  and  $\gamma_i$  are the constants within the range of the considered energy of the fissioning neutrons. Their magnitudes are given together with the error matrices in Tables 1 and 2.

**Table 1. Values of the  $\alpha_i$ ,  $\beta_i$  and  $\gamma_i$  parameters**

Parameter	Fissioning neutron energies	$\alpha_i$	$\beta_i$	$\gamma_i$
$q_1$	TFH	97.242	0.959	0.0
$q_2$	TFH	137.67	0.0	0.0
$q_3$	T	4.312	3.603E-2	4.619E-3
$q_3$	F	4.290	1.523E-1	-2.480E-3
$q_3$	H	4.196	3.380E-1	5.762E-2
$q_4$	T	7.163	-5.789E-2	-2.972E-3
$q_4$	F	6.055	6.879E-2	4.822E-2
$q_4$	H	4.324	1.543E-1	7.649E-2
$q_5$	TFH	8.945E-1	-2.316E-1	1.792E-4
$q_6$	TFH	7.745E-2	8.218E-3	-4.754E-4
$q_7$	T	7.751E-3	-4.630E-3	-4.516E-4
$q_7$	F	3.977E-2	2.444E-3	1.892E-3
$q_7$	H	1.192	-2.730E-2	5.775E-3
$q_8$	T	3.345E-2	-1.221E-3	1.038E-4
$q_8$	F	4.569E-2	-5.389E-4	-1.637E-3
$q_8$	H	3.483E-3	-3.509E-3	1.085E-4

Table 2. Matrices of the  $\alpha_i$ ,  $\beta_i$  and  $\gamma_i$  parameter uncertainties

Parameter	Fissioning neutron energies	A11	A22	A33	A12	A23	A13
q <sub>1</sub>	TFH	1.01E-3	7.07E-5	0.0	2.70E-5	0.0	0.0
q <sub>2</sub>	TFH	6.87E-4	0.0	0.0	0.0	0.0	0.0
q <sub>3</sub>	T	2.49E-4	7.56E-6	1.21E-7	1.79E-5	-4.99E-7	-3.52E-6
q <sub>3</sub>	F	2.87E-4	1.23E-5	1.54E-6	1.39E-6	1.63E-6	-1.56E-5
q <sub>3</sub>	H	1.54E-3	3.01E-4	3.67E-5	-1.28E-4	7.67E-5	-1.43E-4
q <sub>4</sub>	T	6.63E-3	2.76E-4	2.26E-6	1.35E-5	-1.81E-5	-4.72E-5
q <sub>4</sub>	F	8.18E-3	3.27E-4	5.36E-5	3.05E-4	-2.41E-5	-5.24E-4
q <sub>4</sub>	H	2.17E-2	2.96E-3	4.32E-4	-4.79E-3	9.06E-4	-2.51E-3
q <sub>5</sub>	TFH	2.44E-4	9.91E-6	3.08E-7	3.25E-5	-3.69E-7	-4.37E-6
q <sub>6</sub>	TFH	1.54E-6	1.05E-7	2.67E-9	7.03E-8	-5.16E-9	-3.52E-8
q <sub>7</sub>	T	6.24E-6	2.09E-7	4.26E-9	2.55E-7	2.08E-8	-7.49E-8
q <sub>7</sub>	F	6.34E-6	1.11E-6	9.99E-8	6.14E-7	1.33E-7	-3.73E-8
q <sub>7</sub>	H	2.95E-3	4.16E-4	5.39E-5	-3.93E-4	1.28E-4	-2.90E-4
q <sub>8</sub>	T	1.04E-4	3.91E-6	4.39E-8	3.14E-6	-2.63E-7	-1.09E-6
q <sub>8</sub>	F	1.14E-4	6.08E-6	8.70E-7	4.25E-6	2.58E-7	-7.33E-6
q <sub>8</sub>	H	3.40E-4	4.78E-5	7.14E-6	-5.82E-5	1.56E-5	-3.86E-5

In order to determine the dependence of the q<sub>i</sub> (i=1,...,8) parameters on the fissioning neutron energy, it is necessary to perform an analysis using the approximation equation (12) with the objective to determine the analogues between the fission product mass distribution parameters in the framework of its known representation using five Gaussians [5,6]. This analysis showed that in the energy range 0 to 15 MeV, the parameters q<sub>1</sub>, q<sub>2</sub>, q<sub>5</sub>, and q<sub>6</sub> are not dependent on the energy of the fissioning neutrons.

The energy dependence of the remaining parameters can be calculated as follows:

$$q_3(E) = a_1 \sqrt{E_n + E_0 - E_\delta} + b_1, \quad (15)$$

$$q_4(E) = \frac{100}{\sqrt{2\pi} q_3 I_1} \frac{1}{1 + tg^2 \theta}, \quad (16)$$

$$q_7(E) = \frac{400}{\sqrt{2\pi} A_c} \frac{tg^2 \theta}{1 + tg^2 \theta} \quad (17)$$

where

$$\begin{aligned}
 \text{tg}\theta &= a_2(E_n + E_0 - E_\delta) + b_2, \\
 I_1 &= 1 + 1,125q_6^2 + 4,6224q_6^4, \\
 I_2 &= 1 + 9,375q_6^2 + 93,79q_6^4, \\
 q_8(E) &= a_3 \exp(-b_3 \sqrt{E_n + E_0 - E_\delta}),
 \end{aligned}
 \tag{18}$$

and where  $a_i$  ( $i=1,2,3$ ) are the fitting parameters.

The energy dependence of the  $q_3$ ,  $q_4$ ,  $q_7$  and  $q_8$  parameters are determined with the aid of two variables whose numerical values are obtained using the least squares method using reference sets of mass yields for the given compound nucleus (for different  $E$ , in absolute values, in % for each individual fission) more than two ( $N(\bar{Y}) > 2$ ). For  $N(\bar{Y}) = 2$  (which is characteristic for the  $^{240}\text{Pu}+n$ ,  $^{242}\text{Pu}+n$  and  $^{237}\text{Np}+n$  threshold fissioning systems), the values of these parameters are determined by the following formulas using two sets of  $q_i$ :

$$q_3(E_n) = \frac{q_{3F}(\sqrt{E_H + E_0 - E_\delta} - \sqrt{E_n + E_0 - E_\delta}) + q_{3H}(\sqrt{E_n + E_0 - E_\delta} - \sqrt{E_F + E_0 - E_\delta})}{\sqrt{E_H + E_0 - E_\delta} - \sqrt{E_F + E_0 - E_\delta}}. \tag{19}$$

The expressions for  $\text{tg}\theta$  required in the determination of the  $q_4$  and  $q_7$  parameters are:

$$\text{tg}\theta = \frac{S_F(E_H - E_n) + S_H(E_n - E_F)}{E_H - E_F},$$

where

$$\begin{aligned}
 S_F &= \sqrt{\frac{\sqrt{A_c} q_{7F}}{4q_3(I_1 q_{4F} + I_2 q_5)}}, \\
 S_H &= \sqrt{\frac{\sqrt{A_c} q_{7H}}{4q_3(I_1 q_{4H} + I_2 q_5)}}.
 \end{aligned}
 \tag{20}$$

$$q_8(E) = q_{8F} \exp\left(-1,56 \frac{\sqrt{E_n + E_0 - E_\delta} - \sqrt{E_F + E_0 - E_\delta}}{\sqrt{E_H + E_0 - E_\delta} - \sqrt{E_F + E_0 - E_\delta}}\right). \tag{21}$$

The F and H indexes which enter in the expressions (19) and (20) indicate that the values of these parameters are chosen for the fission process induced by "fission spectrum" neutrons and by 14.8 MeV neutrons respectively.

The effectiveness of the method described herein can be tested by comparing it with other calculational and experimental methods for a single or a combination of nuclides and energies of fissioning neutrons. In the performance of these tests it is essential that experimentally determined yield values are not used in these nuclide combinations as reference data in the determination of the parameters used in this method. The reason for this is that if they were used as such, their close agreement with the calculational data would be guaranteed to some extent and would thereby negate the proof of the effectiveness of this method. In this work, a set of fission product mass yields for uranium-238, for a fission neutron energy of 3.9 MeV, served as reference standard. The results of this comparison test are given in Table 3. Their analysis points to a reasonably good agreement between calculated and experimental data in

the entire range of fission product masses (with the exception to some extent in the range of symmetric fission where the central calculated yield values are systematically larger than the experimental data). We believe that these results indicate that this method has a high enough reliability to be used in applied problems.

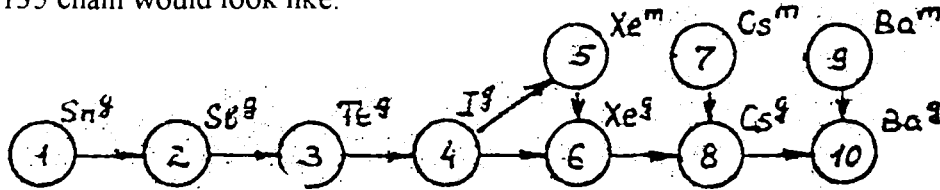
**Table 3. Fission product yields for  $^{238}\text{U}$  for an incident neutron energy of 3.9 MeV**  
(Comparison of calculated with experimental data given in absolute units)

A	Mass Yield (experiment)	Error	Mass Yield (Calculated)	Error
85	0,88	0,04	0,74	0,25
87	1,78	0,08	1,34	0,33
88	2,09	0,15	1,75	0,36
89	2,57	0,29	2,31	0,39
91	3,96	0,28	3,58	0,45
92	4,24	0,25	4,10	0,42
93	4,91	0,32	4,62	0,39
94	5,13	0,39	5,24	0,38
95	5,32	0,19	5,30	0,36
97	5,62	0,15	6,00	0,40
99	6,00	0,22	6,25	0,42
101	7,08	0,51	6,76	0,38
103	6,12	0,18	6,17	0,37
104	4,74	0,29	4,53	0,42
105	4,40	0,27	3,81	0,44
106	2,81	0,30	2,94	0,43
107	1,05	0,27	1,04	0,40
111	0,104	0,013	0,17	0,11
112	0,057	0,017	0,087	0,053
113	0,034	0,008	0,053	0,029
115	0,029	0,003	0,039	0,021
121	0,029	0,003	0,048	0,025
131	3,36	0,10	3,60	0,30
132	4,89	0,14	4,69	0,29
133	6,95	0,25	5,15	0,36
134	7,76	0,42	7,06	0,38
135	6,45	0,40	6,17	0,39
138	5,82	0,18	6,05	0,38
139	5,43	0,60	6,05	0,37
140	6,17	0,48	5,87	0,37
141	5,85	0,56	5,43	0,36
142	4,58	0,28	4,87	0,35
143	4,60	0,28	4,68	0,36
146	3,44	0,31	3,67	0,36
147	2,70	0,20	2,44	0,36
149	1,94	0,20	1,58	0,35
151	0,90	0,06	0,83	0,28
153	0,43	0,08	0,32	0,20

Separation of independent yields between isomeric states of fission products was done with the method described in reference [7] using the spin characteristics of isomeric fission product pairs taken from the most recent publication [8], as well as from the isomeric relationship of independent yields recommended in reference [9] for three neutron energies: namely, thermal, "fission spectrum" and 14.8 MeV. Linear interpolation was used to determine the relationship of independent yields between isomeric states of fission products for intermediate fissioning energies for the three energy ranges described above.

### Calculation of cumulative yields

Let us consider the isobaric fission product decay chain comprising N number of nuclides and assign consecutive numbers to each chain element taking into consideration the possibility of the existence of metastable states with their corresponding branching ratios. As an example, the A=135 chain would look like:



in which the index q corresponds to the ground state, and m to the metastable state. Introducing the following notation where  $f_{ik}$  is the branching ratio (i.e., the probability for the transition from the ith nuclide to the kth nuclide), and  $\hat{Y}_i$  is the evaluated value of the corresponding cumulative yields.

The value of the corresponding cumulative yields for the given isobaric chain can therefore be calculated using the following formula:

$$\hat{Y}_k = \sum_{j=1}^k m_{kj} \hat{y}_{j1}, \quad k=1, \dots, N, \quad (22)$$

or, using matrix notation

$$\hat{Y} = M \hat{y}_1,$$

where the matrix elements are

$$m_{kl} = \begin{cases} \sum_{i=l}^{k-1} f_{ik} \cdot m_{il}, & k > l \\ 1, & k = l \\ 0, & k < l. \end{cases}$$

The uncertainty of the evaluated corresponding cumulative yields are given by:

$$\sigma \bar{Y}_k = \left( \sum_{i=1}^N \sum_{j=1}^N m_{kj} a_{ij}^{-1} m_{ki} \right)^{1/2}, \quad k=1, \dots, N, \quad (23)$$

where  $a_{ij}^{-1}$  is the matrix element of the  $A^{-1}$  matrix from equation (11).

The absolute cumulative yields of the given chain is determined by multiplying by the corresponding mass yield. Their uncertainty is calculated using the method of propagation of errors.

### **The establishment of a permanent fission product yield library.**

In the process of establishing an information system based on empirical and semi-empirical calculational methods for the determination of physical quantities that have not been determined experimentally (such as fission product yields), it is most important to continue to acquire these data, and ascertain the completeness, accuracy and reliability of the used experimental data. The basic principles in the establishment of a library that would serve as a source of data is described below.

All data pertinent to fission product yields that are included in the library are subdivided into three categories: experimental, calculational and evaluated. (Here, as well as in subsequent descriptions, all pertinent data means all actual data and their uncertainties).

The meaning of the first two types of data are self evident. The evaluated data, whose provision is the most important function of this library, is the result of a concerted evaluation effort, whose object is to produce unique values of physical quantities (including fission product yields) based on a few known values of such quantities. The latter are known as "recommended" data. This procedure can have a formal nature, but is usually informal and includes not only procedures and results from formal calculations, but also subjective input of the evaluators which is justified in view of the nature of the operation. Such an approach is conditioned, first of all, by the highly significant volume of original data that are being analyzed, which are very often discrepant from one another; second of all, by the ambiguity of the information itself and the lack of information on the method of their production. Both of these circumstances precludes the use of straightforward formal methods (this is particularly true in the case of experimental data). It is evident that in the process of evaluation of physical quantities, the reliability of calculated yield data to that of the experimental data (fission product yields among others). When both types of data are available, as a rule, the calculated data are excluded from consideration during the preliminary stage of the evaluation.

Such an approach, requiring additional analysis, is acceptable under the following conditions:

- when there is a sharp discrepancy between the experimental values of the yields which exceed by far the values of the uncertainties assigned by the authors,
- when there is serious doubt in the reliability of experimental data obtained from a single experiment,
- when there is a sharp difference between experimental and calculated yield data under the condition that calculated values of other yields determined by the same method are in overwhelming number of cases in agreement with experimental information.

Let us consider the following circumstance. As evidenced from the above, the evaluation of any given fission product yield quantity must, generally speaking, take all of the pertinent information into account. However, from one point of view, the entire volume of information is so large, that its inclusion in the evaluation would require an amount of time which would exceed any reasonable limit. For instance, the measurement of the cumulative yield of barium-140 (lanthanum-140) from thermal neutron fission of uranium-235 is currently described in 38 publications. Similar situations can be observed in the case of other fission products. Although this does not exclude the advisability of a thorough evaluation of the most

important fission products considered in practical applications, it would be evidently illusory to require such an approach for all of the fission products.

On the other hand, the presentation of the fission product yields in the framework of the “three groups” has been formulated by a number of qualified scientists, for instance that published in reference [9]. The sets of fission product mass yields evaluated on the basis of experimental data, given in reference [9], are kept in continuous readiness, and are always used as reference data, i.e. for the determination of parameters used in mathematical formulas.

The first group comprises the following reactions:

- thermal neutron fission: uranium-233,-235, plutonium-239,-241,
- “fission spectrum” neutron fission: thorium-232, uranium-235,-235,-238, neptunium-237, plutonium-238,
- 14 MeV neutron fission: thorium-232, uranium-233,-235,-238.

The listed sets of evaluated yields, including those that are presented below, serve as reference base of the data library. The other sets of evaluated yields which are included in reference [9], are not included in the reference data base inasmuch as they were obtained using calculational methods.

The second group of data which are included in the reference data base for the evaluation of the  $q_i$  parameters determined from equation (13) form the experimental sets of yields for the following reactions:

- thermal neutron fission: thorium-229, americium-241,-242m, curium-245 and californium-249,-251,
- “fission spectrum” neutron fission: uranium-236, plutonium-240,-242,
- 14 MeV neutron fission: uranium-236, neptunium-237, and plutonium-239,-242.

This list was formulated according to the following principle: for each of the listed reactions, there must have existed at least two complete enough sets of consistent experimental yield data. Excluded from this list are the californium-252 thermal fission neutron reaction and the plutonium-240 14 MeV fission reaction, for which only one set of data is known. Nevertheless, they have been included in the list of reference data, first because of their significant influence on the accuracy and reliability of the calculated  $q_i$  parameters, second, due to their completeness, third, because of the recognized qualification of the authors of original experiments, and fourth because these experiments were part of measurement cycles which were united by common authors and procedures. Furthermore, both early and more recent results of these fission reaction experimental cycles are in good agreement with the results of other experimental groups. In comparison with these reactions, the sets of fission reaction data of the second group listed above have two characteristics:

- for some of the fission product masses there exist two or more yield values (according to data of different works); in such cases, these values are averaged, taking their statistical weight into account,
- in the case of some fission products the yield value is absent altogether. In such cases, the following algorithm is used.

If the yield of the considered second group fission reactions had not been investigated, then, the fission product yield was calculated on the basis of the evaluated yield sets from the first group; subsequently, the calculated quantities in this set were replaced by available experimental data or by the average of a number of experimental data. The same procedure is repeated for the next fission reaction from the second group taking the evaluated sets of the first group and the previously supplemented value; the procedure is repeated for two, three or more evaluated supplementary sets. It is obvious that this algorithm is implemented sensibly by first supplementing the better known fission processes, and concluding with the least known process. Note that it is not necessary to execute the secondary recalculation of the lacking data at each stage (with the exception of the last one), because the values of the  $q_i$  parameters change with the exception of the analysis of each subsequent procedure.

The reference base of the library includes sets of neutron fission product mass yields of actinide for energies which are different from the "three group" energy representation. The criteria used for their inclusion in the library coincide with those listed above for the second group of reactions, with the difference that in the case of the reaction being investigated the requirement to have not less than two relatively complete sets of mass yields is, in this case omitted.

At the present time, the reference base of the library consists of the following reaction type (the energy of the fissioning neutrons are given in MeV, and the number of available data sets for those cases in which it exceeds unity is given in parentheses):

- **protoactinium-231**: 3.0,
- **uranium-235**: 0.13, 0.17, 0.3, 0.45, 0.7, 0.9, 1.0, 1.3, 1.7, 2.0 (2), 4.0 (2), 5.5, 6.0 (2), 6.3, 7.1 (2), 8.1 (2), 9.0, 9.1 (2);
- **thorium-232**: 2.0, 3.0 (4), 5.9, 6.4, 6.9, 7.6, 8.0, 11.0;
- **neptunium-237**: 1.1;
- **uranium-238**: 1.5, 2.0 (2), 3.0, 3.9, 4.0, 5.5, 6.0 (20), 6.9, 7.1, 7.7, 8.0, 8.1, 9.0, 9.1;
- **plutonium-239**: 0.13, 0.17, 0.3, 0.45, 0.7, 0.9, 1.0, 1.3, 1.7, 2.0, 3.4, 4.5, 6.1, 7.9.

All these sets of data, determined by the above described algorithm, are used at the last stage of the determination of the parameters used in the universal method to calculate yields for the improvement of the description of their energy dependence (parameters  $q_i$ ,  $i=3,4,7,8$ ). The  $q_i$  parameters for  $i=1,2,5,6$ , whose values in the framework of the chosen analytical approximation are independent of the fissioning neutron energy; they were determined by averaging over all of the obtained values.

Sets of specific fission reaction yields which did not satisfy such stringent criteria were not included in the reference data library, and were used as controls for the verification of the method used to calculate the yields.

The formulation of the reference data library on the basis of independent yields was based on completely different principles than according to masses. The main reason for the difference in this approach lies in the already mentioned fact, that unlike the mass distribution approach, there exists at the present time a generally accepted analytical approximation method to process independent yields (isobaric charge distribution of fission products), namely by using the Gauss distribution corrected for even-odd effects (1).

Correspondingly, the values of the parameters used in this approximation method are used in a number of works which are amenable for the realization of a multigroup representation of the energy spectrum of the fissioning neutrons; according to our point of view, this is adopted in reference [2]. An additional and significant argument advanced in support of the choice of this systems of charge distribution parameters, is the fact that it is taken as the basis for the prediction of independent yields [9] which could not be derived from experiments. This serves as the basis for the constant supply of mass yields in the library that we are developing.

In accordance with such an approach, the reference data which arise as a result of the creation of sets of mass yields, their experimental values are absent in the case of independent yields because the values of the functional parameters of the approximation formulas are known in advance. The following are some of these functional parameters:

- values of the most probable charges  $Z_p(A)$  for the process of thermal fission of uranium-235 [9],
- values of the corrections  $\Delta z_p(A)$  to the Coryell equation (3) which are found with the use of parameters from reference [2],
- values of mass yields  $Y(A)$  taken from the actual library,
- values for the correction for the even-odd effects in the charge distribution.

Thus, with a few exception, the recommended values of independent yields are chosen as their calculational values. The mentioned exceptions include the following cases:

- for the thermal neutron fission of uranium-233, uranium-235, plutonium-239 and plutonium-241, the values listed in reference [9] were used instead of the recommended values derived from independent yields. The reason for this is due to the fact that for the given reactions, a large number of experimental data were included in reference [9]; in the case of mass yields these have a larger degree of reliability than calculational data. Note that inasmuch as the given list of fission processes is overlapped completely by the corresponding mass yields (first group), the non agreement of the two sets is excluded in the normalization.
- the presence of experimental values of independent yields in an individual fission product for other fission reactions. In this case, the algorithm described above (7-11) is implemented. If the number of experimental values of independent yields of any given fission product exceeds unity for the considered fission process, then its weighted average value is calculated.

For any given fission product mass, the independent yields are presented in the library in the charge interval  $([Z_p]-4) \leq Z \leq ([Z_p]+4)$ , where  $[Z_p]$  is the whole number part of the value of the most probable charge for that mass included in the fission reaction being investigated. As a result, the user receives nine individual independent yields for each fission product mass corresponding to his request. It would seem that such a response would be quite adequate for the solution of most applied problems.

### Library of delayed fission neutron groups

The library of fission product yields described above opens the possibility to create a universal information reference system for integral numerical characteristics of delayed fission neutrons.

The most important of these characteristics is the group yield of delayed neutrons represented by the co-called six group approximation, where the groups are formed according to the proximity of the half lives of the corresponding precursors.

Since the delayed neutron yield for the  $j$ th precursor is defined as

$$Y_n(j) = Y_c(j)P_n(j), \quad (24)$$

where  $Y_c(j)$  is the cumulative yield of the  $j$ th precursor,  $P_n(j)$  is the delayed neutron emission probability during its decay, the yield of the  $i$ th delayed neutron group is equal to:

$$Y^{(i)} = \sum_j Y_c(j)P_n(j). \quad (25)$$

The summation for each of the six  $Y^{(i)}$ , using equation (25), are carried out for each precursor; these are then combined in the  $i$ th group in accordance with their half lives. It follows that in the summation of the  $Y^{(i)}$  values for each of the six groups results in the average number of delayed neutrons per fission:

$$\nu_d = \sum_i \sum_j Y_c(j)P_n(j). \quad (26)$$

It is evident that the values of  $P_n$  are strictly spectroscopic characteristics and do not depend on the nature of the fission reaction. These values were chosen in accordance with references [10] and [11]. The subsequent algorithm used in the representation of the delayed neutron group yields in the library is reduced to the solution of equations (24), (25) and (26) using the fission product yield library described above and the corresponding values of  $P_n$ .

It is evident that the quality of the library, constructed in this fashion, can be evaluated only on the basis of a comparison with the corresponding experimental data.

Table 4 lists the results of such a comparison using data for the fission reaction of neptunium-237 and americium-241 measured by American scientists using reactor neutrons [12], and with our measured delayed neutron group yield data for both of these actinides using spectrum neutrons from the fast reactor BR-1 (located at FEI) [13], and also by using 14 MeV neutrons [14]. Overall, it can be said that the agreement in this comparison is good. Such an evaluation may be considered to be of high quality in itself, which also reflects on the quality of the fission product yield library which was used in the calculation of the delayed neutron group yields.

However, the discrepancy of the yields in the 5th group for the fission reaction of neptunium-237 by 14 MeV neutrons and americium-241 with fast neutron must be noted. Since in both of these cases the values of the experimental data exceed the values of the corresponding calculated data, it can be assumed that there exist either one or a few significant delayed

**Table 4. Comparison of calculated and experimental values of delayed neutron group yields (for  $10^4$  fissions)**

Reaction	Ref.	Delayed neutron group						Total per fission
		1	2	3	4	5	6	
A	NP*	3.45 ±0.35	26.3 ±1.8	23.9 ±1.4	45.7 ±2.5	11.9 ±1.0	3.5 ±0.4	114.6 ±3.6
	[12]	4.9 ±1.1	27.5 ±3.5	22.4 ±3.3	42.3 ±6.0	17.1 ±2.2	-	-
	[13]	4.9 ±0.3	31.0 ±0.9	25.1 ±0.9	45.4 ±1.4	12.9 ±1.2	2.7 ±0.7	122 ±3
B	NP	0.837 ±0.099	12.2 ±1.1	6.03 ±0.48	12.5 ±0.9	2.67 ±0.36	0.667 ±0.109	34.9 ±1.6
	[12]	0.7 ±0.3	10.1 ±1.2	7.9 ±1.1	12.6 ±2.0	6.0 ±3.8	-	-
	[13]	1.1 ±0.2	11.6 ±0.9	6.6 ±1.4	13.5 ±0.9	4.9 ±1.0	0.9 ±0.2	39.4 ±2.4
C	NP	2.60 ±0.68	11.2 ±1.7	10.8 ±1.5	19.2 ±2.2	4.24 ±0.55	1.12 ±0.20	49.1 ±3.3
	[14]	3.0 ±0.4	9.9 ±1.1	13.7 ±1.7	18.5 ±3.6	24.0 ±6.8	-	79 ±8

**Annotation:** A =  $^{237}\text{Np}$ f, B =  $^{241}\text{Am}$ f, C =  $^{237}\text{Np}(14\text{MeV})$ , NP = authors' work  
\* calculational results for 2 MeV neutron fission.

neutron precursors which are not included in the reference data (which is unlikely), or due to the use of inadequate values of  $P_n$  (which would seem to be more plausible, taking into account the methodical difficulties in the experimental determination of the spectroscopic characteristics of so many short-lived radionuclides.

There may be still another reason for the observed discrepancy for the fission of neptunium-237 by 14 MeV neutrons. The method to predict fission product yields described above is used in the calculations of delayed neutron yield groups as well. This method is based on the constancy of the  $\sigma(e)$  parameter of the charge distribution of the fragment isobars (2). Such an approach is taken overwhelmingly in most cases of known yield compilations, and currently, there does not seem to be any better alternative. On the other hand, in some cases [15], there is a tendency to widen the charge distribution of fission products by increasing the energy of fissioning neutrons. If this effect does indeed exist, it must be accompanied by a corresponding increase in the independent fission product yields with the accompaniment of a slight divergence from  $Z_p$ , which is observed in the course of the executed comparison.

In any case, more specific conclusion regarding the reasons for the mentioned discrepancies may be arrived at only on the basis of an analysis of results of additional calculational or experimental investigations.

At the present time, the authors of this article are in the process of perfecting the library of delayed neutron group yields. The principle emphasis in this effort consists of including the pertinent experimental information in the library and the development of an optimum method for their renormalization. Attention is also given to the development of a method for the quantitative evaluation of the reliability of the sets of fission product yield data stored in the above mentioned library and to the utilization of experimental integral delayed neutron fission data.

### References

- [1] CORYELL, C.D., et al., *Canad. J. Phys.* 39 (1961) 646.
- [2] NETHAWAY, D.R., Rep. UCRL-51640 (1974).
- [3] CHIMMSLBLAY, D., *Applied non-linear programming*, Mir, Moscow, p.337, [in Russian].
- [4] GUDKOV, A.N., et al., in "Experimental nuclear physics methods at high and low energies", Ehnergoizdat, Moscow (1982) 61 [in Russian].
- [5] MUSGROVE, A.R., COOK, J.L., TRIMBLE, G.D., (*Proc. IAEA Panel Mtg. on Fission Product Nuclear Data, Bologna, 1973*), IAEA, Vienna (1973) 421.
- [6] GUDKOV, A.N., et al., in "Radiation Safety and Shielding of Nuclear Power Plants" 5th Edition, Atomizdat (1981) 59 [in Russian].
- [7] MADLAND, D.G., et al., Rep. LA-6595-MS., Los Alamos (1976).
- [8] *Chart of the Nuclides*, Strasbourg (1992).
- [9] RIDER, B.F., Rep. NEDO-12154-3(B) (1980).
- [10] REEDER, P.L., Rep. PNL-SA-11747 (1983).
- [11] MANEVITCH, L.G., et al., Preprint IAE-4308/4 (1986) [in Russian].
- [12] BENEDETTI, G., et al., *Nucl. Sci. Engin.* 80 (1982) 379.
- [13] GUDKOV, A.N., et al., *At. Energia* 86 (1989) 100 [in Russian].
- [14] BOBKOV, E.Yu., et al., *At. Energia* 67 (1989) 408 [in Russian].
- [15] Shmid, M., et al., *J. Inorg. Nucl. Chem.* 43 (1981) 867.



# THE EVALUATION OF THE $^{237}\text{Np}$ FISSION CROSS SECTION IN THE 20 KEV - 20 MEV ENERGY RANGE.

*V.N. Dushin, V.A. Kalinin, V.I. Shpakov.*

*V.G. Khlopin Radium Institute, Saint Petersburg*

## Abstract

The results of the development of nuclear data evaluation based on the generalized least squares method is presented. The method to interpolate experimental data measured at arbitrary energy points, and their transfer to a fixed energy grid is described. The results of the  $^{237}\text{Np}$  fission cross section measurements performed until 1988 were critically analyzed. A 781x781 covariant matrix was derived from the correlation analysis of the experimental results. The results of the evaluation, and the associate correlation matrix was obtained using the generalized least square method.

## Introduction

The calculation of the accumulation of  $^{237}\text{Np}$  in nuclear reactors is important in the determination of the nuclidic composition of the spent fuel; furthermore, this nuclide is an important component in the thorium fuel cycle. The  $^{237}\text{Np}$  neutron fission cross section was investigated as a standard threshold cross section to serve as an alternative to the  $^{238}\text{U}$  fission cross section standard (which is fully justified by the authors). As a result, the accuracy requirement for the neutron data for this nuclide is fairly high. In particular, the required accuracy of the fission cross section in the energy range from threshold to 20 MeV may not exceed 1 - 5%. The most recent evaluation of the  $^{237}\text{Np}$  fission cross section performed by Derrien [1] was determined only up to a neutron energy of 8 MeV. Also, since the publication of this evaluation, the amount of experimental data increased considerably, primarily as a result of the measurements of the  $^{237}\text{Np}$  fission cross section in the USA, Japan, China and in the former USSR, using new high precision instrumentation. These new data confirmed the inconsistencies in the evaluated fission cross section data presented in the ENDF/B-5 data library. All of these considerations led to the performance of this evaluation.

## Experimental results and the covariant matrix

The results of 24 measurements, performed in the time period spanning the years 1959 - 1987 [2-26], have been included in this evaluation. Most of the data were derived from relative  $\sigma_f^{237}\text{Np}(\sigma_f^7)$  and  $\sigma_f^{235}\text{Np}(\sigma_f^5)$  measurements [2-11]. The results of these measurements were introduced in this evaluation in the form of experimental relative values, renormalized when necessary, to the evaluated  $\sigma_f^5$   $^{235}\text{U}$  values taken from the ENDF/B-5 or ENDF/B-6

libraries. References [12-14] contained absolute values of  $\sigma_f^5$  measurements in which the  $\sigma_f^7$  cross section data was used as standard (the  $^{235}\text{U}$  target was used to measure the neutron flux). In view of the impossibility to reconstruct the original  $\sigma_f^7 / \sigma_f^5$  values, the resulting data of these measurements, preliminarily renormalized, are included in the evaluation as absolute values. Thus, in reference [12], the evaluation of the  $\sigma_f^5$  data taken from the ENDF/B-4 library was used instead of the old Davey compilation. In reference [14], in addition to monitoring the neutron flux using the  $\sigma_f^5$  reaction, the results were normalized to the integral of the  $\sigma_f^7$  ENDF/B-4 cross section in the 1 - 2 MeV energy range. These data were renormalized to the  $\sigma_f^5$  (ENDF/B-6) data and to the corresponding integral taken from Derrien's evaluation. For the sake of completeness, results of relatively old measurements [15-17], in which  $\sigma_f^{238}\text{U}$  was used as the standard, were included in the evaluation. At the same time, the data were renormalized to  $\sigma_f^8$  cross section values taken from the ENDF/B-5 library; these were included in the evaluation as absolute data. References [18-26] contain data from absolute measurements in which the neutron flux was monitored using the (n,p) reaction, activation or the associated particle time correlation method (APTC). In addition, the data included in this evaluation consisted of preliminary cross section measurements obtained by the authors with the APTC method at 4.9 and 18.6 MeV neutron energies in cooperation with the Technical University at Dresden.

The pre-processing of the data consisted of an analysis of the measurement uncertainties in order to determine the magnitude of the correlation between experimental points. It must be mentioned that in spite of the existence of the EXFOR data library, a significant part of the data, in particular those resulting from older measurements, are very poorly documented. In those cases where the information was sufficiently informative, special efforts were made to preserve the values of the uncertainties specified by the authors. In those case where the information on error components was lacking, the authors had to supplement the missing error components derived from an analysis of the experiment and the method used in the processing of the data. Thus, in references [14 and 15], where only statistical errors were given, additional errors arising from the normalization of the determination of the number of fissioning nuclei were added. In reference [22], missing errors in the determination of the target weight and in the fission fragment recording efficiency were added. In the case of references [10 and 11] there is no analysis of the constituent errors; in this case, characteristic correlation values used in similar experiments [7] were used in the determination of the covariance of experimental data. In order to reduce the weight attributed to the data resulting from the rather coarse measurement described in reference [17](which gives only the statistical error information), a higher value was assigned to the total error. Higher total error values were also given to the data published in reference [23], in which error components were assigned unrealistically low values. Furthermore, in a number of measurements where the cross sections vary rapidly with energy, an additional error, attributed to the uncertainty in the energy of the incident neutrons, was assigned to the cross section. It must be noted that in the process of renormalizing cross section values to more up-to-date standard reference data, the authors of this evaluation did not alter the corresponding errors.

A traditional approach was used in the formulation of the full covariance matrix of experimental data  $\mathbf{V}$  which has a dimension of  $(m \times m)$ , where  $m$  is the total number of data. The matrix components had the following form:

$$V_{ij} = \sum S_{ijl} \cdot D_{il} \cdot D_{jl}$$

where  $D_{II}$  is the uncertainty component  $I$  of experimental datum  $I$ ; and where  $S_{ijI}$  is the correlation coefficient between separate error components which satisfies the condition  $-1 < S_{ijI} < 1$  and  $S_{ijI} = 1$ .

Generally, the determination of the values of  $S$  presents a significant difficulty. In the calculation of the covariance, we have attempted to formulate an objective approach. This approach consists in breaking down the errors into components, each of which could be assigned one of three correlation levels: zero-order level ( $S_{ijI} = 0.0$ ) for uncorrelated errors, intermediate level ( $S_{ijI} = 0.7$ ) for partly correlated errors (for instance in the case of quantities measured with the same measurement instrument), and fully correlated level ( $S_{ijI} = 1.0$ ).

Statistical errors and corrections for the background are not amenable for correlation. The determination of errors related to the effectiveness of fission event registration are considered to be fully correlatable. Also fully correlatable are the errors arising in the determination of the target mass, of its nuclear composition, of its half-life, of its normalization and of the neutron source and neutron flux parameters. The results of the target weighing procedure using the same type of instrument but not the one and the same instrument is considered to be partially correlatable, etc...

The magnitude of 0.7 to identify partial correlation was chosen by the authors arbitrarily with the objective to describe a certain average level of connectivity between variables which can be expressed visually in such a way so that the elliptical scattering axes differ by a factor of two. The measurements described in references [6,7,9] were executed at a good metrological level, were well documented and cover a wide neutron energy range. The data that resulted from these measurements were subdivided into neutron energy groups which are associated with specific sources of correlatable (systematic) errors. Because of this, there is a good reason for the correlation values to be energy dependent. In the case of the other measurements the level of correlation does not change from one point to the next.

The possibility for correlation between different measurements was analyzed as well, such as by the use of the same standard reference cross sections, the same target, the same half-life, etc... Such correlations were identified in a few cases, and they were taken into consideration in this evaluation.

The procedure described above made it possible to construct an entire covariant matrix of experimental data including absolute as well as relative data. The resultant matrix had a dimension of  $781 \times 781$ . The covariant matrix turned out to be practically "empty", as the largest correlated block had a dimension of  $280 \times 280$ .

### **Generalized Least Squares Method**

Evaluation is understood to mean the processing of information contained in the results of measurements and calculations, carried out on the basis of hypotheses regarding the nature of data, and the subsequent thorough analysis of these data, and the derivation of procedures used in obtaining data and the methods used in their processing. At the present time, a widely used method in the evaluation procedure is the generalized least squares (LS) method which is based on three assumptions:

- a) the measurement results and the evaluated parameters are linearly dependent,
- b) there are no correlations between the evaluated parameters and the results, and
- c) the uncertainties of the parameters and those of the measurement results have a normal distribution.

These approximations are extremely general, are weak enough and are applicable in practically all interesting cases. The approximations of the generalized least-squares method imply that the initial parameter approximations are close to their exact values, the covariant matrix reflects a realistic magnitude of the measurement errors, and that the linearisation of the measured functional is acceptable. The departure of the distribution of the error of the measured quantities from a normal distribution which has been observed in individual cases is most likely due to the existence of an unaccounted correlation of data. Such distributions may be reduced to a normal shape at the expense of a corresponding transformation of variables.

Using the nomenclature of reference [27], we have:

- D - measurement results, dimension m vector
- V - measurement covariance (m × m) matrix
- P' - parameters for the evaluation of dimension n vector
- P - result of parameter evaluation dimension n vector
- M - matrix of covariance parameters P (n × n)
- M' - matrix of covariance parameters P' (n × n).

The expression which connects the measurement results with the parameters, written with the use of the sensitivity coefficients matrix G, is:

$$\mathbf{D}' = \mathbf{D} + \mathbf{G} \cdot (\mathbf{P}' - \mathbf{P}) \quad \text{where } \mathbf{G} = \delta\mathbf{D}/\delta\mathbf{P}$$

where  $\mathbf{D}'$  is the dimension vector n, and  $\mathbf{G}$  is the (n × m) matrix.

In conformance with the convention used in the least-squares method, it follows that in order to determine the values of the P parameters it is necessary to minimize a  $\chi^2$  type expression for the collections of data and parameters:

$$Q = (\mathbf{D} - \mathbf{D}')^t \mathbf{V}^{-1} (\mathbf{D} - \mathbf{D}') + (\mathbf{P} - \mathbf{P}')^t \mathbf{M}^{-1} (\mathbf{P} - \mathbf{P}')$$

By calculating the minimum value of the functional Q ( $\delta Q/\delta P = 0$ ), one obtains:

$$\mathbf{P}' - \mathbf{P} = (\mathbf{M}^{-1} + \mathbf{G}^t \mathbf{V}^{-1} \mathbf{G})^{-1} \mathbf{G}^t \mathbf{V}^{-1} (\mathbf{D} - \mathbf{D}')$$

Or, by introducing the expression  $\mathbf{N} = \mathbf{G} \cdot \mathbf{M} \cdot \mathbf{G}^t$ , one obtains:

$$\mathbf{P}' - \mathbf{P} = \mathbf{M} \mathbf{G}^t (\mathbf{N} + \mathbf{V})^{-1} (\mathbf{D} - \mathbf{D}')$$

and for the covariant matrix of results one obtains:

$$(\mathbf{M}' - \mathbf{M}) = -\mathbf{M} \mathbf{G}^t (\mathbf{N} + \mathbf{V})^{-1} \mathbf{G} \mathbf{M} \quad (1)$$

Note that there is another approach (one that has not been used), consisting of the Baiesov approximation and the method of the maximum probability function, which leads to the same results. That approach [30] requires the minimization of each element of the P parameter vector. The relationship obtained by this method is similar to the LS method. From our point of view, however, the LS method is more straightforward, and the covariance matrix elements maintain their physical meaning (such as the evaluation of the standard deviation) and does not introduce any substantial limitations. In addition, the LS method makes it possible to obtain useful relationships for the evaluation of a significant amount of information (in terms of the logarithm of the ratios of the standard deviation parameters prior to and after the processing of the experimental results) produced in the course of the experiment. References [28,31,32] contain a certain amount of useful relationships for the evaluation of experimental results and degrees of importance (objective, in the sense of lowering the standard deviation level) of the measurements for the entire functional, namely the neutron fission cross section in the given case.

### **Evaluation of the cross section value in metric space**

The classical relationships of the LS method, are by their very nature intended to be used for the evaluation of physical quantities which are inexorably related to each other by linear relationships. In the concept of the LS method, it is not foreseen to use information relating to space structure (configurational or energy space, etc...) represented by physical quantities. For instance, there is no mechanism for the use of information to characterize the shape of a curve, which is difficult to formulate in any event. The main reason for this inadequacy is due to the necessity to represent uninterrupted/continuous physical quantities with the use of a discreet model. The LS method uses only discreet values in a non-metric space (!); consequently, it does not have mechanisms which operate on sequential information and mechanisms able to compare spatially distributed quantities. The approaches which do exist are based on the reduction of continuous physical quantities to discreet representations using various methodologies whose use depends on the physical nature of the investigated quantity. Thus, for the evaluation of the energy dependence of nuclear data, the methodology proposed in the work described in reference [31] is based on the use of spline fitting approximation based on the use of a discreet energy grid with the subsequent evaluation of coefficients. The authors of this evaluation have used a combination of a discreet energy grid with a varying interpolation of the experimental data.

Assuming that the energy dependence of the  $^{237}\text{Np}$  fission cross section can be represented by a smooth curve, and that the energy coordinates of the experimental points are known to an accurate enough degree so as to allow its single-valued distribution between the energy points of the grid of the evaluated parameters. On that basis, it can be expected that the vector of the searched for parameters P (having an infinite dimension by its nature) will be described accurately enough by the discreet approximation based on previously assigned energy points, and that they will be determined to a high degree of constancy for this evaluation.

The proposed procedure is described in Figure 1, where:

$\sigma_j$  - is the cross section of the jth experimental point,

$G_{i,j}^*$  - is the sensitivity coefficient of the jth experimental point on the ith member of the P parameter.

$$\sum G^*_{i,j} = 1.0$$

- - experimental point
- - "a priori" cross section

The following linear expression was used by the authors to calculate the sensitivity coefficients

$$G^*_{i,j} = (E_j - E_i) / (E_{j+1} - E_i) \quad (2)$$

under the condition that  $E_i < E_j < E_{i+1}$ , more exactly, these equations are used for the formulation of the discrete energy grid for the experimental data and the parameters. The sensitivity coefficients  $G$  in the LS equations (1) are calculated in a traditional manner using

$$G = G^* \cdot (\delta D / \delta p)$$

In this manner, each experimental point influences only the cross section being evaluated at two energies, close enough to the energy value of the experimental point. It can be said that equation (2) introduces the linear metric with certain limitations. The soundness of such a choice is "absolutely not absolute".

For the construction of the interpolation scheme we took advantage of the fact that the LS method understands the concept of "a priori information". Under these conditions, it is only logical to take the evaluated data from existing evaluated data libraries (such as ENDF/B, ENDL, etc..) whose energy dependence can be used to interpolate the experimental data using the energy points of the energy grid of the evaluated parameters (P). In such a scheme, only existing information ("new" experimental data based on new measurements, and "old" experimental data existing in data libraries, i.e., "a priori" data) can be used, which, to our mind, does not coarsen the original data (because that is done by the averaging procedure) and does not introduce additional information as may happen in the case of spline approximations.

On the other hand, in the course of an evaluation of the vector parameter (P) components for which there are existing equations which characterize any measured and/or a priori known properties of its components, one could attempt using a gradual, step by step, approach based on the concepts embodied in the statistical regularization method devised by Turchin. Under such conditions, one could adopt the concept of continuity or smoothness of a curve, of "form" dependence, as well as the correlation matrix of components of the evaluated vector. For instance, assuming that one knew the second moment of the probability distribution of the entire collection of experimental data (i.e., the correlation matrix), using Baies' formulas, minimizing the amount of additional information (in the sense of Kulback?) in the probability distribution, one can write:

$$P' - P = [E + \alpha^2 \cdot V^{-1}]^{-1} \cdot (D' - D)$$

$$M' = \alpha^2 \cdot [E + \alpha^2 \cdot V^{-1}]^{-1}$$

where  $E$  is the unitary matrix and  $\alpha$  is the regularization parameter.

Under these conditions, the amount of information that is contained in the experimental data and in the "a priori" parameters does not change, and additional criteria in the construction of sensitivity coefficients are not introduced; this is an important point if one is to maintain the objectivity of the evaluation procedure. As a matter of fact, these relationships speak only to the fact that the components of the P parameter are continuous functions of the argument (i.e., there is a transition from a vector representation to a functional and operational representation). Such an approach provides the possibility to introduce supplementary information conveying "limitation", "smoothness", "monotony", and other such properties to the components of the P parameter.

### **Execution of the programming and results of the cross section evaluation**

The LSM algorithm was programmed for the EC-1045 computer using the FORTRAN-77 computer language. The sub-programs which executed the matrix operations embodied special procedures designed to conserve the accuracy of the data (in particular, iterational constructions of reverse matrices).

Two separate calculational procedures were implemented: one consisted of a sequential treatment of data resulting from individual measurements (i.e., measurement blocks not correlated with other measurements), and the other one in which all of the data were treated simultaneously. Both procedures produced practically identical results, but differed significantly in the time taken for the computation: the difference being proportional to the dimensions of the calculated matrices. Thus, the sequential treatment required approximately 40 minutes of computation, and the other more than 2 hours. With regard to the memory required for the executed algorithm, depended on the dimensions of the covariant matrices and were equal to approximately  $(6 \times m \times m)$  8 bytes, or about 30 Mbytes of operational memory.

As indicated above, a significant part of the experimental data included in this evaluation consisted of data from relative measurements. In the course of the pre-processing of the data, data from all relative measurements were represented in the form of  $\sigma_f^7 / \sigma_f^5$  ratios with a corresponding increase in the magnitude of the evaluated vector P. The  $^{237}\text{Np}$  fission cross section was represented by an 80 point approximation, the values of the chosen energies can be seen in Table 1, which also lists the results of the evaluation. The  $^{235}\text{U}$  fission cross section is represented by 98 points. Thus, in total, 178 cross section values were evaluated. The  $^{237}\text{Np}$  "a priori" information was taken from the ENDF/B-4 evaluated data library. A certain amount of influence of the "a priori" values on the evaluation results was ascertained for uncertainties smaller than 20 - 30 %, which could be attributed to "a priori" quantities, and a certain increase in the stability of the operation of the algorithm could be observed by reducing the level of the "a priori" uncertainties. This increase manifested itself by a reduction of the scatter of the evaluated dispersion results (matrix M) when the initial/original data were altered. All of the major calculations were performed with an 80% uncertainty level for "a priori" information. Two different approaches were used in the assignment of "a priori" data to  $\sigma_f^{235}\text{U}$ : taking the data and their corresponding errors from the ENDF/B-5 and ENDF/B-6 data libraries. As the level of the uncertainties assigned to the fission cross section of  $\sigma_f^{235}\text{U}$  is extremely low in both /B-5 and /B-6 ENDF versions, no significant changes occurred in the values of the  $^{235}\text{U}$  fission cross section and in the level of their error due to the use of new experimental  $\sigma_f^7 / \sigma_f^5$  information.

Figure 2 shows the input data from absolute measurements used in the evaluation and the resulting evaluation curve (given in the form of cross section as a function of energy).

Figure 3 shows the input data from relative measurements ( given in the form of the ratio  $\sigma_f^7 / \sigma_f^5$  as a function of energy).

Table 1 lists the results of the evaluation of the  $^{237}\text{Np}$  fission cross section; the listed results were obtained using  $\sigma_f^5$   $^{235}\text{U}$  data from ENDF/B-5. In Figure 4, these results are shown together with the evaluation results obtained using  $\sigma_f^5$   $^{235}\text{U}$  data from ENDF/B-6. Cross sections  $\sigma_f^7$  which were taken from ENDF/B-6 and ENDF/B-4 were used as “a priori” data. As can be seen, both calculational approaches yield practically the same results. However, the errors results obtained with the ENDF/B-6 data are unbelievably low, namely less than one percent. We believe that these results are due to non-physical uncertainties in the uranium-235 cross section file in ENDF/B-6. The structure of the experimental data is such that the relative measurements have a dominant influence. This is due to the fact that lower uncertainty values are assigned as a result of simpler method and processing procedure, and also because the number of relative measurements is noticeably larger. As a result, the evaluation using data from relative measurements is given more weight, which correspondingly increases the role of the  $^{235}\text{U}$  fission cross section and the level of its errors.

In the 14 to 15 MeV neutron energy range, there is a noticeable increase in the cross section curve which is caused by the inclusion of well corroborated data of Garlea [8], Zasadny [24] and Dushin [25]. A particularly strong influence is exerted by the absolute measurement of Dushin et al. [25]. A detailed analysis of the available documentation of these data, made it possible to assign to these absolute measurements an error of 1% which is at the same level, and in part even lower than that of relative measurements. The breakdown of the  $\sigma_f$  evaluated data curve above 15 MeV is caused by the absence of data in comparison to the accuracy of the cross section in the 14 MeV region. Above 15 MeV, the cross section curve depends primarily on the data of Carlson [22], and on the well substantiated metrological level measurement of Behrens [6]. The smooth dependence of the ENDF/B-6 evaluation along the upper data corridor is supported only by the old data of Rago and Goldstein[17], whose analysis did not permit assigning an error of less than 10% to these data. Thus, the physically unsubstantiated breakdown of the evaluated curve, which lies within the boundaries of the assigned errors, is supported from one side by the lack and significant scatter of the experimental data , and on the other hand by the fact that the LS method is not designed to use information about the smoothness of the cross section.

The value of  $\chi^2$  for one degree of freedom, was calculated for the entire array of data which would characterize the consistency of the evaluated curve with the experimental results; the result of this calculation yielded a value of  $\chi^2_1 = 4.75$  which indicates the existence of a statistical inconsistency of the original/initial data and the corresponding results of the evaluation. The usual recommendation of the LS procedure consists of multiplying the errors by the square root of  $\chi^2_1$  which has the objective to formally fulfill the requirement of equating the chi-square value to the degrees of freedom. Accordingly, the errors would have to be multiplied by a value of approximately 2.2. The final version of the evaluated cross sections (where the values of  $\sigma_f^5$  are taken from ENDF/B-5) together with the corrected errors is listed in Table 1. The noticeable departure of the chi-square value from unity indicates that on the average, we made an error of a factor of two in the assignment of errors

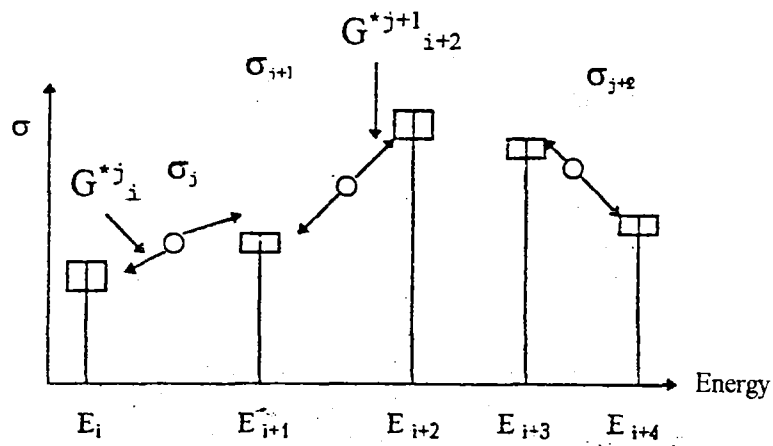
to the “a priori” and experimental data. This exercise has revealed the basic shortcomings of the LS methodology which consists of the absence of a validation mechanisms for the assignment of errors to the initial data; this forces one to use the empirical technique of multiplying the errors by chi-square.

Table 2 illustrates the structure of the correlational matrix of the evaluated  $^{237}\text{Np}$  fission cross section, which is given in terms of averaged values. Because of the averaging procedure, it is practically impossible to reproduce elements of the non-correlational linkage of neighboring fission cross sections values . The evaluated cross section values for neighboring energy values are non-correlated to a level of 20 to 30 %(!), and as can be seen from the values listed in the table, the cross section values at lower energies are correlated to a level of 10 to 20 %. The non-correlation depends on the chosen cross section interpolation procedure.

## Conclusion

The results of the nuclear data evaluation procedure based on the LSM methodology as well as the vector evaluation algorithms, are described. All of the available  $^{237}\text{Np}$  fission cross section data were used in the evaluation procedure. The evaluated  $^{237}\text{Np}$  fission cross section data, listed in Table 1, are in extremely good agreement with the ENDF/B-6 evaluation with the exception of the region above 15 MeV where there is a pronounced lack of experimental data.

The experience gained from the processing of the experimental data using the LS methodology leads to the conclusion that the evaluation of nuclear data still requires a fair amount of artifice and intuition, and at the present time cannot be considered to be a formal procedure.



**Figure 1. Superposition of the discrete energy grid for the  $P(E_i)$  parameters with arbitrary measurement energy points  $\sigma_{j_r} N_p$ .**

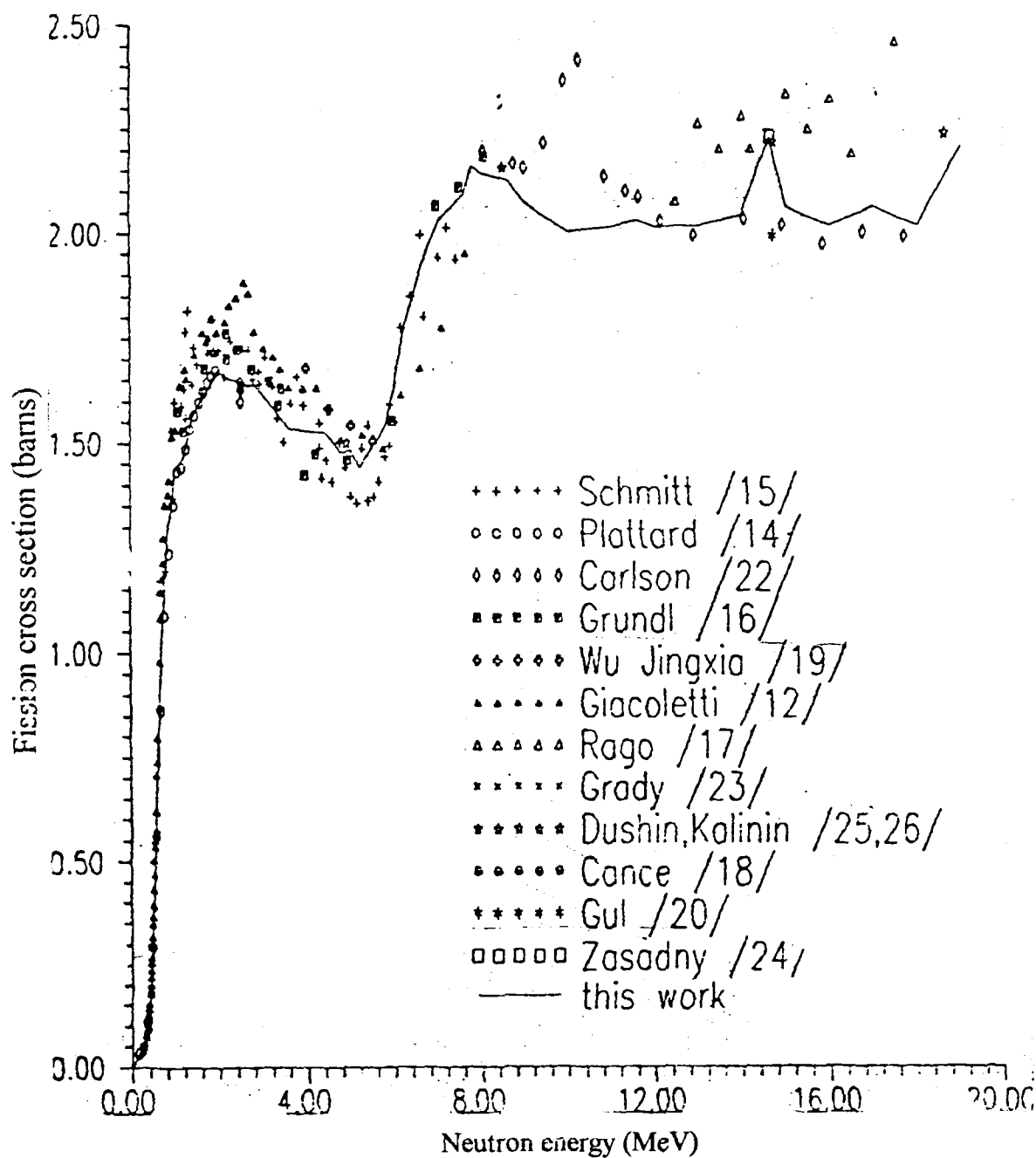


**Figure 2. Results of the neptunium fission cross section evaluation using absolute measurement data**

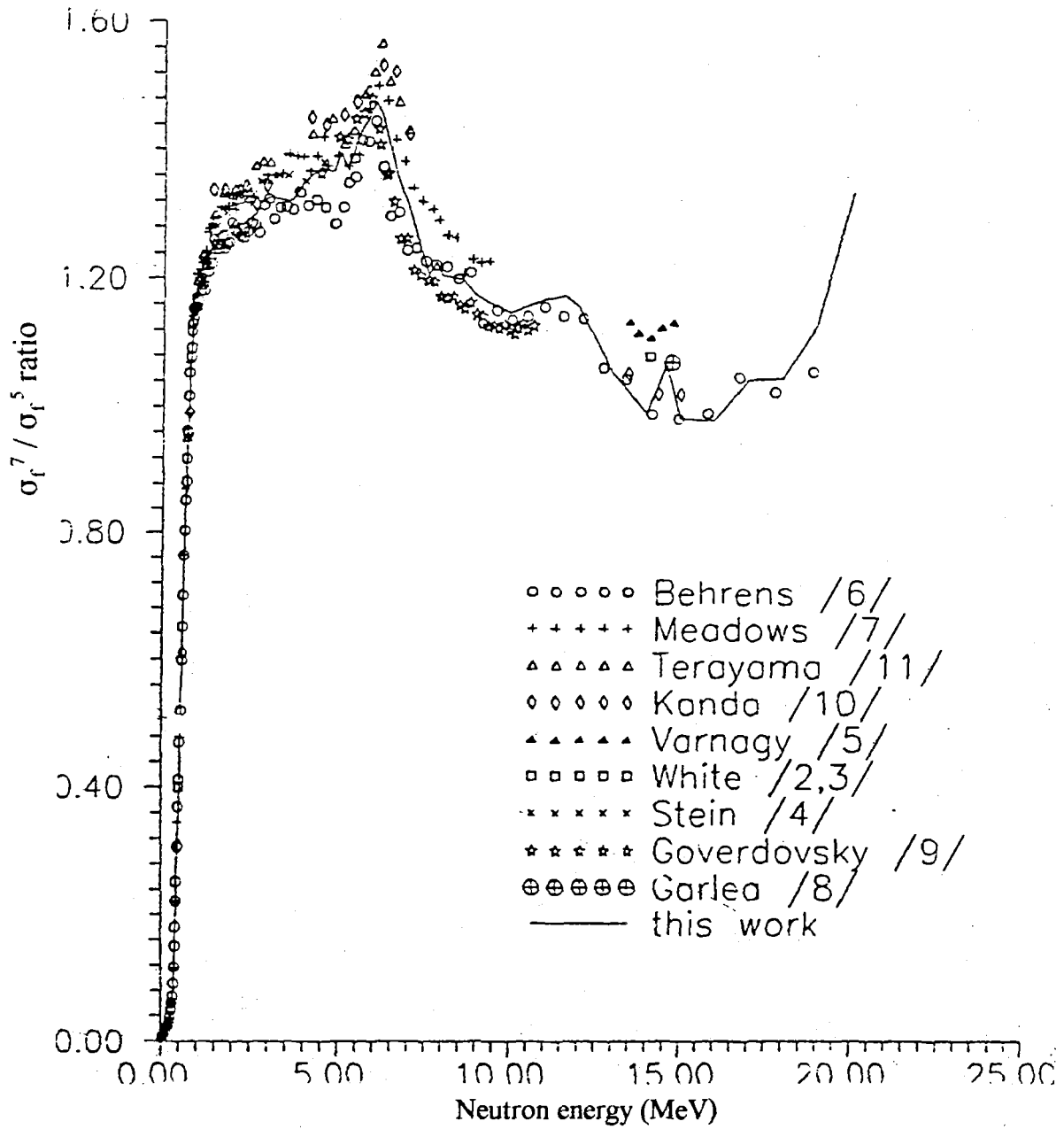


**Figure 3. Results of the neptunium fission cross section data from relative measurements given in the form of the  $\sigma_f^7 / \sigma_f^5$  ratio**

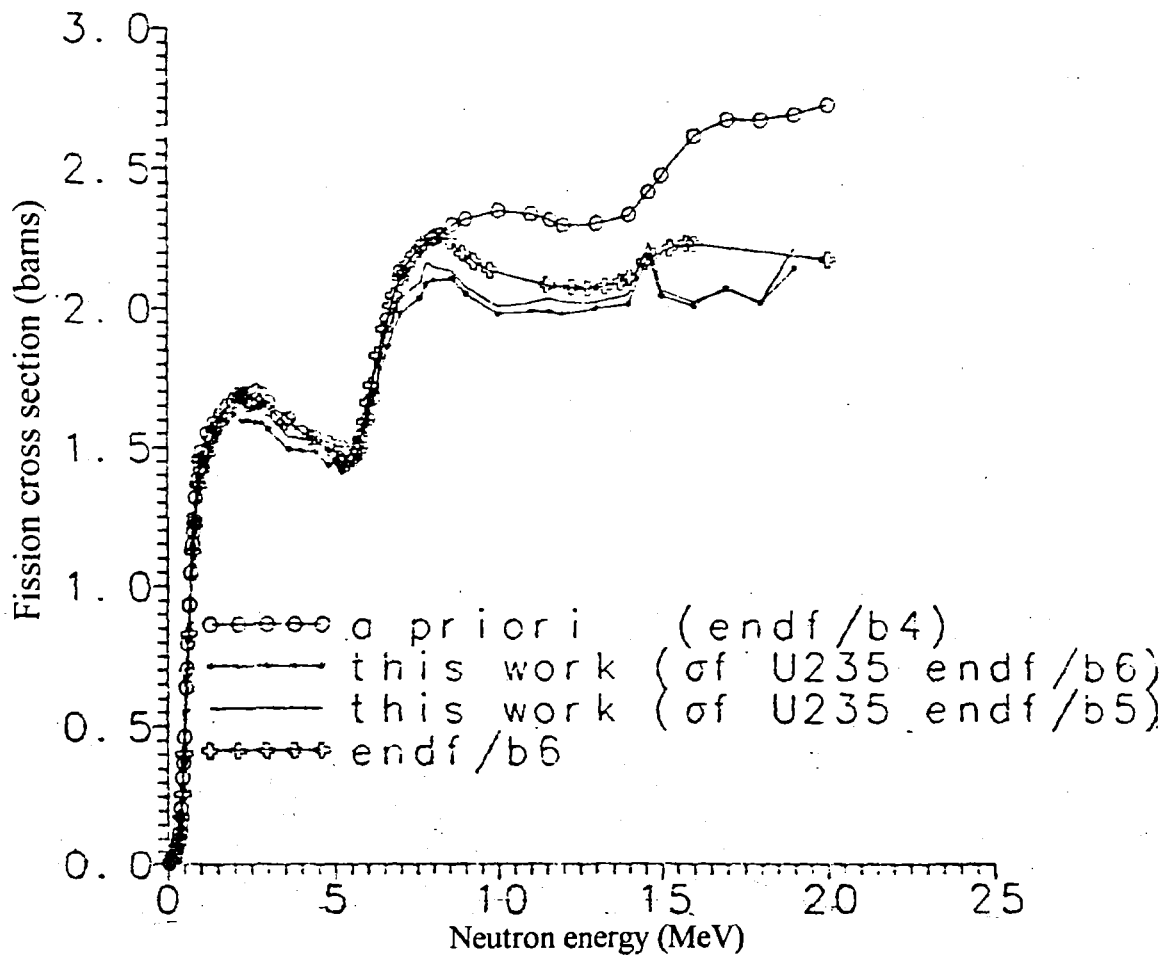


Figure 4. Comparison of the "a priori" data and data taken from ENDF/B-6 with the authors' evaluation of the  $^{237}\text{Np}$  fission cross section.

**Table 1.  $^{237}\text{Np}$  fission cross section evaluation results**

(Reference data taken from the ENDF/B-5 evaluated data file,  
uncertainties have been corrected)

N <sup>o</sup>	E, MeV	$\sigma_f$ , b	Error, b	N <sup>o</sup>	E, MeV	$\sigma_f$ , b	Error, b
1	0.024	0.0039	.0013	41	1.200	1.4652	.0300
2	0.030	0.0031	.0011	42	1.400	1.5635	.0332
3	0.040	0.0118	.0024	43	1.600	1.6036	.0411
4	0.045	0.0135	.0053	44	1.800	1.6417	.0431
5	0.050	0.0133	.0042	45	2.000	1.6747	.0413
6	0.065	0.0099	.0031	46	2.200	1.6539	.0455
7	0.070	0.0138	.0035	47	2.400	1.6497	.0405
8	0.076	0.0141	.0060	48	2.600	1.6365	.0370
9	0.080	0.0147	.0064	49	2.800	1.6383	.0427
10	0.090	0.0177	.0035	50	3.000	1.6152	.0374
11	0.100	0.0177	.0075	51	3.600	1.5367	.0486
12	0.110	0.0189	.0042	52	4.000	1.5295	.0458
13	0.150	0.0261	.0053	53	4.400	1.5279	.0427
14	0.159	0.0249	.0075	54	4.800	1.4786	.0451
15	0.180	0.0308	.0057	55	5.000	1.4845	.0464
16	0.200	0.0340	.0042	56	5.200	1.4418	.0389
17	0.224	0.0348	.0044	57	5.600	1.5067	.0418
18	0.250	0.0444	.0051	58	5.800	1.5441	.0480
19	0.268	0.0461	.0088	59	6.000	1.6418	.0477
20	0.269	0.0489	.0044	60	6.200	1.7612	.0400
21	0.300	0.0660	.0055	61	6.600	1.9184	.0418
22	0.333	0.0897	.0081	62	7.000	2.0323	.0422
23	0.350	0.1083	.0106	63	7.600	2.0942	.0651
24	0.372	0.1323	.0150	64	7.800	2.1644	.0708
25	0.400	0.1784	.0130	65	8.000	2.1470	.0649
26	0.450	0.2987	.0174	66	8.600	2.1314	.0537
27	0.470	0.3853	.0315	67	9.000	2.0779	.0482
28	0.500	0.3788	.0178	68	10.000	2.0053	.0460
29	0.550	0.5856	.0306	69	11.000	2.0204	.0752
30	0.570	0.6951	.0462	70	11.600	2.0369	.1142
31	0.600	0.7215	.0269	71	12.000	2.0216	.1274
32	0.650	0.9361	.0361	72	13.000	2.0230	.1148
33	0.700	1.0582	.0280	73	14.000	2.0504	.1074
34	0.750	1.1311	.0460	74	14.600	2.2383	.0809
35	0.775	1.2039	.0629	75	15.000	2.0678	.1009
36	0.800	1.2478	.0579	76	16.000	2.0257	.1405
37	0.850	1.3078	.0482	77	17.000	2.0726	.1619
38	0.900	1.3341	.0469	78	18.000	2.0257	.1646
39	0.950	1.3920	.0497	79	19.000	2.2231	.1705
40	1.000	1.4420	.0341	80	20.000	2.7353	1.155



## References

- [1] DERRIEN, H., DOAT, J.P., FORT, E., Evaluation of the  $^{237}\text{Np}$  fission cross section, INDC(FR)-42/L, IAEA, Vienna (1980).
- [2] WHITE, P.H., HODKINSON, J.D., WALL, G.I., in Proc. Int. Symp. on Phys. and Chem. of Fission, Salzburg, Vol. 1 (1965) 219.
- [3] WHITE, P.H., WARNER, G.P., J. Nuc. Energy 21 (1967) 671.
- [4] STEIN, W.E., SMITH, R.K., SMITH, H.L., in Proc. Int. Conf. on Neutron Cross Sections and Technology, Washington D.C., NBS Spec. Pub. 299 1 (1968) 627.
- [5] VARNAGY, M., CSIKAI, J., Nucl. Instr. Meth. 196 (1982) 465.
- [6] BEHRENS, J.W., et al., Nucl. Sci. Eng. 80 (1982) 393.
- [7] MEADOWS, J.W., Nucl. Sci. Eng. 85 (1983) 271.
- [8] GARLEA, I., et al., Rev. Romaine de Physique 29 (1984) 421.
- [9] GOVERDOVSKIY, A.A., et al., Atom. Ehnerg. 5 2 (1985) 137.
- [10] KANDA, K., et al., Rep. JAERI-M-85-035 (1985) 220.
- [11] TERAYAMA, H., KARINO, Y., MANABE, F., et al., Rep. NEANDC(J)-122 (1986).
- [12] GIACOLETTI, R.J., et al., Nucl. Sci. Eng. 48 (1972) 412.
- [13] DAVEY, W.B., Nucl. Sci. Eng. 26 (1966) 149.
- [14] PLATTARD, S., BLONS, J., PLAYA, D., Nucl. Sci. Eng. 61 (1976) 477.
- [15] SCHMITT, H.W., MURRAY, R.B., Phys. Rev. 116 (1959) 1575.
- [16] GRUNDL, J.A., Nucl. Sci. Eng. 30 (1967) 39.
- [17] RAGO, P.F., GOLDSTEIN, N., Health Phys. 14 (1968) 595.
- [18] CANCE, M., GRENIER, G., in Proc. Intern. Conf. Nucl. Data for Sci. and Techn., Antwerp (1982) 51.
- [19] JINGXIA, W., et al., Chin. J. of Nucl. Phys. 6 (1984) 369.
- [20] GUL, K., AHMAD, M., ANWAR, M., et al., Nucl. Sci. Eng. 94 (1986) 42.
- [21] PERKIN, J.L., et al., J. Nucl. Eng. 19 (1965) 423.

- [22] CARLSON, A.D., PATRICK, B.H., in Proc. Intern. Conf. on Nucl. Cross Sect. for Techn., Washington D.C. 1980, NBS Spec. Pub. 594 (1981) 971.
- [23] GRADY, D.J., BALDWIN, G.T., KNOLL, G.F., *ibid.* (1981) 976.
- [24] ZASADNY, J., Trans. At. Nucl. Soc. 47 (1984) 425.
- [25] DUSHIN, V.N., et al., Proc. IAEA Cons. Mtg. on U235 Fast Neutron Fission Cross Section, Smolenice, CSSR, 1983. IAEA Rep. INDC(NDS)-146 (1983) 53.
- [26] KALININ, V.A., KOVALENKO, S.S., KUZMIN, V.N., et al., Problems in Nuclear Science and Technology, Series: Nuclear Constants No.4 (1987) 3 [in Russian].
- [27] MANNHART, W., a Small Guide to Generate Covariance of Experimental Data, PTB-FMRB-84, ISSN 0341-666, PTB Braunschweig (1981).
- [28] MUIR, D.W., (Proc. IAEA Spec. Mtg. on Covariance Methods and Practices in the Field of Nuclear Data., Vienna, 1986), INDC(NDS)-192/L, IAEA, Vienna (1988) 113.
- [29] USACHEV, L.N., BOBKOV, Yu.G., Perturbation Theory and Planning of Experiments in the Field of Nuclear Data for Reactors, Moscow, Atomizdat (1980) [in Russian].
- [30] VAN'KOV, A.A., VOROPAEV, A.I., YUROVA, L.N., Analysis of a Reactor Physics Experiment, Moscow, Atomizdat (1977) [in Russian].
- [31] UENOHARA, Y., KANDA, Y., Proc. Intern. Conf. Nuclear Data for Science and Technology, Antwerp (1982) 639.
- [32] YUSDIBEKOV, N.R., TSATSKIN, M.L., Operation of Multiply Connected Control Systems, Moscow, Nauka (1990) [in Russian].
- [33] ARLT, R., HERBACH, C.M., JOSCH, M., et al., Proc. Adv. Gp. Mtg. On Nuclear Standard Reference Data, Geel, Belgium, 1984. IAEA-TECDOC-335 (1985) 174.
- [34] MERLA, K., Preprint 05-02-87, Technical University of Dresden, GDR (1987).



## EVALUATION OF PHOTONEUTRON REACTION CROSS SECTIONS OF RADIOACTIVE FISSION PRODUCT NUCLEI.

*Yu.N. Shubin, A.G. Gusseyenov, N.S. Rabotnov, V.P. Lunev.*

*State Research Centre of the Russian Federation  
Institute of Physics and Power Engineering, Obninsk*

### Abstract

Photonuclear reaction data have been calculated for long-lived fission products using a simple photoabsorption model and the data from the systematics of giant dipole resonances in spherical and deformed nuclei. Cross sections for the  $(\gamma, n)$ ,  $(\gamma, 2n)$  and  $(\gamma, 2n)$  reactions for gamma ray energies ranging up to 50 MeV are presented for 17 nuclei.

### Introduction

One of the stages in the development of an ecologically optimized nuclear fuel cycle will consist in the development of procedures to burn or transmute highly radioactive nuclear waste. There are two basic types of nuclear waste that are the cause of great concern, namely transactinides and fission products which have a high yield and have half-lives of a few tens of years. The most likely means to execute these procedures is the utilization of the hard neutron spectrum which exists in fast reactors. However, there is another method that offers a potential possibility, namely, using beams of charged particle, high energy neutrons or gamma rays generated by high energy proton or electron accelerators. In order to be able to implement such methods using accelerators, there is a need to produce evaluated nuclear data which describe the interaction of these high energy particles with radioactive nuclides. As experimental data for these reactions do not exist, there is a need to develop reliable calculational methods to generate the corresponding reaction cross sections and spectra, as well as to perform a broad investigation of existing methods that have been tested with stable isotopes.

One of the first steps of this investigation consists of performing calculations whose results lead to the data needed to implement the above mentioned procedures for the transmutation of long-lived isotopes. The energy dependence of the following photonuclear reaction cross section isotopes were evaluated:

$^{90}\text{Sr}$  ( $T_{1/2} = 29.1$  y),  $^{126}\text{Sn}$  ( $T_{1/2} = 1 \cdot 10^5$  y.),  $^{137}\text{Cs}$  ( $T_{1/2} = 30.1$  y.),  $^{93}\text{Zr}$  ( $T_{1/2} = 1.53 \cdot 10^6$  y.),  
 $^{94}\text{Nb}$  ( $T_{1/2} = 2.3 \cdot 10^4$  y.),  $^{96}\text{Zr}$  ( $T_{1/2} = 3.56 \cdot 10^{17}$  y.),  $^{99}\text{Tc}$  ( $T_{1/2} = 2.111 \cdot 10^5$  y.),  
 $^{107}\text{Pd}$  ( $T_{1/2} = 6.5 \cdot 10^6$  y.),  $^{108}\text{Ag}$  ( $T_{1/2} = 127$  y.),  $^{121}\text{Sn}$  ( $T_{1/2} = 55$  y.),  $^{129}\text{I}$  ( $T_{1/2} = 1.57 \cdot 10^7$  y.),  
 $^{135}\text{Cs}$  ( $T_{1/2} = 2.3 \cdot 10^6$  y.),  $^{147}\text{Sm}$  ( $T_{1/2} = 1.06 \cdot 10^{11}$  y.),  $^{148}\text{Sm}$  ( $T_{1/2} = 7.0 \cdot 10^{15}$  y.),  
 $^{151}\text{Sm}$  ( $T_{1/2} = 90$  y.),  $^{158}\text{Tb}$  ( $T_{1/2} = 180$  y.),  $^{166}\text{Ho}$  ( $T_{1/2} = 81.6$  h.).

## 1. Models and methods used in the photoneutron reaction cross section evaluations

### a) Spherical nuclei

The total photoabsorption cross section  $\sigma_\gamma(E_\gamma)$  for stable nuclides has been thoroughly investigated up to  $E_\gamma$  energies ranging from 25 to 30 MeV, as well as the basic components of the total cross section in this energy range, namely, the  $(\gamma,n)$  and  $(\gamma,2n)$  reactions. For other isotopes data exists for the  $(\gamma,3n)$  reactions in the vicinity of the threshold. Data that were available in the middle of the seventies have been compiled and published in the well known Berman data atlas. All of these data provide the basis to conclude that the energy dependence of the indicated cross sections reveal simple and universal regularities which makes it possible to evaluate these cross sections for those isotopes that are not being investigated, including the radioactive target nuclei as well, to a high degree of reliability. To a smaller degree of confidence, it is possible to extrapolate the corresponding data up to energies of 50 MeV.

The observed regularities can be summarized as follows:

1. The energy dependence of  $\sigma_\gamma(E)$  is dominated by the "gigantic resonance" which can be satisfactorily described by the following lorentzian

$$\sigma_\gamma(E) = \sigma_0 / \left( 1 + (E^2 - E_0^2) / E_\gamma^2 \cdot \Gamma^2 \right), \quad (1)$$

where  $\sigma_0$  is the value of the resonance cross section,  $E_0$  is the resonance energy, and  $\Gamma$  is the resonance width. Table 1 lists experimentally determined gigantic resonance parameters for spherical nuclei in the energies of interest which were taken from the atlas [1].

2. Above the  $(\gamma,n)$  reaction threshold, the increase of the neutron width quickly overwhelms the competing radiative decay; as a result, the contribution of this channel can be neglected.

3. For energies above  $E_0$ , on the right side of the gigantic resonance the cross section can noticeably exceed the lorentzian extrapolation, sometimes by a factor of two. There is a tendency to consider this to be a contribution of resonances of other multiplicities, primarily quadrupolarity (see for instance reference [2]). If one approximates this contribution by a lorentzian as well, then its characteristics are most probably the following:

- (I) the resonance energy is larger than the dipolar resonance by 10-15 MeV,
- (ii) its amplitude is one order of magnitude lower, and
- (iii) its width is approximately the same.

The relationship of the probability of emission of the number of neutrons in the confines of the allowed energy balance, is described satisfactorily by the evaporation model in which the neutron spectrum has a Maxwellian distribution

$$f(E_n, T) \cdot dE_n = C \cdot E_n \cdot e^{-E_n/T} \cdot dE_n \quad (2)$$

The thermodynamic temperature  $T$  for the purpose of our analysis may be defined by Dilg's formula [3] ("back-shifted model")

$$T = (1 + (1 + 4aE)^{1/2}) / 2a, \quad E = U - \Delta, \quad (3)$$

where  $U$  is the excitation energy, and the  $a$  and  $\Delta$  parameters are systematized as in reference [3]. This systematization gives the possibility to evaluate the values of these parameters for the radioactive nuclides of interest to our analysis.

All of the "giant resonance" parameters and neutron spectra of interest to us are obtained to a relatively low degree of accuracy; as a result, the following additional simplifying assumptions may be justifiably introduced in the calculations:

1. The stepwise energy dependence of the neutron energy  $T = T_x$  is constant for  $B_{xn} < E_\gamma < B_{(x+1)n}$ , where  $B_{xn}$  is the threshold of the  $(\gamma, xn)$  reaction.
2. At each energy, only two competing photoneutron reactions with a number of emitted neutron are taken into account.
3. Omission of those reactions for which  $x > 3$  and  $E_\gamma < 50$  MeV.

Together with the mentioned omission of the radiation width this leads to the following expressions for the  $(\gamma, xn)$  reactions:

$$\sigma(\gamma, n) = \begin{cases} \sigma_\gamma, & \text{for } B_n < E_\gamma < B_{2n} \\ \sigma_\gamma - \sigma(\gamma, 2n), & \text{for } B_{2n} < E_\gamma < B_{3n} \end{cases} \quad (4-a)$$

$$\alpha(\gamma, 2n) = \begin{cases} \sigma_\gamma \cdot \frac{\int_0^{E_\gamma - B_{2n}} f(E, T_2) \cdot dE}{\int_0^{E_\gamma - B_n} f(E, T_2) \cdot dE}, & \text{for } B_{2n} < E_\gamma < B_{3n} \\ \sigma_\gamma - \alpha(\gamma, 3n), & \text{for } B_{3n} < E_\gamma < B_{4n} \end{cases} \quad (4-b)$$

$$\alpha(\gamma, 3n) = \sigma_\gamma \frac{\int_{E_1 + E_2 < E_\gamma - B_{3n}} dE_1 dE_2 f(E_1, T_3) f(E_2, T_2)}{\int_{E_1 + E_2 < E_\gamma - B_{2n}} dE_1 dE_2 f(E_1, T_3) f(E_2, T_2)}. \quad (5)$$

Introducing expression (2) into these formulas and performing the integration, gives

$$\sigma(\gamma, 2n) = \sigma_\gamma \cdot \left( 1 - \frac{E_\gamma - B_{2n} + T_2}{T_2} \right) \cdot e^{-(E_\gamma - B_{2n})/T_2}, \quad (6)$$

$$\alpha(\gamma, 3n) = \sigma_\gamma \cdot I(E_\gamma - B_{3n}) / I(E_\gamma - B_{2n}),$$

where

$$I(E) = T_3^2 - T_3 \cdot (E + T_3) \cdot e^{-E/T_3} - (1 + E/T_2) \cdot e^{-E/T_2} \cdot T^2 - e^{-E/T} \cdot T \cdot (E + T) + e^{-E/T} \cdot (2T^3 - 2T^2 \cdot (T + E) \cdot e^{-E/T} - E^2 \cdot T \cdot e^{-E/T}) / T_2, \quad (7)$$

where  $T = T_3 T_2 / (T_3 + T_2)$ .

The totality of the parameter values for spherical nuclei which were used in the calculations is listed in Table 2.1. The threshold values for the reactions (binding energy) were taken from reference [4].

The results of the calculated  $(\gamma,n)$  reactions for spherical nuclei are given in Tables 3.1 and 3.2, for  $(\gamma,2n)$  reactions in Tables 4.1 and 4.2 and for  $(\gamma,3n)$  reactions in Tables 5.1 and 5.2. The calculational results for the  $(\gamma,n)$ ,  $(\gamma,2n)$  and  $(\gamma,3n)$  reactions and their sums are shown in Figures 1 - 6, for the  $^{90}\text{Sr}$ ,  $^{93}\text{Zr}$ ,  $^{99}\text{Tc}$ ,  $^{129}\text{I}$ ,  $^{137}\text{Cs}$ , and  $^{148}\text{Sm}$  isotopes.

#### b) Deformed nuclei

In contrast to nuclides that had been under consideration earlier, in the case of strongly deformed nuclei such as  $^{151}\text{Sm}$ ,  $^{158}\text{Tb}$  and  $^{166}\text{Ho}$ , in the process of the calculation of the photonuclear reaction cross sections it is necessary to take the breakup of the giant resonances into consideration. The photoabsorption cross section is the sum of two giant resonances, dipole and quadrupole. Thus, in the case of strongly deformed nuclei we have adopted the following simple assumptions regarding the nature of this breakup:

1. Each giant resonance is represented by the sum of two lorentzians.
2. Each lorentzian is defined by three parameters:  $\sigma_0$  which is the value of the cross section of the resonance,  $E_0$  is the resonance energy, and  $\Gamma$  the resonance width. It is assumed that the amplitude of the quadrupole resonance is 10 times smaller than the dipole resonance, that the resonance energy is greater by 10 MeV, that the widths are equal, and that these assumptions refer to each constituent lorentzian.
3. The thermodynamical temperature  $T$  is evaluated with the use of the Gilg formula [3],  $U$  is the excitation energy, and the  $a$  and  $\Delta$  parameters are systematized as in reference [3].
4. It is assumed that the energy dependence of the temperature has a stepwise character, that  $T = T_x$  is constant for  $B_{xn} < E_\gamma < B_{(x+1)n}$ , where  $B_{xn}$  is the threshold of the  $(\gamma,xn)$  reaction.
5. For each energy, only two competing photoneutron reactions each having a number of emitted neutrons are taken into account.
6. For  $E_\gamma < 50$  MeV, and for reactions which emit charged particles, photoneutron reactions for which  $x > 3$  are omitted.

The totality of the parameter values used in the calculation of photonuclear reaction cross sections of deformed nuclei are listed in Table 2.2. The threshold values (binding energies) are taken from reference [4].

The results of the calculated  $(\gamma,n)$  reactions for deformed nuclei are given in Tables 3.3, for  $(\gamma,2n)$  reactions in Tables 4.3 and for  $(\gamma,3n)$  reactions in Tables 5.3. The calculational results for the  $(\gamma,n)$ ,  $(\gamma,2n)$  and  $(\gamma,3n)$  reactions for  $^{151}\text{Sm}$  and  $^{166}\text{Ho}$  and their sums are shown in Figures 7 and 8.

**Table 1. Giant dipole resonance parameters for spherical nuclei of intermediate mass** (see equation (1) in the text). (The atomic weight is not indicated if the parameters were determined for a natural mixture)..

Нуклид	$E_0$	$\sigma_0$	$\Gamma$	Нуклид	$E_0$	$\sigma_0$	$\Gamma$
-Rb	16.80	190	4.47	118-Sn	15.59	256	4.77
-Sr	16.84	206	4.50		15.44	279	4.86
89-Y	16.79	185	3.95	119-Sn	15.53	253	4.81
	16.74	226	4.25	120-Sn	15.40	280	4.89
	16.83	205	3.69		15.37	285	5.10
90-Zr	16.85	185	4.02	124-Sn	15.19	283	4.81
	16.74	211	4.16		15.28	276	4.80
91-Zr	16.58	184	4.20	-Sb	15.48	277	5.05
92-Zr	16.26	166	4.68	-Te	15.40	297	5.32
92-Mo	16.82	162	4.14	133-Cs	15.25	287	5.02
93-Nb	16.59	200	5.05		15.34	317	5.31
94-Zr	16.22	161	5.29	138-Ba	15.26	327	4.61
94-Mo	16.36	185	5.50	-Ba	15.29	356	4.89
96-Mo	16.20	185	6.01	139-La	15.24	336	4.47
98-Mo	15.80	189	5.94	-Ce	14.95	351	4.64
100-Mo	15.74	171	7.81		15.15	324	4.42
103-Rh	16.16	191	7.26	141-Pr	15.23	341	4.00
-Pd	15.92	199	7.18		15.04	347	4.49
107-Ag	15.90	150	6.71		15.36	332	4.07
-Ag	16.07	199	7.38	-Nd	14.92	315	4.70
-Cd	15.81	227	6.22	142-Nd	14.94	359	4.44
115-In	15.63	266	5.24	143-Nd	15.01	349	4.75
	15.72	247	5.60	144-Nd	15.05	317	5.28
116-Sn	15.68	266	4.19	144-Sm	15.32	383	4.45
	15.56	271	5.08	145-Nd	14.95	296	6.31
117-Sn	15.66	254	5.02	146-Nd	14.74	310	5.78
	15.64	259	5.04				

Table 2.1. Tabulated parameters used in the calculations of photonuclear reaction cross sections. ("Нуклид" = nuclide, "мб" = mb and "МэВ" = MeV.) (The parameters for the "quadrupole" resonance were determined using the following parameter:  $F_v = F_v^{qp} + 10$  MeV;  $\sigma_0 = \sigma_0^{qp} \cdot 0.1$ ;  $\Gamma = \Gamma^{qp}$ ).

Нуклиды	<sup>90</sup> Sr	<sup>92</sup> Zr	<sup>90</sup> Zr	<sup>94</sup> Nb	<sup>99</sup> Tc	<sup>107</sup> Pd	<sup>108</sup> Ag	<sup>121</sup> Sn	<sup>128</sup> Sn	<sup>129</sup> I	<sup>135</sup> Cs	<sup>137</sup> Cs	<sup>147</sup> Sm	<sup>148</sup> Sm
$E_0^1$ , МэВ	16.8	16.3	16.0	16.5	16.0	16.0	16.0	15.5	15.0	15.5	15.0	15.2	14.8	14.8
$\sigma_{01}$ , мб	200.0	170.0	160.0	200.0	190.0	200.0	180	260	280.0	300	300	300.0	320	200.0
$\Gamma_{11}$ , МэВ	4.2	5.0	5.5	5.0	6.5	7.0	7.0	5.0	4.8	5.0	5.0	4.8	5.0	5.0
$B_{1n}$ , МэВ	7.806	6.750	7.840	7.230	8.890	6.530	7.27	6.18	8.196	8.84	8.82	8.279	6.37	8.14
$B_{2n}$ , МэВ	14.169	15.400	14.310	16.050	16.280	16.090	16.81	15.28	13.928	15.68	15.71	15.049	14.80	14.51
$B_{3n}$ , МэВ	25.282	23.290	22.500	23.950	25.670	23.170	24.73	21.77	22.420	24.80	24.70	23.940	21.56	22.94
$B_{4n}$ , МэВ		35.27	29.26	35.99	33.58	33.19	34.58	31.10	15.0	31.91	31.88	15.0	32.11	29.76
$a$ , МэВ	10.0	12.3	11.0	12.0	13.0	15.0	14.8	16.4	1.5	15.5	15.0	0.0	18.0	16.8
$\Delta$ , МэВ	1.5	0.8	0.8	-0.75	-0.5	-0.4	-0.9	0.9	0.83	-0.3	-0.2	0.92	-1.0	0.64
$T_1$ , МэВ	1.03	0.95	1.01	1.06	1.04	0.92	0.97	0.78	1.09	0.93	1.00	1.17	0.83	0.83
$T_2$ , МэВ	1.40	1.29	1.31	1.35	1.32	1.19	1.24	1.00	1.30	1.18	1.20	1.38	1.06	1.07
$T_3$ , МэВ	1.72	1.52	1.56	1.64	1.56	1.41	1.47	1.28		1.39	1.41		1.27	1.26

Table 2.2. Parameters used for photonuclear reaction calculations for deformed nuclei.

Нуклид	$E_0^1$ , МэВ	$\sigma_{01}$ , мб	$\Gamma_{11}$ , МэВ	$E_0^2$ , МэВ	$\sigma_{02}$ , мб	$\Gamma_{12}$ , МэВ	$B_{1n}$ , МэВ	$B_{2n}$ , МэВ	$B_{3n}$ , МэВ	$B_{4n}$ , МэВ	$a$ , МэВ	$\Delta$ , МэВ	$T_1$ , МэВ	$T_2$ , МэВ	$T_3$ , МэВ
<sup>151</sup> Sm	12.4	176	3.0	15.7	230	5.2	5.59	13.58	9.55	27.76	18.2	-1.0	0.79	1.01	1.17
<sup>159</sup> Tb	12.2	190	2.8	15.8	230	5.0	6.75	15.36	22.44	31.26	18.0	-1.0	0.82	1.05	1.24
<sup>166</sup> Ho	12.1	230	2.5	15.7	290	5.0	6.24	14.23	20.92	29.38	18.0	-0.9	0.82	1.04	1.23

Table 3.1. Energy dependence of the ( $\gamma, n$ ) reaction cross sections for spherical nuclei.

$E_\gamma$	$^{90}\text{Sr}$	$^{93}\text{Zr}$	$^{96}\text{Zr}$	$^{94}\text{Nb}$	$^{99}\text{Tc}$	$^{107}\text{Pd}$	$^{108}\text{Ag}$
7.0		4.37				10.73	
7.5		5.33		5.91		13.06	11.75
8.0	4.68	6.50	8.06	7.19		15.84	14.26
8.5	5.67	7.90	9.82	8.73		19.17	17.25
9.0	6.88	9.61	11.96	10.59	19.27	23.16	20.85
9.5	8.36	11.71	14.58	12.87	23.36	27.98	25.18
10.0	10.17	14.30	17.83	15.67	28.34	33.81	30.43
10.5	12.44	17.54	21.87	19.16	34.44	40.88	36.79
11.0	15.29	21.61	26.94	23.53	41.93	49.47	44.52
11.5	18.92	26.80	33.35	29.06	51.14	59.89	53.90
12.0	23.61	33.44	41.48	36.14	62.45	72.48	65.23
12.5	29.76	42.03	51.80	45.25	76.23	87.52	78.77
13.0	37.92	53.17	64.81	57.05	92.74	105.11	94.60
13.5	48.88	67.53	80.89	72.33	111.92	125.00	112.50
14.0	63.72	85.70	99.95	91.84	133.08	146.27	131.64
14.5	81.70	107.64	119.63	115.94	154.51	167.13	150.42
15.0	96.71	131.76	126.73	143.65	173.40	184.99	166.49
15.5	106.75	153.47	119.32	171.41	186.43	197.04	177.33
16.0	108.55	154.52	101.10	192.69	191.09	201.32	181.19
16.5	99.02	133.71	78.07	191.89	184.58	188.47	177.86
17.0	79.51	102.76	55.96	163.16	157.36	154.25	166.94
17.5	56.75	72.49	38.05	123.96	122.46	115.95	139.13
18.0	37.27	48.39	25.02	87.43	89.90	82.45	106.24
18.5	23.40	31.32	16.15	58.98	63.56	56.51	76.89
19.0	14.43	19.96	10.34	38.84	43.89	37.81	53.79
19.5	8.89	12.66	6.60	25.31	29.88	24.92	36.82
20.0	5.51	8.03	4.23	16.44	20.19	16.29	24.88
20.5	3.45	5.12	2.72	10.70	13.60	10.60	16.69
21.0	2.19	3.28	1.76	7.00	9.17	6.89	11.16
21.5	1.40	2.13	1.15	4.61	6.20	4.49	7.46
22.0	0.91	1.39	0.76	3.07	4.21	2.94	5.01
22.5	0.60	0.92	0.51	2.07	2.89	1.93	3.37
23.0	0.40	0.62		1.41	1.99	1.28	2.29
23.5	0.28			0.98	1.39		1.56
24.0	0.19				0.98		1.07
24.5	0.14				0.69		0.74
25.0	0.10				0.49		
25.5					0.34		

Table 3.2. Energy dependence of the( $\gamma$ ,n) reaction cross sections for spherical nuclei.

$E_\gamma$	$^{121}\text{Sn}$	$^{126}\text{Sn}$	$^{129}\text{I}$	$^{135}\text{Cs}$	$^{137}\text{Cs}$	$^{147}\text{Sm}$	$^{148}\text{Sm}$
7.0	6.89					10.56	
7.5	8.51					13.12	
8.0	10.47					16.26	
8.5	12.85	18.79			18.65	20.13	24.94
9.0	15.77	23.29	22.36	26.89	23.05	24.94	30.97
9.5	19.38	28.97	27.55	33.39	28.58	30.96	38.58
10.0	23.88	36.21	34.07	41.64	35.61	38.57	48.29
10.5	29.53	45.54	42.34	52.23	44.62	48.28	60.79
11.0	36.70	57.68	52.94	65.91	56.30	60.78	76.99
11.5	45.88	73.58	66.62	83.69	71.56	76.99	98.06
12.0	57.73	94.43	84.37	106.74	91.57	98.06	125.31
12.5	73.12	121.50	107.37	136.27	117.71	125.30	159.84
13.0	93.05	155.60	136.80	172.78	151.13	159.84	201.59
13.5	118.56	192.70	173.19	214.79	191.76	201.58	247.47
14.0	150.09	204.37	215.04	256.83	236.22	247.47	289.59
14.5	186.36	187.58	256.93	288.96	275.82	289.59	316.36
15.0	222.67	150.96	288.99	301.01	298.36	316.35	294.59
15.5	250.46	108.04	301.03	289.98	278.92	313.97	228.53
16.0	255.62	70.56	280.35	255.85	218.69	256.21	157.91
16.5	210.76	43.36	220.67	195.60	153.47	182.01	101.59
17.0	149.22	25.75	156.36	137.16	100.78	119.06	62.72
17.5	96.19	15.05	104.20	91.72	63.79	74.27	37.88
18.0	58.66	8.76	67.11	59.78	39.63	45.15	22.65
18.5	34.69	5.10	42.47	38.47	24.42	27.11	13.51
19.0	20.20	2.99	26.67	24.63	15.03	16.20	8.07
19.5	11.69	1.76	16.72	15.77	9.26	9.69	4.84
20.0	6.76	1.05	10.51	10.13	5.73	5.81	2.93
20.5	3.92	0.63	6.64	6.55	3.57	3.51	1.79
21.0	2.29	0.38	4.23	4.27	2.24	2.14	1.10
21.5	1.35	0.24	2.72	2.82	1.42	1.32	0.69
22.0	0.80	0.15	1.77	1.89	0.91	0.82	0.44
22.5			1.17	1.29	0.59		0.29
23.0			0.79	0.90	0.39		
23.5			0.54	0.63	0.26		
24.0			0.38	0.45			
24.5			0.27	0.31			

**Table 3.3. Energy dependence of the ( $\gamma,n$ ) reaction cross sections for deformed nuclei.**

$E_\gamma$	$^{151}\text{Sm}$	$^{158}\text{Tb}$	$^{166}\text{Ho}$
6.00	9.05	8.64	
6.50	11.45	10.98	12.74
7.00	14.47	13.95	16.15
7.50	18.31	17.76	20.54
8.00	23.27	22.73	26.27
8.50	29.79	29.39	33.95
9.00	38.56	38.53	44.55
9.50	50.66	51.46	59.71
10.00	67.82	70.37	82.31
10.50	92.69	98.66	117.24
11.00	128.59	140.47	171.23
11.50	176.65	195.06	244.21
12.00	226.66	242.71	303.11
12.50	254.38	253.54	303.91
13.00	252.75	236.60	275.59
13.50	243.68	222.57	261.11
14.00	227.50	223.37	268.20

$E_\gamma$	$^{151}\text{Sm}$	$^{158}\text{Tb}$	$^{166}\text{Ho}$
14.50	194.52	236.32	281.28
15.00	156.19	253.00	259.46
15.50	116.65	260.84	212.21
16.00	80.43	225.84	155.53
16.50	51.55	167.77	103.90
17.00	31.26	112.67	64.88
17.50	18.29	71.05	38.85
18.00	10.51	43.23	22.75
18.50	5.99	25.85	13.22
19.00	3.42	15.37	7.68
19.50	1.97	9.17	4.50
20.00		5.53	2.67
20.50		3.39	1.62
21.00		2.14	
21.50		1.39	
22.00		0.90	

**Table 4.1. Energy dependence of the ( $\gamma,2n$ ) reaction cross sections for spherical nuclei**

$E_\gamma$	$^{90}\text{Sr}$	$^{93}\text{Zr}$	$^{96}\text{Zr}$	$^{94}\text{Nb}$	$^{99}\text{Tc}$	$^{107}\text{Pd}$	$^{108}\text{Ag}$
14.5	2.00		1.20				
15.0	13.16		13.98				
15.5	34.85	0.47	35.98				
16.0	65.39	13.56	59.56				
16.5	97.37	35.84	77.72	8.81	2.40	9.15	
17.0	119.24	56.06	87.19	30.17	18.51	33.19	1.75
17.5	124.57	68.27	88.69	50.72	38.14	57.21	16.71
18.0	116.67	72.29	84.86	63.94	54.01	74.70	35.19
18.5	102.69	70.67	78.30	69.42	64.08	84.64	50.14
19.0	87.82	66.05	70.86	69.38	68.92	88.41	59.81
19.5	74.44	60.26	63.56	66.17	69.95	87.95	64.76
20.0	63.23	54.37	56.91	61.51	68.57	84.98	66.26
20.5	54.11	48.92	51.12	56.45	65.86	80.76	65.53
21.0	46.81	44.13	46.21	51.59	62.59	76.13	63.56
21.5	41.01	40.06	42.17	47.22	59.27	71.62	61.03
22.0	36.45	36.74	38.94	43.47	56.20	67.54	58.42
22.5	32.92	34.15	36.47	40.43	53.57	64.06	56.01
23.0	30.30	32.27	35.06	38.12	51.49	61.23	53.97
23.5	28.51	31.52	33.70	36.56	49.97	59.89	52.34
24.0	27.55	30.85	32.57	36.49	48.96	57.69	51.10
24.5	27.45	30.59	31.39	36.26	48.28	55.18	50.10
25.0	28.23	30.34	29.84	36.52	47.66	51.82	49.63

Table 4.1. (Cont.)

$E_\nu$	$^{90}\text{Sr}$	$^{93}\text{Zr}$	$^{96}\text{Zr}$	$^{94}\text{Nb}$	$^{99}\text{Tc}$	$^{107}\text{Pd}$	$^{108}\text{Ag}$
25.5	29.87	29.57	27.59	36.65	46.74	47.38	48.10
26.0	31.63	27.76	24.53	35.84	45.47	41.95	45.65
26.5	32.42	24.72	20.84	33.48	43.06	35.92	42.07
27.0	31.05	20.81	16.98	29.58	39.76	29.80	37.51
27.5	27.54	16.74	13.41	24.85	35.72	24.06	32.43
28.0	23.00	13.05	10.36	20.12	31.30	19.00	27.31
28.5	18.57	9.99	7.90	15.92	26.85	14.75	22.51
29.0	14.76	7.58	5.99	12.44	22.63	11.31	18.24
29.5	11.67	5.73	4.51	9.66	18.80	8.58	14.58
30.0	9.22	4.32	3.40	7.48	15.43	6.47	11.52
30.5	7.28	3.25	2.55	5.78	12.53	4.84	9.03
31.0	5.75	2.44	1.91	4.46	10.09	3.61	7.01
31.5	4.53	1.83	1.43	3.44	8.07	2.68	5.41
32.0	3.58	1.37	1.07	2.65	6.40	1.98	4.15
32.5	2.81	1.03	0.80	2.04	5.05	1.45	3.17
33.0	2.21	0.77	0.59	1.56	3.96	1.07	2.41
33.5	1.73	0.57	0.44	1.20	3.09	0.78	1.82
34.0	1.36	0.43	0.33	0.92	2.40	0.57	1.37
34.5	1.06	0.32	0.24	0.70	1.85	0.41	1.03
35.0	0.82	0.23	0.18	0.53	1.43	0.30	0.77
35.5	0.64	0.17	0.13	0.40	1.09	0.22	0.57
36.0	0.50	0.13	0.10	0.31	0.84	0.15	0.42
36.5	0.38	0.09	0.07	0.23	0.64	0.11	0.31
37.0	0.30	0.07	0.05	0.17	0.48	0.08	0.23
37.5	0.23	0.05	0.04	0.13	0.37	0.06	0.17
38.0	0.17	0.03	0.02	0.10	0.28	0.04	0.12
38.5	0.13	0.02	0.02	0.07	0.21	0.03	0.09
39.0	0.10	0.02	0.01	0.05	0.15	0.02	0.06
39.5	0.08	0.01	0.01	0.04	0.11	0.01	0.05
40.0	0.06	0.01		0.03	0.08	0.01	0.03
40.5	0.04			0.02	0.06		0.02
41.0	0.03			0.01	0.05		0.01
41.5	0.02			0.01	0.03		
42.0	0.02			0.01	0.02		
42.5	0.01				0.02		
43.0	0.01				0.01		
43.5					0.01		

Table 4.2. Energy dependence of the (n,2n) reaction cross sections for spherical nuclei.

E.	<sup>121</sup> Sn	<sup>126</sup> Sn	<sup>129</sup> I	<sup>135</sup> Cs	<sup>137</sup> Ba	<sup>147</sup> Sm	<sup>148</sup> Sm
13.5		2.97					
14.0		32.33					
14.5		81.15					
15.0		129.91				5.15	24.55
15.5	5.27	161.67			17.07	42.79	70.49
16.0	40.56	171.37	9.64	6.32	53.25	83.20	107.31
16.5	77.95	164.47	41.46	31.85	83.31	108.67	126.15
17.0	100.81	149.15	70.95	56.09	99.42	118.53	130.09
17.5	108.62	131.41	88.82	71.47	103.67	117.75	125.03
18.0	106.48	114.42	95.78	78.42	100.52	111.26	115.73
18.5	99.27	99.46	95.39	79.51	93.69	102.44	105.14
19.0	90.23	86.84	90.94	77.18	85.52	93.21	94.84
19.5	81.14	76.44	84.71	73.19	77.32	84.59	85.57
20.0	72.84	68.02	78.07	68.66	69.74	77.03	77.62
20.5	65.67	61.32	71.78	64.27	63.06	70.72	71.09
21.0	59.72	56.14	66.24	60.43	57.37	65.73	65.95
21.5	54.98	52.33	61.64	57.38	52.70	62.06	62.20
22.0	51.90	49.82	58.11	55.29	49.05	60.22	59.83
22.5	49.05	48.65	55.71	54.27	46.43	58.48	58.82
23.0	46.59	48.48	54.48	54.33	44.88	56.83	59.23
23.5	44.08	48.80	54.40	55.30	44.40	54.59	60.18
24.0	41.26	48.55	55.29	56.65	44.99	51.05	60.52
24.5	37.84	46.57	56.57	57.39	45.50	45.67	58.46
25.0	33.48	42.13	57.46	56.68	44.68	38.55	53.14
25.5	28.12	35.60	56.31	53.39	41.32	30.67	45.22
26.0	22.28	28.30	52.54	48.03	35.79	23.24	36.41
26.5	16.76	21.54	46.50	41.48	29.49	17.04	28.16
27.0	12.14	15.96	39.39	34.75	23.56	12.25	21.23
27.5	8.60	11.65	32.32	28.48	18.51	8.72	15.74
28.0	6.01	8.44	25.95	22.97	14.39	6.17	11.56
28.5	4.18	6.08	20.52	18.30	11.11	4.35	8.42
29.0	2.90	4.37	16.05	14.44	8.52	3.06	6.10
29.5	2.01	3.13	12.44	11.29	6.51	2.15	4.40
30.0	1.39	2.24	9.57	8.76	4.94	1.51	3.16
30.5	0.96	1.60	7.31	6.75	3.73	1.05	2.26
31.0	0.66	1.14	5.56	5.17	2.80	0.74	1.61
31.5	0.46	0.81	4.20	3.94	2.09	0.51	1.14
32.0	0.31	0.57	3.15	2.98	1.56	0.36	0.81
32.5	0.22	0.40	2.36	2.24	1.16	0.25	0.57
33.0	0.15	0.28	1.76	1.68	0.85	0.17	0.40
33.5	0.10	0.20	1.30	1.26	0.63	0.12	0.28
34.0	0.07	0.14	0.96	0.93	0.46	0.08	0.20
34.5	0.04	0.10	0.71	0.69	0.33	0.05	0.14

Table 4.2. (Cont.)

$E_\gamma$	$^{121}\text{Sn}$	$^{126}\text{Sn}$	$^{129}\text{I}$	$^{135}\text{Cs}$	$^{137}\text{Cs}$	$^{147}\text{Sm}$	$^{148}\text{Sm}$
35.0	0.03	0.07	0.52	0.51	0.24	0.04	0.10
35.5	0.02	0.04	0.38	0.37	0.17	0.02	0.07
36.0	0.01	0.03	0.27	0.27	0.13	0.01	0.05
36.5	0.01	0.02	0.20	0.20	0.09	0.01	0.03
37.0		0.01	0.14	0.14	0.06		0.02
37.5		0.01	0.10	0.10	0.04		0.02
38.0			0.07	0.07	0.03		0.01
38.5			0.05	0.05	0.02		
39.0			0.04	0.04	0.01		0.01
39.5			0.02	0.03	0.01		
40.0			0.02	0.02			
40.5			0.01	0.01			
41.0			0.01	0.01			

Table 4.3. Energy dependence of the  $(\gamma, 2n)$  reaction cross sections for deformed nuclei.

$E_\gamma$	$^{151}\text{Sm}$	$^{158}\text{Tb}$	$^{166}\text{Ho}$
14.0	16.18		
14.5	58.84		7.94
15.0	108.94		52.49
15.5	152.80	2.06	110.92
16.0	179.97	32.47	159.22
16.5	187.44	71.27	184.72
17.0	179.65	98.45	188.30
17.5	163.67	110.37	177.86
18.0	145.16	111.02	161.17
18.5	127.40	105.47	143.27
19.0	111.84	97.44	126.75
19.5	98.95	89.17	112.72
20.0	89.83	81.92	101.63
20.5	80.83	76.46	93.80
21.0	72.95	73.28	90.59
21.5	65.83	72.31	89.13
22.0	58.57	71.61	86.54
22.5	49.72	68.62	77.53
23.0	39.73	62.48	65.21
23.5	30.76	56.47	54.31
24.0	23.76	51.28	45.63

$E_\gamma$	$^{151}\text{Sm}$	$^{158}\text{Tb}$	$^{166}\text{Ho}$
24.5	18.442	46.53	38.48
25.0	14.22	41.58	32.07
25.5	10.74	35.92	25.91
26.0	7.83	29.55	20.01
26.5	5.50	23.05	14.76
27.0	3.75	17.24	10.50
27.5	2.51	12.50	7.30
30.5	0.21	1.49	0.74
31.0	0.14	1.04	0.50
31.5	0.09	0.72	0.34
32.0	0.06	0.50	0.23
32.5	0.04	0.34	0.16
33.0	0.03	0.23	0.11
33.5	0.02	0.16	0.07
34.0	0.01	0.11	0.05
34.5	0.01	0.07	0.03
35.0	0.01	0.05	0.02
35.5	0.03	0.02	
36.0	0.02	0.01	
36.5	0.01	0.01	
37.0		0.01	

Table 5.1. Energy dependence of the ( $\gamma,3n$ ) reaction cross sections for spherical nuclei.

$E_\gamma$	$^{90}\text{Sr}$	$^{93}\text{Zr}$	$^{96}\text{Zr}$	$^{94}\text{Nb}$	$^{99}\text{Tc}$	$^{107}\text{Pd}$	$^{108}\text{Ag}$
23.5			0.23			0.01	
24.0		0.06	0.85			0.28	
24.5		0.41	2.01	0.02		1.31	
25.0		1.24	3.73	0.25		3.33	
25.5	0.00	2.64	5.85	0.92		6.23	0.15
26.0	0.04	4.50	8.08	2.16		9.66	0.78
26.5	0.29	6.51	10.07	3.86	0.13	13.14	2.08
27.0	0.86	8.28	11.55	5.72	0.64	16.27	3.95
27.5	1.71	9.57	12.47	7.40	1.59	18.77	6.11
28.0	2.64	10.35	12.90	8.71	2.92	20.55	8.28
28.5	3.50	10.73	12.97	9.62	4.44	21.67	10.27
29.0	4.22	10.81	12.80	10.19	5.99	22.22	11.93
29.5	4.80	10.71	12.49	10.50	7.44	22.32	13.24
30.0	5.25	10.48	12.08	10.61	8.71	22.10	14.19
30.5	5.58	10.18	11.62	10.58	9.76	21.64	14.81
31.0	5.81	9.83	11.14	10.45	10.58	21.03	15.16
31.5	5.95	9.45	10.65	10.24	11.18	20.32	15.28
32.0	6.01	9.06	10.16	9.97	11.58	19.55	15.22
32.5	6.01	8.67	9.69	9.67	11.80	18.76	15.02
33.0	5.96	8.29	9.24	9.35	11.88	17.97	14.73
33.5	5.88	7.91	8.80	9.01	11.85	17.19	14.35
34.0	5.76	7.55	8.39	8.67	11.72	16.44	13.94
34.5	5.62	7.21	8.00	8.33	11.52	15.72	13.49
35.0	5.46	6.88	7.64	8.00	11.27	15.03	13.03
35.5	5.30	6.57	7.29	7.68	10.99	14.38	12.56
36.0	5.13	6.28	6.97	7.36	10.68	13.76	12.10
36.5	4.95	6.01	6.67	7.07	10.35	13.18	11.65
37.0	4.78	5.75	6.39	6.78	10.02	12.64	11.21
37.5	4.61	5.51	6.12	6.51	9.69	12.12	10.79
38.0	4.44	5.28	5.87	6.25	9.37	11.64	10.39
38.5	4.28	5.07	5.64	6.00	9.05	11.19	10.00
39.0	4.13	4.87	5.42	5.77	8.74	10.76	9.64
39.5	3.98	4.68	5.21	5.55	8.44	10.36	9.29
40.0	3.83	4.51	5.02	5.34	8.15	9.99	8.96
40.5	3.69	4.34	4.84	5.15	7.88	9.63	8.65
41.0	3.56	4.18	4.67	4.96	7.61	9.29	8.35
41.5	3.44	4.03	4.50	4.79	7.36	8.98	8.07
42.0	3.32	3.89	4.35	4.62	7.12	8.68	7.80
42.5	3.21	3.76	4.21	4.47	6.89	8.39	7.55
43.0	3.10	3.64	4.07	4.32	6.67	8.12	7.31

Table 5.1. (Cont.)

$E_\gamma$	$^{90}\text{Sr}$	$^{93}\text{Zr}$	$^{96}\text{Zr}$	$^{94}\text{Nb}$	$^{99}\text{Tc}$	$^{107}\text{Pd}$	$^{108}\text{Ag}$
43.5	3.00	3.52	3.94	4.18	6.47	7.87	7.08
44.0	2.90	3.41	3.82	4.05	6.27	7.63	6.86
44.5	2.81	3.30	3.70	3.92	6.08	7.39	6.65
45.0	2.73	3.20	3.59	3.80	5.90	7.18	6.46
45.5	2.64	3.10	3.48	3.68	5.73	6.97	6.27
46.0	2.56	3.01	3.38	3.57	5.56	6.77	6.09
46.5	2.49	2.93	3.28	3.47	5.41	6.58	5.92
47.0	2.42	2.84	3.19	3.37	5.26	6.39	5.75
47.5	2.35	2.76	3.10	3.28	5.11	6.22	5.60
48.0	2.28	2.69	3.02	3.19	4.98	6.05	5.45
48.5	2.22	2.62	2.94	3.10	4.85	5.89	5.30
49.0	2.16	2.55	2.86	3.02	4.72	5.74	5.17
49.5	2.10	2.48	2.79	2.94	4.60	5.60	5.04
50.0		2.42	2.73	2.87	4.49	5.46	4.91

Table 5.2. Energy dependence of the  $(\gamma,3n)$  reaction cross sections for spherical nuclei.

$E_\gamma$	$^{121}\text{Sn}$	$^{126}\text{Sn}$	$^{129}\text{I}$	$^{135}\text{Cs}$	$^{137}\text{Cs}$	$^{147}\text{Sm}$	$^{148}\text{Sm}$
22.5	0.24					0.62	
23.0	1.31	0.08				2.39	
23.5	3.54	0.70				5.68	0.10
24.0	6.98	2.38				10.37	0.91
24.5	11.42	5.27			0.08	15.81	3.03
25.0	16.32	8.98			0.50	20.95	6.37
25.5	20.80	12.67	0.14	0.21	1.84	24.78	10.24
26.0	23.98	15.59	0.84	0.98	3.61	26.94	13.79
26.5	25.52	17.47	2.29	2.37	5.54	27.65	16.55
27.0	25.68	18.43	4.25	4.15	7.32	27.38	18.41
27.5	24.94	18.70	6.38	6.04	8.83	26.52	19.50
28.0	23.73	18.52	8.37	7.83	10.01	25.36	19.98
28.5	22.34	18.07	10.08	9.37	10.90	24.08	20.02
29.0	20.92	17.44	11.44	10.62	11.50	22.76	19.73
29.5	19.56	16.72	12.44	11.57	11.86	21.47	19.23
30.0	18.27	15.97	13.12	12.23	12.03	20.23	18.59
30.5	17.09	15.20	13.51	12.63	12.03	19.07	17.88
31.0	16.00	14.44	13.67	12.82	11.91	17.98	17.12
31.5	15.01	13.71	13.65	12.85	11.69	16.98	16.35
32.0	14.11	13.01	13.48	12.73	11.41	16.04	15.60
32.5	13.28	12.35	13.22	12.52	11.09	15.18	14.87
33.0	12.53	11.74	12.88	12.23	10.73	14.39	14.17
33.5	11.85	11.16	12.49	11.89	10.36	13.66	13.50

Table 5.2. (Cont.)

E <sub>γ</sub>	<sup>121</sup> Sn	<sup>126</sup> Sn	<sup>129</sup> I	<sup>135</sup> Cs	<sup>137</sup> Cs	<sup>147</sup> Sm	<sup>148</sup> Sm
34.0	11.22	10.62	12.07	11.53	9.99	12.99	12.88
34.5	10.65	10.11	11.64	11.14	9.61	12.36	12.29
35.0	10.13	9.65	11.20	10.75	9.25	11.79	11.74
35.5	9.64	9.21	10.77	10.36	8.90	11.26	11.22
36.0	9.20	8.81	10.35	9.97	8.56	10.76	10.74
36.5	8.79	8.43	9.95	9.60	8.23	10.30	10.29
37.0	8.40	8.08	9.56	9.24	7.92	9.88	9.87
37.5	8.05	7.75	9.19	8.89	7.62	9.48	9.47
38.0	7.72	7.44	8.84	8.56	7.34	9.11	9.10
38.5	7.41	7.15	8.50	8.25	7.08	8.76	8.76
39.0	7.13	6.88	8.18	7.95	6.83	8.43	8.43
39.5	6.86	6.63	7.88	7.67	6.59	8.12	8.13
40.0	6.60	6.39	7.60	7.40	6.36	7.84	7.84
40.5	6.37	6.17	7.33	7.15	6.15	7.56	7.57
41.0	6.14	5.96	7.08	6.90	5.94	7.31	7.31
41.5	5.93	5.76	6.84	6.68	5.75	7.06	7.07
42.0	5.73	5.57	6.61	6.46	5.57	6.83	6.84
42.5	5.55	5.39	6.40	6.25	5.40	6.62	6.62
43.0	5.37	5.22	6.19	6.06	5.23	6.41	6.42
43.5	5.20	5.06	6.00	5.87	5.07	6.21	6.22
44.0	5.04	4.91	5.81	5.69	4.92	6.03	6.03
44.5	4.89	4.76	5.64	5.53	4.78	5.85	5.85
45.0	4.74	4.62	5.47	5.36	4.64	5.68	5.69
45.5	4.60	4.49	5.31	5.21	4.51	5.52	5.52
46.0	4.47	4.36	5.16	5.07	4.39	5.37	5.37
46.5	4.35	4.24	5.01	4.93	4.27	5.22	5.22
47.0	4.23	4.13	4.88	4.79	4.16	5.08	5.08
47.5	4.11	4.02	4.74	4.66	4.05	4.94	4.94
48.0	4.00	3.91	4.62	4.54	3.94	4.81	4.82
48.5	3.90	3.81	4.50	4.42	3.84	4.69	4.69
49.0	3.79	3.71	4.38	4.31	3.75	4.57	4.58
49.5	3.70	3.62	4.27	4.20	3.65	4.46	4.46
50.0	3.61		4.16	4.10		4.35	

Table 5.3. Energy dependence of the ( $\gamma,3n$ ) reaction cross sections for deformed nuclei.

$E_\gamma$	$^{151}\text{Sm}$	$^{158}\text{Tb}$	$^{166}\text{Ho}$
19.50			
20.00	0.09		
20.50	1.14		
21.00	3.93		
21.50	8.58		0.20
22.00	14.72		1.60
22.50	21.22		4.73
23.00	26.63	0.12	9.01
23.50	30.78	0.96	13.96
24.00	34.37	2.96	19.46
24.50	37.71	6.17	25.34
25.00	40.55	10.35	31.12
25.50	42.29	14.91	35.91
26.00	42.39	19.01	38.80
26.50	40.84	21.92	39.45
27.00	38.18	23.44	38.34
27.50	35.06	23.81	36.27
28.00	31.94	23.41	33.68
28.50	29.05	22.58	31.13
29.00	26.49	21.53	28.73
29.50	24.26	20.40	26.55
30.00	22.31	19.27	24.59
30.50	20.62	18.17	22.85
31.00	19.14	17.12	21.29
31.50	17.84	16.14	19.90
32.00	16.69	15.23	18.65
32.50	15.67	14.39	17.53
33.00	14.75	13.61	16.52
33.50	13.93	12.89	15.61
34.00	13.18	12.23	14.78
34.50	12.51	11.62	14.02

$E_\gamma$	$^{151}\text{Sm}$	$^{158}\text{Tb}$	$^{166}\text{Ho}$
35.00	11.89	11.06	13.33
35.50	11.32	10.54	12.70
36.00	10.81	10.07	12.11
36.50	10.33	9.62	11.57
37.00	9.88	9.21	11.07
37.50	9.47	8.83	10.61
38.00	9.09	8.47	10.18
38.50	8.73	8.13	9.78
39.00	8.40	7.82	9.40
39.50	8.09	7.53	9.05
40.00	7.79	7.26	8.72
40.50	7.52	7.00	8.41
41.00	7.26	6.75	8.12
41.50	7.01	6.53	7.84
42.00	6.78	6.31	7.58
42.50	6.56	6.10	7.34
43.00	6.35	5.91	7.10
43.50	6.15	5.72	6.88
44.00	5.97	5.55	6.67
44.50	5.79	5.38	6.47
45.00	5.62	5.22	6.28
45.50	5.46	5.07	6.10
46.00	5.30	4.93	5.93
46.50	5.16	4.79	5.76
47.00	5.02	4.66	5.60
47.50	4.88	4.54	5.45
48.00	4.75	4.42	5.31
48.50	4.63	4.30	5.17
49.00	4.51	4.19	5.04
49.50	4.40	4.08	4.91

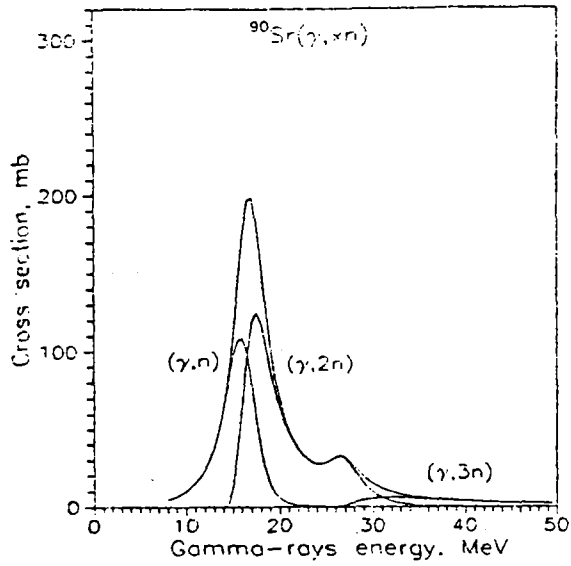


Figure 1. Photoneutron reaction cross section for the spherical  $^{90}\text{Sr}$  nuclide.

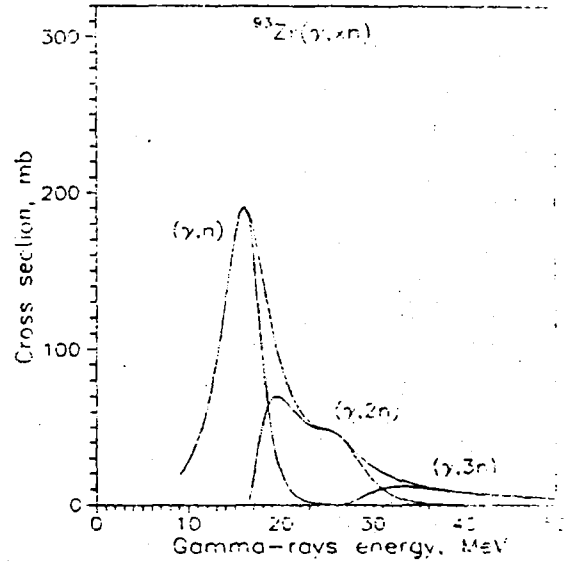


Figure 2. Photoneutron reaction cross section for the spherical  $^{93}\text{Zr}$  nuclide.

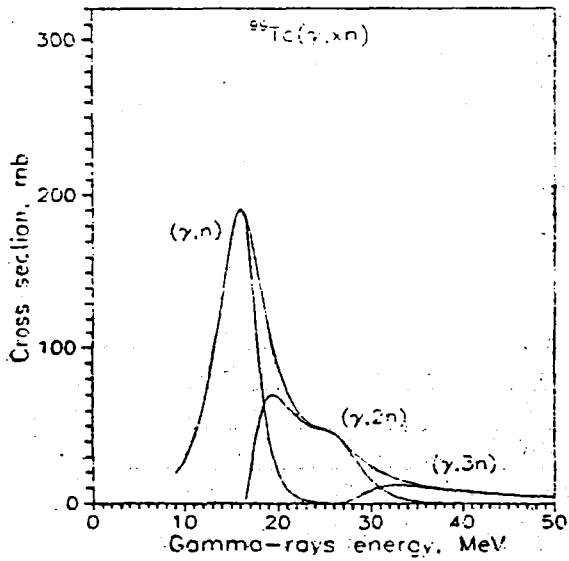


Figure 3. Photoneutron reaction cross section for the spherical  $^{99}\text{Tc}$  nuclide.

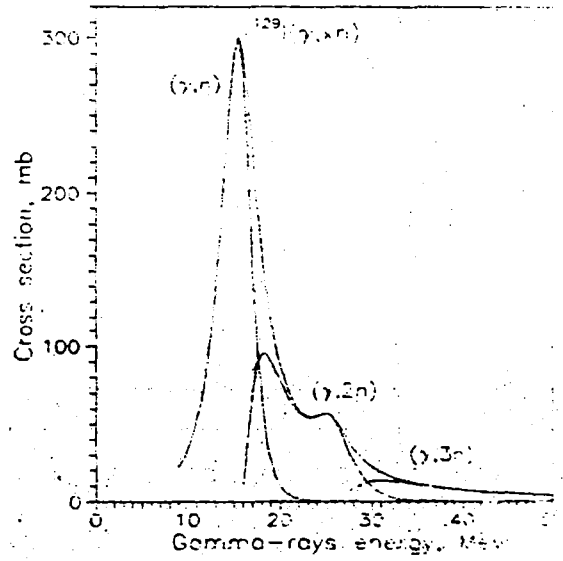


Figure 4. Photoneutron reaction cross section for the spherical  $^{129}\text{I}$  nuclide.

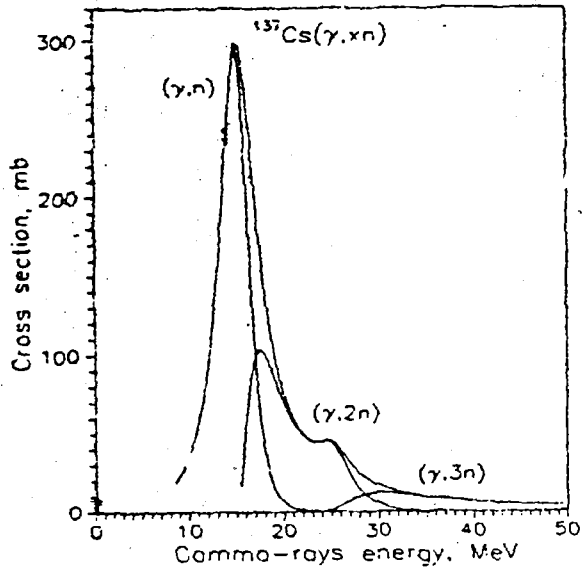


Figure 5. Photoneutron reaction cross section for the spherical  $^{137}\text{Cs}$  nuclide.

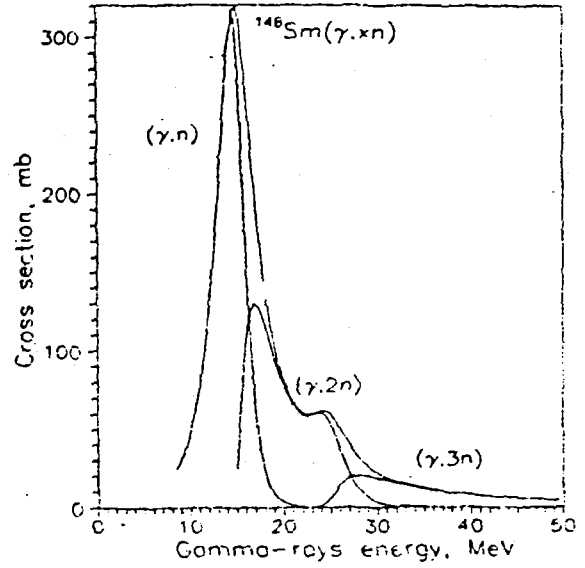


Figure 6. Photoneutron reaction cross section for the spherical  $^{148}\text{Sm}$  nuclide.

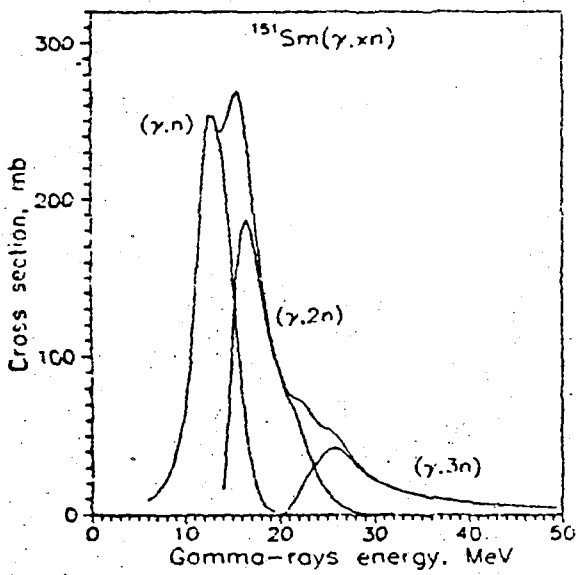


Figure 7. Photoneutron reaction cross section for the deformed  $^{151}\text{Sm}$  nuclide.

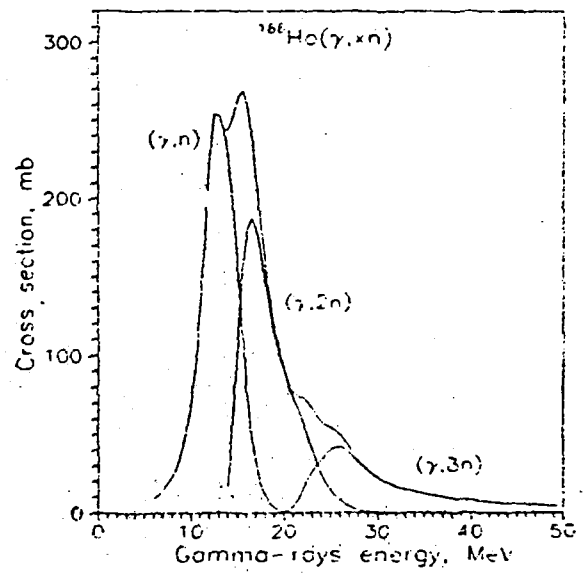


Figure 8. Photoneutron reaction cross section for the deformed  $^{166}\text{Ho}$  nuclide.

### References

- [1] BERMAN, B.L., Atomic Data and Nucl. Data Tabl. 15 (1975) 319.
- [2] FULTZ, S.F., et al., Phys. Rev. 186 (1969) 1255.
- [3] DILG, W., et al., Level density parameters for the back-shifted Fermi gas model in the mass range  $40 < A < 250$ . Nucl. Phys. A217 (1973) 269.
- [4] KRAVZOV, V.A., Atomic masses and nuclear binding energies, Moscow, Atomizdat (1974).



# ANALYSIS OF REACTION RATE MEASUREMENTS FOR THE DETERMINATION OF NEUTRON ENERGY SPECTRA.

*A.V. Zvonarev, G.N. Manturov, Yu.S. Khomyakov, A.M. Tsibulya*

*State Research Centre of the Russian Federation  
Institute of Physics and Power Engineering, Obninsk*

*V.P. Netsvet, N.V. Skorikov*

*Mangyshlaksk Atomic Energy Plant*

*I.M. Proshin*

*Moscow Institute of Engineering Physics, Moscow*

## Abstract

A maximum likelihood technique for the reconstitution of neutron spectra from reaction rate measurements has been developed. Results of spectrum index measurements in the BR-1 and the BN-350 reactors are presented. An estimate is made of the uncertainties and the results of the correlation matrix unfolding.

## Introduction

In the course of analyzing experiments designed to measure reaction cross section ratios averaged over reactor spectra, one very often encounters the following situation. Assuming that the value obtained as a result of calculations differs from the experimental value by 10%. If one then assumes that the reason for this difference is due to the cross section of the reaction being investigated, it is sensible to question its processing; if, on the other hand, the reason for this difference is due to the neutron spectrum, it is then necessary to investigate the reason for the discrepancy and to attempt to correct it. The latter procedure may necessitate the correction of other cross sections (for instance, the scattering cross section of reactor materials).

Reference [1] describes the analysis of cross section ratios for a large number of nuclides measured on the BR-1 reactor. Since many of these measurement results revealed differences between calculated and measured values, the conclusion was made that in view of the systematic character of these discrepancies, it was unlikely that they could be ascribed to the

cross section of these reactions. At the same time, it was noticed that for most reactions, the adjustment of the high energy range of the calculated spectrum led to an improved agreement. A similar situation was observed by the authors in the analysis of reaction cross section ratio measurements for structural materials measured in the BN-350 reactors.

This has led to the need to develop a specific methodology for the analysis of such situations. This methodology is based on the reconstitution of a multigroup neutron spectrum using experimental values of the reaction cross section ratio and the evaluation of the errors of the reconstituted spectrum.

### **The methodology for the reconstitution of a multigroup neutron spectrum using the maximum probability method.**

#### *Statement of the problem*

From a mathematical point of view, the problem of neutron spectrum reconstitution is reduced to solving a system of integral equations:

$$q_i = \int_0^{E^{up}} \sigma_i(E) \varphi(E) dE, \quad i=1, \dots, n; \quad (1)$$

where  $q_i$  is the measured rate of reaction I,  $\sigma_i(E)$  is the cross section of reaction I,  $\varphi(E)$  is the neutron spectrum,  $n$  is the number of measured reactions and  $E^{up}$  is the upper boundary of the spectrum. If the total energy range is subdivided into a number of intervals, the problem is reduced to solving the equivalent system of algebraic equations:

$$q_i \sum_{j=1}^m \sigma_{ij} \varphi_j, \quad i=1, \dots, n, \quad (2)$$

where  $m$  is the number of energy intervals.

The main difficulty is that the posed problem is not correct; that is, it does not have a single-valued and unique solution [2]. Actually, there is a need to determine a continuous function for the neutron spectrum  $\varphi(E)$  or a set of parameters  $\varphi_j$ , whose number is larger than the number of equations (for  $m > n$ ), using a relatively small number of intervals  $q_i$ . This means that in order to solve the problem it is necessary to introduce additional information related to the investigated spectrum which can be obtained from general considerations (for instance on the basis of some physical premise).

Another difficulty is that the measured reaction rate  $q_i$  and the reaction cross section  $\sigma_i$  are known to some degree of accuracy. It is therefore impossible to guarantee an exact solution of equation (1) for the actual spectrum  $\varphi(E)$ . Furthermore, there are additional difficulties of a calculational character related to the stability of the solution and to the inversion of a badly defined matrix which can lead to solutions that are inconsistent with the physics of the problem (negative or oscillating solutions).

The given problem has been investigated in great detail. At the present time, iterative methods are the most popular, they have replaced such engineering methods as the effective threshold cross section method.

After considering well known algorithms, such as SAND-II and others, the authors did not find the answer to two pertinent questions. First, it was not clear how the physically based limitations, which solves the uniqueness problem, affect the neutron spectrum function  $\varphi(E)$ . Second, it was difficult to evaluate the errors of the reconstructed spectrum function which apparently may be obtained only by "shaking them loose" from the original data (?).

The authors believe that the indicated methods (or others like them) serve only as the foundation for the development of more specific and physically substantiated methods. In this case, the methods that are preferable are those that offer the most options to solve this problem. The method that is considered by the authors to be the most preferable is the maximum likelihood method, which allows the superposition of statistical type constraints on the desired solutions. The actual constraints can be chosen on the basis of the physical nature of the problem. The important factor in favor of such a choice is the statistical method which, in contrast to those proposed above, makes it possible to evaluate the uncertainties in the reconstructed spectrum, which is of extreme importance in the analysis of the experiment. In conclusion, let us note that the algorithm used by the authors and described below is close to that used in the STAYSL [3] program developed in other countries.

### *The mathematical formalism*

Let us assume that the group reaction cross sections  $S = \{\sigma_i^g\}$  and the a priori spectrum  $F = \{\varphi_i\}$ , as well as their uncertainties (more exactly represented by the covariance matrices  $W_\sigma$  and  $W_\varphi$ ) are known prior to performing the experiment. If one then takes the experimental results into consideration, it is possible to obtain new, more accurate values of  $S'$  and  $F'$  and their covariance matrices  $W_{\sigma'}$  and  $W_{\varphi'}$ . In order to obtain these values it is expedient to use the principle of maximum likelihood, whose evaluated values have a number of desirable features: they are consistent, effective(?), asymptotically normal and have a minimum of possible errors [16]. The principle of the maximum likelihood method has the objective to choose such values of evaluated parameters which would maximize the probability to obtain such values as a result of experiments.

If one accepts that the distribution function has the shape of a Gaussian, and that  $Q$ ,  $S$ , and  $F$  are independent of each other, then the probability can be expressed as follows:

$$L(Q') = \exp(0,5 \cdot (Q'' - Q')^T V^{-1} (Q'' - Q')) \times \quad (3)$$

$$\times \exp(0,5 \cdot (S' - S)^T W_\sigma^{-1} (S' - S) + 0,5 \cdot (F' - F)^T W_\varphi^{-1} (F' - F))$$

where  $V$  is the covariance matrix of the measurement errors, and  $Q''$  represents the unknown "actual" values of the reaction rates. Let us introduce the generalized vector  $P = (S, F)^T$  and a sensitivity coefficient matrix  $H$  which would allow a linear connection between  $Q''$ ,  $P$  and  $P'$  in the vicinity of point  $P$  (better known as the "linear hypothesis")

$$Q'' = Q + H(P' - P) \quad (4)$$

The problem is then reduced to the maximization of the probability  $L(Q')$  or equivalently to the minimization of the quadratic form:

$$S^2 = 0,5 \cdot (Q - Q' + H(P' - P))^T V^{-1} (Q - Q' + H(P' - P)) + \quad (5)$$

$$+ 0,5 \cdot (P' - P)^T W_p^{-1} (P' - P),$$

where

$$W_p = \begin{pmatrix} W_\sigma & 0 \\ 0 & W_\varphi \end{pmatrix}.$$

The solution of this equation leads to the well known expression:

$$P' - P = W_p H^T (V + H W_p H^T)^{-1} (Q' - Q), \quad (6)$$

and the covariant error matrix based on the new 'a posteriori' evaluations of P is

$$W_p' = W_p - W_p H^T (V + H W_p H^T)^{-1} H W_p. \quad (7)$$

### *Features of the methodology*

The 'a priori' values  $\varphi_i$  and  $W_\varphi$  is in fact that additional information which was mentioned above, which is required as a result of the incorrectly stated problem. Moreover,  $W_\varphi$  together with  $\varphi_i$  prescribe a channel within whose boundaries it is expedient to make corrections to the initial spectrum; at the expense of the correlation of the uncertainties it can reflect the interdependence of neutron fluxes in different energy groups, in other words it introduces constraints on the shape of the spectrum.

As a rule, 'a priori' information on neutron spectra in reactor systems may be obtained only as a result of solving the transport equation. Even the representation of the smoothness of the spectrum and of the generalized characteristics are derived from the given equation. At the same time, the neutron spectrum also has a fine resonance structure. To reconstitute this structure on the basis of the limited number of measured information is considered by the authors to be impossible. It would only be possible to undertake such a reconstitution in the region of broad resonances, such as the broad sodium resonance in fast reactors using a sodium coolant (Incidentally, this is only feasible by using the same resonance of the  $^{23}\text{Na}(n,\gamma)$  reaction, however, it is not entirely clear whether such a reconstitution is an exercise in self-deception).

The actual methodology is based on the multigroup approach using the 28-group BNAB [4] constants. As the BNAB data library is used extensively in reactor and shielding calculations, it makes it possible to use the calculated spectra as the initial approximation without having to perform additional calculations. Methods for the calculation and analysis of sensitivities, the evaluation of uncertainties of various functions of the neutron field [5,6] are developed in the framework of this system of constants. The latter, simplifies the evaluation of the  $W_\varphi$  matrix. Considering the normalized function  $\varphi_i$  as a bi-linear functions, it is possible, using the

perturbation theory, to evaluate the sensitivity of reaction cross sections which are used in the calculation, and using the covariance matrices of their uncertainties it is possible to evaluate the constant component of  $W_\varphi$ . Using the same method, it is also possible to evaluate the technological uncertainty in the calculation of the  $\varphi_j$  function using uncertainties of the technological parameters, namely of the composition and dimensions of each zone. Most difficult is the evaluation of the methodical component  $W_\varphi$ ; this depends to a large degree on the experience and intuitive sense of the investigator. One of the most objective methods to perform such an evaluation is by comparing spectra which have been calculated using various methods and calculational programs.

Let us note that the notation  $\sigma_j$  in equation (2) is understood to mean the group averaged blocked cross sections which are produced in the BNAB methodology. Among other things, the resonance structure of cross sections is taken into account by resonance selfshielding factors. This also simplifies the problem to account for the resonance structure of the neutron flux density. The notation  $\varphi_j$  represents the group neutron flux.

### *Provision of the nuclear constants*

In order to implement these calculations with the use of the BNAB data, it was necessary to create a special 28-group cross section data library for dosimetry reactions. The group reaction cross sections were calculated with the use of the GRUKON program [7] using evaluated data from various data libraries: the non-Russian libraries ENDF/B-5 and 6, JENDL-2 and 3, and the Russian libraries BOSPOR-80 [8], BOSPOR-86 [9] and FOND [10] (the data from the FOND library shall be designated as BNAB-90). The cross section library is accompanied by a library of covariance matrices of the data's uncertainties. The dosimetry reaction matrices, taken from the ENDF/B-5 library, were those of Nolthenius and Zijp [11]. In all of the other cases, the matrices were evaluated by G.N. Manturov.

### *Provision of the calculational programs*

The computational programs assembled for this project were based on the program complex CORE and the additional set of programs INDEKC [5]. This set of programs comprises three data libraries consisting of: the results of measurements and calculations (Q'-Q) named LEMEX, the sensitivities of measured quantities of the constants (H) named LSENS, and the matrices of the constants' uncertainties ( $W_\varphi$ ,  $W_\sigma$ ) named LUND. The work was performed on an IBM PC/AT.

### *Reconstitution of the neutron spectrum of the BR-1 reactor*

Results of cross section measurements performed on the BR-1 reactor for a large number of nuclides and results of their calculational analysis are reported in reference [1]. An analysis of the neutron spectrum based on these measurements is also reported in that report.

For the purpose of this experiment, the BR-1 reactor was used as a plutonium fueled fast critical assembly which has a hard neutron spectrum (at the present time, the reactor is fueled

with uranium). The spectrum in the central measurement channel was calculated using the CRAB-1 [12], MMKFK [13] and DOT-3 [14] computer programs using the nuclear data from the BNAB-78 data library. The results of these calculations were in good agreement with each other. The comparison of the discrepancies between the calculational and experimental results with the data uncertainties made it possible to come to the conclusion that the latter contribute the determining contribution to the overall uncertainty of the calculated spectrum. The evaluation of the constant/(data?) which constitutes the errors in the calculation of neutron group spectra was performed on the basis of the calculation of their sensitivities to the data which are used in these calculations. The evaluated uncertainties of the group constants given in the BNAB-78 [4] were used subsequently. Based on the assumption that the neutron fission spectrum depends on one parameter only, namely on the average energy, it was calculated from the evaluation of the covariational matrix of the uncertainties. All of the necessary calculations for the transfer of the data uncertainties to the calculated neutron spectrum with the use of sensitivity coefficients were executed with the aid of the INDEKC [5] set of computer programs. The evaluated uncertainties of the calculated spectrum and their correlations are listed in Table 1. It must be noted that the principal contribution to the uncertainties of the group spectra (normalized to unity) consists of the errors associated with the plutonium-239 inelastic scattering cross section and the plutonium-239 fission spectrum (in the upper groups).

Having evaluated the covariational matrix  $W_\phi$  and the errors of the measured reaction cross sections, it is now possible to evaluate the error in the measurement of the ratio of the corresponding reaction cross sections:

$$W_q = H_\sigma W_\sigma H_\sigma^T + H_\phi W_\phi H_\phi^T, \quad (8)$$

where  $H_\sigma$  and  $H_\phi$  are the sensitivities of the ratios of the measured cross sections to the reaction cross sections and group neutron fluxes respectively, and where  $W_\sigma$  and  $W_\phi$  are their corresponding covariant errors matrixes. The first term of equation (8) will be designated below as the constant component, and the second term as the spectral component. Having acquired the knowledge of  $W_\phi$ , it is now possible to execute the procedure for the reconstitution of the "real" spectrum. (Although it seems to the authors that it is more sensible to speak of the correction of the calculational spectrum.) Only the reactions listed in the upper part of Table 2 were used in the reconstitution of the spectrum, as most of them pertain to the so-called "dosimetry reactions" whose cross sections are well known. Furthermore, the reactions included in this set encompass practically the entire energy range of the investigated spectrum. The lower part of the table is comprised of the remaining measured reactions which had not been used in the correction procedure.

Table 2 contains the values of the ratios of calculated to measured data, prior to and after the execution of the spectrum reconstitution procedure. Two results are obtained as a result of the reconstitution: the first takes into account only the new, corrected/adjusted group spectrum values, while the second includes the reaction cross section corrections as well, which occurs automatically in the course of the reconstitution procedure (these are listed only for those reactions that are included in the reconstitution process). The table also lists the values of the various types of error: experimental errors of the measured parameters, the error arising in their calculations, their components, as well as the spectral component of the calculational error of the indicated parameters arising after the spectrum reconstitution.

As observed in many cases, the spectral component prior to the execution of the reconstitution procedure is significantly larger. After the reconstitution procedure, for those reaction cross sections which have a low level of uncertainty, the spectral component are lower in the case of most reactions. The discrepancies between the calculated and measured data (see column 4) which remain after the reconstitution process are due mainly to the errors of the reaction cross sections.

The results given in Table 2 clarify the problem that was stated at the beginning of this article. In the case of most threshold reactions, the main divergence between calculation and experiment is apparently due to the large uncertainties in the calculated neutron spectrum in the higher energy groups. At the same time, the agreement between calculation and measurement in the case of the  $^{47}\text{Ti}(n,p)$  reaction appears to be accidental and is the result of the compensation of the errors in the calculated spectrum and in the cross section of the given reaction. In other words, there is a need to correct the reaction cross section. The large discrepancies in the reactions in the lower part of the table may be explained only by the large uncertainties in the reaction cross sections. Experimental data may be used to produce more exact evaluations.

Table 3 shows the results of correcting the calculational spectrum, and Table 4 shows the matrix that correlates the errors in the reconstituted spectrum. The largest differences between the reconstituted and calculated spectra are observed in the upper energy range. One of the main questions which arises in the reconstitution process concerns the influence that the covariance matrix of the a priori calculated spectrum errors has on the final result

The extent of this influence was evaluated for two possible cases. In one case all of the elements of the  $W_{\varphi}$  matrix were increased by a factor of four (i.e., by a factor of two in the case of the errors), in the other case, the diagonalized  $W_{\varphi}$  matrix was analyzed. The results of this evaluation are given in Figure 1. It turns out that the reconstituted results are more sensitive to the structure of the covariance matrix than to the absolute values of the assumed errors. By increasing the values of the errors by a factor of two, the character of the deviation of the reconstituted spectrum from the calculated spectrum was conserved. The actual deviations were changed somewhat but not to any large extent. The changes in the  $W_{\varphi}$  matrix itself led to a significantly different resultant spectrum (see for instance, the -1 group). In the present case this can be easily explained. In the case of the BNAB data library, the range of sensitivity of many reaction indicators includes the first group and affects the zero group only slightly. The correction of the fraction of the first neutron group is specified on the basis of high experimental values of reaction rates. Inasmuch as the upper part of the neutron spectrum is close to the neutron fission spectrum, which is reflected in the  $W_{\varphi}$  matrix, the number of neutrons in the first group leads to its increase in the zeroth and in the minus first groups. Otherwise, the shape of the spectrum will be different from the fission spectrum. However, if the error correlation in these groups is altered, i.e., assuming that we don't know anything about the shape of the spectrum above 6.5 MeV, (except for its initial approximation), then the method will correct the spectrum only in the region of reaction-detector sensitivity. The neutron spectrum in the lower groups (10 to 12) is reconstituted also as a result of the  $W_{\varphi}$  matrix correlation. In this manner, the  $W_{\varphi}$  matrix steers the reconstitution process; the given example illustrates the possibilities to introduce additional information about the investigated spectrum into the reconstitution procedure.

The maximum refinement of the spectrum also occurs in its high energy region. One has to

take into account, however, that a reduction of the spectral component the uncertainties in the calculation of the reaction rates in the spectrum reconstitution process occurs not only at the expense of a reduction in the dispersion of the group neutron fluxes, but also at the expense of changes in the correlation of errors of various energy groups.

As regards the reasons for the discrepancies between the initial, calculational and reconstituted spectra, the most likely explanation lies in the uncertainties in the inelastic scattering cross section and in the plutonium-239 fission spectrum, both of which contribute to the initial contribution to the errors in the calculation. Another spectrum calculation has been performed for the center of the BR-1 reactor using the new version of the BNAB-90 group constants. The results of this calculation, listed in Table 3 show good agreement with the reconstituted spectrum. On one hand, this confirms the correctness of the conclusions reached in this study, and on the other hand it confirms the accuracy of the BNAB-90 data.

### ***Results of the reconstitution of the neutron spectrum in the BN-350 reactor***

Table 5 lists results of measurements made using the BN-350 reactor and their comparison with calculated data. The measured data were obtained using needle-shaped (?) activation detectors which were irradiated in the space between fuel elements of the reactor. In contrast to the reactions that were measured in the BR-1 reactor, the actual measurement results were announced first. The calculation of the neutron flux was made with the TRIGEX [15] program using the nuclear data from the BNAB-78 library.

Here, it can also be observed that there is a systematical divergence between calculation and measurement for threshold reactions which can be eliminated by correcting the calculated spectrum. This systematical divergent character can also be observed in individual reactions, particularly in the  $^{47}\text{Ti}(n,p)$  reaction, in the case of two different spectra. The situation is more complicated in the case of the capture cross section, where it is much more difficult to detect this systematic behavior. The reason for this is due to the fact that in the case of the BN-350 reactor, a significant part of the spectrum falls in the resonance region of the capture cross sections of many indicators, a situation which is practically non-existent in the case the BR-1 reactor.

A significant divergence between the reconstituted and the calculated spectra can be observed in the case of the neutron spectrum in the BN-350 reactor, particularly in the high energy part of the spectrum. In the low energy part of the spectrum, the change of the spectrum as a result of the correction occurs principally at the expense of the error correlation of the initial spectrum. This can be observed in Figure 2, where the influence of the covariant matrix  $W_{\varphi}$  on the effects of reconstitution may be observed. The properties of the deviation of the reconstituted spectrum from the initial and calculated spectra, is the same when using the new version of the BNAB-90 data. This confirms the physics nature of the reconstituted results. It can therefore be concluded that the experimental data measured in the BN-350 reactor supports the changes that had been made in the BNAB-90 nuclear data.

### ***Conclusion***

The methodology presented in this report has shown to be effective in the analysis of experiments conducted with reactor spectra. The most difficult aspect of this procedure lies in the evaluation of the covariant matrix of the initial spectrum, which exerts a significant

influence on the reconstitution results. At the same time, this methodology makes it possible to introduce into the reconstitution process, physically based considerations on the shape of the spectrum which depend on the actual characteristics of the neutron-physical systems.

This project on the analysis of the ratios of cross sections of a large number of reactions, measured in the spectra of the BN-350 and BR-1 reactors, provides information required for the testing and correction of nuclear cross sections. Neutron spectra of the BN-350 and BR-1 reactors as well as the evaluation of the uncertainties of the results have been reconstituted based on the results of measurements.

Special attention has been given to the systematic discrepancies between calculated and measured threshold reactions. This discrepancy has been observed in the plutonium fueled BR-1 reactor as well as in the uranium fueled BN-350 power reactor. The most likely cause for this discrepancy lies in the uncertainties in the neutron fission spectrum and in the inelastic scattering cross section data stored in the BNAB-78 data library. Using data from the new version of the data library, BNAB-90, which incorporates improved nuclear data and a revised version of the fission spectrum, as given in reference [16], leads to a significantly better agreement between calculation and experiment.

## References

- [1] ZVONAREV, A.V., et al., Problems in Nuclear Science and Technology. Series: Nuclear Constants No. 3 (1990) 67. [in Russian].
- [2] TICHONOV, A.N., ARSEININ, V.N., Methods to Solve Certain Problems, Nauka, Moscow, Principal publication house of physico-mathematical literature (1979). [in Russian].
- [3] PEREY, F.G., Least Squares Dosimetry Unfolding. The STAY/SL Program. Report ORNL/TM-6062 also ENDF-254 (1977).
- [4] NIKOLAEV, M.N. (Edit.), Group Constants for Reactor and Shielding Calculations, Ehnergoizdat, Moscow (1981). [in Russian].
- [5] MANTUROV, G.N., Computer Programs for the Analysis of Reactor Characteristics Sensitivities to Nuclear Data, Preprint FEI-1034, Obninsk (1980). [in Russian].
- [6] BOLYATKO, V.V., et al., Uncertainties in Radiation Shielding Calculations, Ehnergoatomizdat, Moscow (1983). [in Russian].
- [7] SINITSA, V.V., et al., "GRUKON - Collection of computer programs for the calculation of group constants", in Nuclear Physics Research in the USSR. Annotation of programs. Vol. 27, Atomizdat, Moscow (1979). [in Russian].
- [8] BYCHKOV, V.M., ZOLOTAREV, K.I., PASHCHENKO, A.B., Problems in Nuclear Science and Technology. Series: Nuclear Constants No. 3(42) (1981) 60. [in Russian].

- [9] MANOCHIN, V.N., et al., "Activation cross sections induced by fast neutrons", Handbook on Nuclear Activation Data, IAEA, Vienna (1987) 305.
- [10] KOSHSHEEV, V.N., NIKOLAEV, M.N., Problems in Nuclear Science and Technology. Series: Nuclear Constants, No. 5(59) (1984) 16. [in Russian].
- [11] NOLTHENIUS, H.J., ZIJP, W.L., "Uncertainty and correlation data for the ENDF/B-V dosimetry file (version 2)". (Proc. IAEA Consultants Meeting on Radiation Damage Estimates for Reactor Structural Materials, Santa Fe, New Mexico, USA, 1985). IAEA Report INDC(NDS)-179/G. Vienna (1986).
- [12] SAVOS'KIN, M.M., et al., Problems in Nuclear Science and Technology. Series: Nuclear Constants, No. 6(43) (1984) 44. [in Russian].
- [13] MAYOROV, V.V., Problems in Nuclear Science and Technology. Series: Nuclear Constants, No. 8(21) (1981). [in Russian].
- [14] INSTITUTE OF ATOMIC ENERGY, User manual for the DOT-III computer program, Rep. IAE N 36/290083 (1983). [in Russian].
- [15] SEREGIN A.S., Problems in Science and Technology. Series: Nuclear Constants No. 4(33) (1983).
- [16] CHOMYAKOV, Yu.S., NIKOLAEV, M.N., DOLGOV, E.V., TSIBULYA, A.M., Problems in Science and Technology. Series: Nuclear Constants, No. 1 (1991) 70. [in Russian]

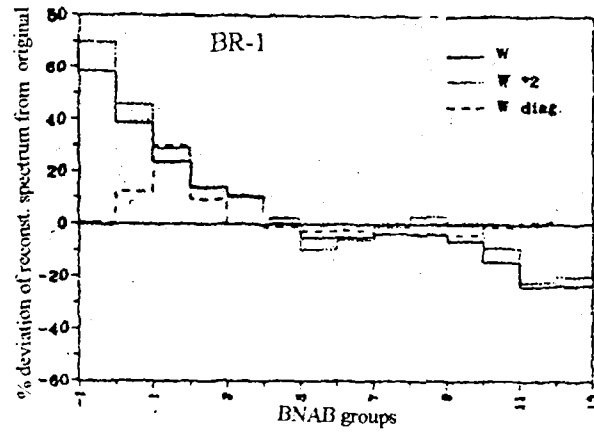


Figure 1. Deviation of the reconstituted neutron spectrum for the BR-1 reactor from the original spectrum for various  $W$  matrices.

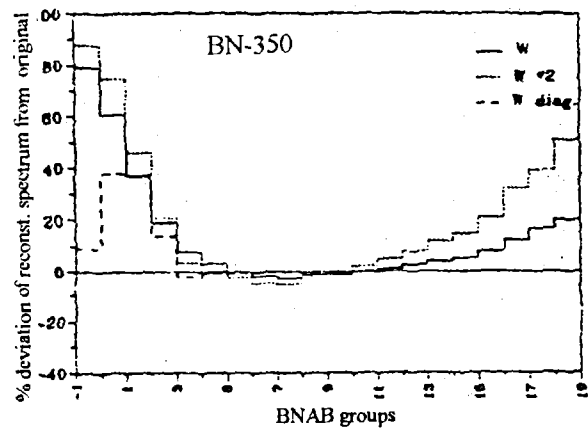


Figure 2. Deviation of the reconstituted neutron spectrum for the BN-350 reactor from the original spectrum for various  $W$  matrices



Table 2. Ratios of calculated data relative to the reaction cross sections measured on the BR-1 reactor and various component errors.

Reaction	Library	Calculation/measurement			Uncertainties %			
		Init. $\sigma$ , $\varphi$	Corrected		Exper.	Const. comp.	Spectral comp.	
			$\varphi$	$\sigma$ , $\varphi$			Before	After
1	2	3	4	5	6	7	8	9
<sup>27</sup> Al(n, $\alpha$ )	ENDF/B6	.178	.989	.999	5.0	8.8	13.9	4.3
<sup>48</sup> Ti(n,p)	ENDF/B6	.728	.917	.991	5.0	11.2	13.7	4.0
<sup>59</sup> Co(n, $\alpha$ )	ENDF/B6	.754	.945	.982	4.5	6.8	13.5	3.9
<sup>54</sup> Fe(n, $\alpha$ )	БОСП.86	.614	.760	1.02	4.0	18.0	12.9	3.6
<sup>56</sup> Fe(n,p)	ENDF/B5	.790	.976	.994	3.5	6.1	12.8	3.6
<sup>46</sup> Ti(n,p)	ENDF/B6	.784	.927	.995	5.0	12.8	11.1	2.9
<sup>27</sup> Al(n,p)	ENDF/B6	.895	1.06	1.02	8.0	11.2	11.0	2.9
<sup>54</sup> Fe(n,p)	БОСП.86	.887	1.01	1.01	4.0	4.1	9.6	2.7
<sup>58</sup> Ni(n,p)	ENDF/B6	.912	1.03	1.01	5.0	8.0	9.3	2.7
<sup>47</sup> Ti(n,p)	ENDF/B6	1.09	1.23	1.02	5.0	11.0	9.0	2.7
<sup>238</sup> U(n,f)	БНАБ-90	.907	.988	.993	4.0	4.0	7.8	2.8
<sup>115</sup> In(n,n')	ENDF/B5	.875	.941	.989	6.0	12.4	7.1	2.6
<sup>237</sup> Np(n,f)	БНАБ-90	.990	1.03	1.00	4.0	9.9	4.6	2.3
<sup>55</sup> Mn(n, $\gamma$ )	ENDF/B6	1.27	1.21	1.01	5.0	25.4	4.7	2.4
<sup>239</sup> Pu(n,f)	БНАБ-90	.936	.943	.962	4.0	3.3	1.0	0.6
<sup>238</sup> U(n, $\gamma$ )	БНАБ-90	1.04	1.00	1.00	4.0	4.6	3.3	1.2
<sup>58</sup> Fe(n, $\gamma$ )	ENDF/B5	.836	.796	.976	4.5	15.9	4.1	2.2
<sup>59</sup> Co(n, $\gamma$ )	ENDF/B6	.873	.843	.935	5.0	7.6	3.5	1.4
<sup>63</sup> Cu(n, $\gamma$ )	ENDF/B6	1.01	.972	.996	5.0	15.9	3.2	1.3
<sup>197</sup> Au(n, $\gamma$ )	ENDF/B6	.968	.928	.956	5.0	4.6	4.6	2.1
<sup>24</sup> Mg(n,p)	ENDF/B6	.787	.993		5.0		13.7	4.2
<sup>50</sup> Cr(n, $\gamma$ )	БНАБ-90	1.34	1.31		8.0		2.5	1.2
<sup>59</sup> Co(n,p)	БОСП.86	.608	.727		5.0		11.6	3.0
<sup>64</sup> Ni(n, $\gamma$ )	БНАБ-90	1.60	1.56		5.0		1.9	.6
<sup>93</sup> Nb(n,2n)	БОСП.86	1.68	2.29		3.5		18.8	5.9
<sup>93</sup> Nb(n, $\alpha$ )	БНАБ-90	1.23	1.56		6.0		14.1	4.4
<sup>92</sup> Mo(n,p)	ENDF/B5	.429	.506		5.0		10.9	2.8
<sup>92</sup> Mo(n, $\alpha$ )	ENDF/B5	.49	.63		10.0		14.5	4.2
<sup>98</sup> Mo(n, $\gamma$ )	БНАБ-90	1.51	1.48		4.0		1.5	.5
<sup>94</sup> Zr(n, $\gamma$ )	ENDF/B6	1.35	1.32		6.0		1.6	.4
<sup>96</sup> Zr(n, $\gamma$ )	JENDL-1	7.04	7.00		5.0		1.1	.8
<sup>232</sup> Th(n,f)	БНАБ-90	.845	.928		5.0		8.1	2.8
<sup>233</sup> U(n,f)	БНАБ-90	1.00	.999		2.0		.2	.2
<sup>234</sup> U(n,f)	БНАБ-90	.899	.930		4.0		4.4	2.1
<sup>236</sup> U(n,f)	БНАБ-90	.891	.949		4.0		6.5	2.5
<sup>240</sup> Pu(n,f)	БНАБ-90	.869	.900		3.0		4.6	2.2
<sup>241</sup> Pu(n,f)	БНАБ-90	1.03	1.02		3.0		.1	.1
<sup>232</sup> Th(n, $\gamma$ )	БНАБ-90	.918	.886		5.0		3.0	1.0
<sup>236</sup> U(n, $\gamma$ )	БНАБ-90	.869	.834		7.0		3.6	1.3
<sup>237</sup> Np(n, $\gamma$ )	БНАБ-90	1.15	1.10		7.0		5.9	3.0
<sup>232</sup> Th(n,2n)	БНАБ-90	.841	1.06		5.0		3.8	4.3
<sup>238</sup> U(n,2n)	БНАБ-90	.768	.969		5.0		3.6	4.2

Annotations: 1) the reactions which were included in the correction process are listed in the upper part of the table; 2) the initial values of the cross sections and of the spectra used in the calculation are listed in the second column; 3) initial cross sections and corrected spectrum used in the calculations are listed in the third column; 4) corrected cross sections and neutron spectrum are listed in the fourth column.

**Table 3. Initial (calculated using BNAB-78 data) and reconstituted BR-1 reactor neutron spectra, their uncertainties, and the BR-1 recalculated spectrum using BNAB-90 data.**

g	Spectra		Deviation of recon. from init. %	Uncertainties %		Calculated spectrum BNAB-90 )
	Init. Calc. (BNAB-78 )	Reconstituted		Initial	Reconst.	
-1	.000010	.000016	58.4	30.0	9.8	.000015
0	.000504	.000703	38.9	20.0	6.5	.000677
1	.0110	.0137	23.9	12.3	4.0	.0140
2	.0554	.0634	13.9	9.7	3.3	.0639
3	.113	.126	10.8	7.9	2.8	.123
4	.177	.182	2.6	6.5	4.1	.187
5	.165	.157	-5.0	5.9	5.4	.170
6	.191	.182	-4.8	5.3	3.6	.178
7	.143	.138	-3.7	7.4	4.1	.132
8	.0834	.0805	-3.9	9.8	6.4	.0729
9	.0419	.0395	-6.2	11.6	7.9	.0373
10	.0139	.0120	-14.4	14.9	10.2	.0131
11	.0049	.00375	-23.9	18.3	12.1	.0080
12	.000279	.000215	-23.2	20.0	14.5	.000631

**Table 4. Covariant matrix of errors of the BR-1 reconstituted spectrum**

<b>g</b>	<b>Stand. dev. %</b>	<b>Correlation matrix</b>																	
-1	9.8	1.00																	
0	6.5	1.00	1.00																
1	4.0	1.00	1.00	1.00															
2	3.3	.27	.27	.27	1.00														
3	2.8	.27	.27	.27	.67	1.00													
4	4.1	-.26	-.26	-.26	.56	.56	1.00												
5	5.4	-.20	-.20	-.20	-.37	-.32	-.23	1.00											
6	3.6	.00	.00	.00	-.64	-.63	-.74	.66	1.00										
7	4.1	.23	.23	.23	-.33	-.40	-.60	-.51	.05	1.00									
8	6.4	.16	.16	.16	-.02	-.09	-.21	-.83	-.37	.74	1.00								
9	7.9	.06	.06	.06	.07	.03	.04	-.89	-.54	.60	.90	1.00							
10	10.1	-.17	-.17	-.17	.18	.16	.34	-.83	-.69	.33	.72	.87	1.00						
11	12.1	-.35	-.35	-.35	.22	.18	.50	-.63	-.65	.06	.47	.66	.82	1.00					
12	14.5	-.27	-.27	-.27	.19	.16	.41	-.51	-.54	.05	.38	.58	.74	.93	1.00				

**Table 5. Ratios of calculated data relative to the reaction cross sections measured on the BN-350 reactor and various component errors.**

Reaction	Library	Calculation/measurement			Uncertainties %			
		Init. $\sigma$ , $\varphi$	Corrected		Exper.	Const. comp.	Spectral comp.	
			$\varphi$	$\sigma, \varphi$			Before	After
1	2	3	4	5	6	7	8	9
$^{55}\text{Mn}(n,2n)$	ENDF/B6	.499	.809	.984	10.0	24.5	22.8	8.9
$^{48}\text{Ti}(n,p)$	ENDF/B6	.690	.941	.991	5.0	11.2	13.8	4.9
$^{59}\text{Co}(n,\alpha)$	ENDF/B6	.727	.986	.991	6.5	6.5	13.5	4.8
$^{54}\text{Fe}(n,\alpha)$	БООП.86	.667	.885	1.01	5.5	18.0	12.7	4.3
$^{56}\text{Fe}(n,p)$	БООП.86	.752	.995	.997	3.5	6.2	12.6	4.2
$^{60}\text{Ni}(n,p)$	ENDF/B6	.645	.830	.910	5.5	7.4	11.8	3.9
$^{46}\text{Ti}(n,p)$	ENDF/B6	.782	.955	.997	4.2	12.8	10.4	3.8
$^{54}\text{Fe}(n,p)$	БООП.86	.928	1.05	1.03	5.5	4.2	8.5	3.7
$^{58}\text{Ni}(n,p)$	ENDF/B6	0.916	1.02	1.01	4.0	7.7	8.2	3.6
$^{47}\text{Ti}(n,p)$	ENDF/B6	1.12	1.23	1.02	5.0	11.0	7.8	3.6
$^{55}\text{Mn}(n,\gamma)$	ENDF/B6	.740	.770	.969	6.0	20.8	3.7	3.2
$^{58}\text{Fe}(n,\gamma)$	ENDF/B6	1.09	1.11	1.01	4.0	13.2	1.8	1.6
$^{59}\text{Co}(n,\gamma)$	ENDF/B6	.699	.758	.936	5.0	11.1	6.6	5.8
$^{50}\text{Cr}(n,g)$	БНАБ-90	1.14	1.14	1.14	5.0	12.4	1.5	1.3
$^{59}\text{Co}(n,p)$	БООП.86	.607	.761	.761	4.5	21.5	11.2	3.9
$^{64}\text{Ni}(n,\gamma)$	БНАБ-90	1.83	1.83	1.83	6.0	9.8	1.3	1.2
$^{92}\text{Mo}(n,p)$	ENDF/B5	.436	.524	.524	5.0	9.4	9.9	3.6
$^{92}\text{Mo}(n,\alpha)$	ENDF/B5	.588	.816	.816	10.0	9.3	14.6	5.2
$^{98}\text{Mo}(n,\gamma)$	БНАБ-90	1.19	1.21	1.21	5.0	6.6	1.5	1.3
$^{94}\text{Zr}(n,\gamma)$	ENDF/B6	1.22	1.21	1.21	5.0	7.4	.7	.6
$^{96}\text{Zr}(n,\gamma)$	JENDL-1	2.61	2.67	2.67	5.0	6.7	1.8	1.6
$^{238}\text{U}(n,f)$	БНАБ-90	.972	1.03	1.03	5.0	4.5	6.8	3.8
$^{238}\text{U}(n,\gamma)$	БНАБ-90	1.00	1.01	1.01	3.0	3.8	1.3	1.1
$^{238}\text{U}(n,2n)$	БНАБ-90	.917	1.26	1.26	10.5		14.1	5.4
$^{236}\text{U}(n,f)$	БНАБ-90	.954	.995	.995	5.0		5.6	3.4
$^{236}\text{U}(n,\gamma)$	БНАБ-90	.960	.968	.968	8.0		1.2	1.0
$^{239}\text{Pu}(n,f)$	БНАБ-90	.997	.994	.994	2.5	4.8	.8	.7
$^{240}\text{Pu}(n,f)$	БНАБ-90	1.04	1.05	1.05	5.0		3.4	2.4
$^{241}\text{Pu}(n,f)$	БНАБ-90	1.16	1.15	1.15	4.0		.2	.1
$^{237}\text{Np}(n,f)$	БНАБ-90	.928	.939	.939	5.0	9.7	4.3	3.0
$^{237}\text{Np}(n,\gamma)$	БНАБ-90	.946	.953	.953	5.5		1.3	1.1
$^{233}\text{U}(n,f)$	БНАБ-90	.999	.996	.996	8.0		.3	.3
$^{232}\text{Th}(n,f)$	БНАБ-90	.912	.978	.978	7.0	5.2	6.9	3.7

Annotations: 1) the reactions which were included in the correction process are listed in the upper part of the table; the remaining reactions are listed in the lower part of the table; 2) the initial values of the cross sections and of the spectra used in the calculation are listed in the second column; 3) initial cross sections and corrected spectrum used in the calculations are listed in the third column; 4) corrected cross sections and neutron spectrum are listed in the fourth column.

**Table 6. Initial (calculated using BNAB-78 data) and reconstituted BN-350 reactor neutron spectra, their uncertainties, and the BN-350 recalculated spectrum using BNAB-90 data.**

E	Spectra		Deviation of recon. from init. %	Uncertainties %		Calculated spectrum BNAB-90
	Init. Calc. BNAB-78	Reconstituted		Initial	Reconst.	
-1	.000033	.000005	79.5	28.2	11.3	.000006
0	.000060	.000097	60.9	21.6	8.6	.000085
1	.00140	.00193	37.5	13.3	5.3	.00176
2	.00901	.0108	19.3	10.3	5.1	.0123
3	.0238	.0257	7.8	7.8	4.6	.0240
4	.0483	.0500	3.3	5.9	4.5	.0522
5	.0602	.0603	.1	4.0	3.6	.0692
6	.148	.145	-1.8	2.9	2.8	.147
7	.153	.149	-2.8	2.5	2.4	.150
8	.157	.155	-1.2	1.4	1.3	.154
9	.147	.145	-1.4	3.0	2.9	.144
10	.106	.106	.2	2.9	2.7	.103
11	.0705	.0715	1.3	3.4	3.1	.0726
12	.0391	.0401	2.5	4.1	3.7	.0407
13	.0117	.0122	4.1	5.4	5.0	.0124
14	.0168	.0177	5.2	5.5	4.9	.0173
15	.00591	.00637	7.8	6.9	6.1	.00650
16	.00160	.00180	12.2	9.7	8.5	.00187
17	.000300	.000351	16.9	12.9	11.4	.000366
18	.000083	.000100	20.2	15.4	13.7	.000099

Table 7. Covariant matrix of the errors of the initial (calculated) spectrum

$\lambda$	Stand. dev. %	Correlation matrix																			
-1	28.2	1.00																			
0	21.6	1.00	1.00																		
1	13.3	1.00	1.00	1.00																	
2	10.3	.74	.74	.74	1.00																
3	7.8	.59	.59	.59	.81	1.00															
4	5.9	.42	.42	.42	.61	.79	1.00														
5	4.00	.23	.23	.23	.35	.52	.65	1.00													
6	2.9	.03	.03	.03	.08	.19	.22	.71	1.00												
7	2.5	-.15	-.15	-.15	-.19	-.12	-.20	.09	.67	1.00											
8	1.4	-.33	-.33	-.33	-.46	-.54	-.61	-.57	-.25	.51	1.00										
9	3.0	-.21	-.21	-.21	-.29	-.37	-.42	-.47	-.38	-.12	.72	1.00									
10	2.9	-.18	-.18	-.18	-.26	-.36	-.37	-.57	-.68	-.50	-.13	-.06	1.00								
11	3.4	-.16	-.16	-.16	-.23	-.35	-.33	-.56	-.73	-.64	-.22	-.04	.89	1.00							
12	4.1	-.12	-.12	-.12	-.19	-.30	-.27	-.49	-.69	-.69	-.20	-.14	.78	.90	1.00						
13	5.4	-.08	-.08	-.08	-.13	-.24	-.19	-.38	-.64	-.71	-.24	-.12	.64	.81	.93	1.00					
14	5.5	-.09	-.09	-.09	-.13	-.24	-.20	-.38	-.61	-.67	-.23	-.12	.57	.74	.86	.91	1.00				
15	6.9	-.07	-.07	-.07	-.10	-.20	-.26	-.32	-.55	-.63	-.23	-.10	.47	.63	.76	.78	.97	1.00			
16	9.7	-.04	-.04	-.04	-.06	-.16	-.11	-.25	-.49	-.62	-.22	-.09	.37	.56	.67	.74	.91	.99	1.00		
17	12.9	-.02	-.02	-.02	-.04	-.13	-.07	-.19	-.44	-.59	-.22	-.08	.30	.50	.60	.70	.85	.95	.99	1.00	
18	15.4	-.01	-.01	-.01	-.02	-.11	-.05	-.17	-.44	-.62	-.22	-.07	.28	.50	.59	.69	.83	.94	.97	.99	1.00



---

Nuclear Data Section  
International Atomic Energy Agency  
P.O. Box 100  
A-1400 Vienna  
Austria

e-mail, INTERNET: [SERVICES@IAEAND.IAEA.OR.AT](mailto:SERVICES@IAEAND.IAEA.OR.AT)  
fax: (43-1)20607  
cable: INATOM VIENNA a  
telex: 1-12645 atom a  
telephone: (43-1)2060-21710

---

online: TELNET or FTP: [IAEAND.IAEA.OR.AT](http://IAEAND.IAEA.OR.AT)  
username: IAEANDS for interactive Nuclear Data Information System  
username: ANONYMOUS for FTP file transfer  
username: FENDL for FTP file transfer of FENDL files  
For users with web-browsers: <http://www-nds.iaea.or.at>

---